UNESCO - INTERNATIONAL UNION OF GEOLOGICAL SCIENCES

EARTH PROCESSES IN GLOBAL CHANGE

Climates of the Past

Editors: J. Meco and N. Petit-Maire

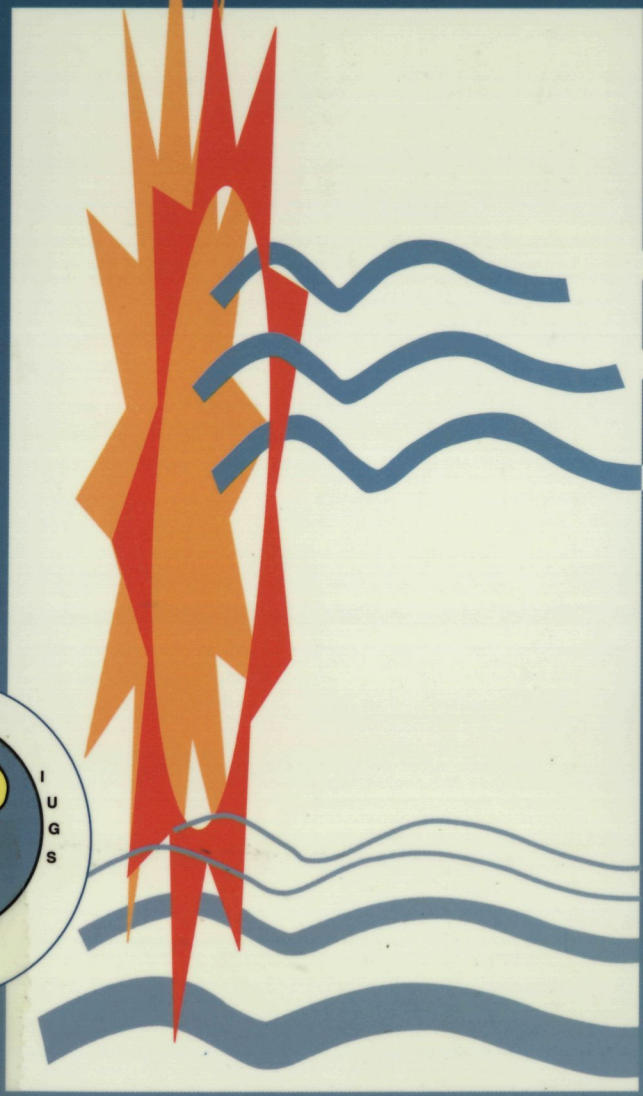

UNIVERSIDAD DE LAS PALMAS DE GRAN CANARIA
SERVICIO DE PUBLICACIONES

Climates of the Past

Editors
J. Meco and N. Petit-Maire

Proceedings of the CLIP meeting held June 2-7, 1995
Lanzarote and Fuerteventura (Canary Islands, Spain)

International union of Geological Sciences
Unesco

Earth Processes in Global Change

Universidad de Las Palmas de Gran Canaria
SERVICIO DE PUBLICACIONES

CLIP Meeting (1995. Lanzarote y Fuerteventura, Islas Canarias)

Climates of the past: proceedings of the CLIP meeting held june 2-7, 1995 Lanzarote and Fuerteventura (Canary Islands, Spain) / Editors J. Meco and N. Petit-Maire; International Union of Geological Sciences, Unesco, [Programme] Earth Processes in Global Change. -Las Palmas de Gran Canaria: Universidad, 1997
157 p.: il.; 30 cm
ISBN 84-89728-18-6

1. Climatología - Congresos 2. Cambios climáticos - Congresos I. Meco, J. II. Petit-Maire III. International Union Geological Scienses IV. Unesco V. Earth Processes in Global Change VI. Universidad de Las Palmas de G. C. VII. Título
55.583

Edita: Universidad de Las Palmas de Gran Canaria
Servicio de Publicaciones

Realización: Daute Diseño, S.L.

Depósito Legal: G.C. - 51 - 1997

Foreword

We warmly thank IUGS, UNESCO, ANDRA and the French Committee of Geology for the support which allowed CLIP members to meet in the Canary Islands.

The Clip meeting held in June 1995 in the two easternmost Canary islands would not have been possible without the very important support provided by several high personalities in the Canary Government, in Las Palmas de Gran Canaria University and among the Fuerteventura and Lanzarote authorities. We are particularly grateful to M. Cabrera Cabrera, Vice-Councillor foe Culture and Sports, F. Rubio Royo, Rector of Las Palmas de Gran Canaria University, M. Lobo Cabrera, Chairman of Research, E. Pérez Parrilla, President of Cabildo and C. García Déniz, Councillor for Culture in Lanzarote, J.J. Herrera Velázquez, President of Cabildo and M. Cabrera González Councillor for Culture in Fuerteventura. We warmly thank H. Umpiérrez Sánchez, J. Morales Teixidor, A. Carrasco Martín, D. Ortega Reguilón, V. Lloret LLinares and I. Hernández Díaz who proved extremely helpful in the organisation of the workshop.

The Clip members who attended were from 12 countries: Australia, Canadá, China, France, Germany, Indonesia, Morocco, Senegal, Spain, UK, USA and Venezuela. Most of them had never visited the Islands before. All of them were impressed by their exciting geological features, their impressive landscapes and their development.

A hearty «Gracias» to all those who participated in the success of the meeting.

J. Meco, Professor ULPGC
N. Petit-Maire, President CNF/INQUA
DRE/CNRS

Contents:

INTRODUCTION

THE ROLE OF EARTH SCIENCES IN THE ANTICIPATION OF FUTURE CLIMATIC CHANGE AND THE UNESCO-IUGS PROGRAMME "CLIMATES OF THE PAST"

The world socio-economic and political structures rest, for a large part, upon the present-day climatic conditions, widely dictating the regional availability of fresh water, food and shelter. The study of long term geological records has shown that the present-day scenario is only transitory within the huge variability of the Earth's climate. Changes in the solar energy received by the planet have induced, at least in the last million years, alternate cold and warm phases: over the last 20,000 years only, the average global temperature has shifted from a glacial maximum (-3°C relative to nowadays global average) to a warm pattern (+1°C global average). The climate optimum peaked between 9,500 and 7,000 years ago, then slowly degradated, due to the astronomical long trend presently leading the globe toward a new cold phase. However, Man is now interfering with this trend: a rapid global warming is induced by the emission into the atmosphere of radiative gases (CO_2, CH_4, water vapour, *etc.*) the natural ratio of which is already significantly enhanced. Theoretical models, used to generate possible future scenarios, anticipate a minimal warming of +1°C in the XXIth century and try to predict its effects on the regional climates. The uncertainty of such models is wide, due to the complexity of the interactive processes involved: atmosphere, ocean, ice, continental surfaces. Moreover, they cannot easily consider, at their wide temporal and spatial scale, the huge geographic diversity of the continents and its regional consequences.

Thus, the only efficient method for anticipating the effects of future climatic change (whatever it will be, natural or man-made) on the Earth's landscapes, hydrology and ecosystems, is to use *the actual archives provided by geological deposits* on the paleoenvironments corresponding to colder or warmer scenarios in the recent past. Cores from polar ice yield past surface temperatures, indicate periods of dust flows, wind-blown from arid areas and even, thanks to the air bubbles trapped in the ice, the past composition of the atmosphere (CO_2, CH_4). Ocean-floor sediments provide Foraminifera shells, the analysis of which indicates past sea surface temperatures and global ice-volume, lake sediments provide records of the hydrological evolution of regional areas. Pollen in geological layers indicate the past vegetal cover. Changes from aeolian sediments (loess, sand dunes) to paleosols indicate evolution from an arid to a more humid climate. Animal remains also imply different biotopes. Man himself is a climatic marker when archaeological sites are found in present-day uninhabited deserts. Most of those geological and biological indicators can be dated with a greater and greater precision by the physico-chemical methods.

Thus, Geology allows to evaluate the type and *amplitude* of past environmental changes in each region, but also the *velocity* of change and even, at times, their impact on human life, migrations and civilisations.

Whatever our climatic future, a naturally colder world or a pollution induced warmer world, *it happened before* (even if at different rates and for different reasons), and Earth Sciences, a real Key of the Future, can tell us what happened in each case.

A colder world ?

Geological records all show that natural global coolings (related with a reduction of the insolation) have been very slow. Changes take place at the scale of millenia: ice caps grow, oceanic currents and trade winds intensify, the oceans' level lowers, the permanently frozen areas, the cold-dry steppes and the tropical deserts expand. These patterns are non-linear, with oscillatory warmer / colder episodes progressively heading towards the maximal glacial patterns. The last one has produced very severe environmental degradation: in northern Africa, the Sahara desert has expanded 400 km to the South of its present-day boundary, the Amazone and other rain forests have considerably reduced, while sea-level was 130 m lower than nowadays and ice mountains over Greenland reached a 4,000 m height.

The natural trend (reduction of insolation) currently running towards such a scheme does not threaten our near future, since the cooling is estimated to -0.01°C/century However, Earth Sciences have established that, since the end of the last optimum, about 6,000 years ago, sea surface temperatures have lowered by 0.5°C. The average of 500 curves of local sea-level changes dropped 1.5 m. Mountains glaciers advanced both in the Himalaya and the Alps. In northern Africa, the 100 mm isohyet (mean annual average of rainfall) has migrated 500 km southwards.

A warmer world ?

Due to its proximity in time, the last natural shift from a colder to a warmer scenario (16,000 to 10,000 years before present) is well documented and precisely radiocarbon dated in ice, ocean and continental sediments. The rise in insolation coincides with a rise of the carbon dioxyde and methane ratios in our atmosphere. All warming signals rapidly increase in intensity, although in a non-linear pattern. The first consequence was sea-level rise, due to ice-melting and thermic expansion of the ocean. Between about 20,000 years and 10,000 years before present, the sea-level changed from -130 m to -35 m relative to the current level. Two abrupt pulses took place, with respective rises of 2.5 m and 3.7 m / century ! Atmospheric circulation slowed up, oceanic cores progressively displayed less dust layers, due to weaker aeolian ablation over the vast deserts of the preceeding glacial phase, which began to receive increased rainfall. The arid and semi-arid ecozones, as well as the cold-dry steppes in Central Asia and the permafrost area, began to shift back.

. *Those processes, in contrast with those associated to global cooling, were very rapid:* over about 8,000 years, the average temperature of the Earth's surface shifted from about -3°C to +1°C, relative to the present-day one. While sea-level rise, connected with ice-melting, was completed about 6,000 years ago, changes in atmospheric circulation have induced, as early as 10,000 years ago, a complete overthrow of the glacial environments. In the tropical deserts, fresh water lakes and swamps appeared widely in all the closed depressions. Paleobotanics and paleontology bring evidence to a northwards shift of vegetal and animal species up to 22°N. Rainfall over the Sahara is estimated to have been 50 times higher than at present, during the optimum. Thus, in the span of 10,000 years (16,000 to 8,000 years BP), the desert belt in northern Africa moved about

1,000 km to the North. A similar evolution is recorded by Earth Sciences in the Arab Peninsula, Rajahstan and China. The palynological records in Brasil also show the expansion of the rain forest during this wet phase. In Russia, the permafrost southern limit migrated northwards, ice-rich deposits thawed and warming induced the mammoth-fauna extinction.

Thus, all geological records show that past warmings (of moderate intensity relative to the expected pollution forcing) had a wide and rapid impact upon landscapes, hydrology and the biosphere. In the tropical arid areas, in particular, increase of precipitation induced *presence of abundant surface fresh-water* and *a regeneration of the biosphere*, at the scale of several centuries.

The UNESCO-IUGS Programme " Climates of the Past"

The actual paleosituations known thanks to Geology must be considered together with the theoretical results of climatic models, if one wants to anticipate our future with a major efficiency. The greatest attention should be given to the most sensitive transitory areas between the main ecozones (polar, temperate, humid tropics), such as the deserts margins, the periglacial area and the coastal zones at the interface of oceanic and continental processes. Earth Sciences have to be integrated at a privileged rank into all the "Global Change" programs, as a major key to the anticipation of our climatic and environmental future. In this scope, a joint UNESCO-IUGS Programme "Earth Processes in Global Change" was created in september 1992 and a Pilot Project "Climates of the Past " (CLIP) initiated in January 1993. Its specific objecives are at three levels:

- To facilitate contacts between geoscientists working in different areas, to encourage synthetic work and to create a network of members in different fields of Earth Sciences liable to collaborate and widen the scope of their regional or thematic work. These aims are achieved through annual or biannual meetings, held in locations having provided major results on past environmental changes related with Global Changes. In 1993, the scientists having studied results on sea-level change in Barbados have presented their work in the field to our members. In 1994, our Indonesian colleagues presented to us their research and problems in the Indo-Pacific area, a key zone for the understanding of oceanic circulation. In 1995, the workshop took place in the Eastern Canary Islands, where marine terraces and thick continental deposits alternating aeolian formations (testifying for an arid climate) and paleosols (testifying for a humid climate) are currently studied by CLIP members from Canada, France, Morocco, Spain and UK.

In 1996, the meeting has held along the northern coast of Venezuela, where marine terraces were related with neotectonics along this southern margin of the Caribbean plate. In 1997, it will take place in northeastern Australia, where major research has taken place.

Other collaborations were established and are current : Brasil-France (dating of submarine "glacial" canyons at the mouth of the Amazone), Indonesia- France (dating of marine terraces), Indonesia- Australia (coral reefs, isotopic analyses), France-Spain (radiocarbon dating, U/Th dating, stable isotopes analyses), Canada-Morocco-Spain (TL and OSL dating), Venezuela - France (radiocarbon and U/th dating of marine terraces and archaeological Sites).

-To publish (in coll. with CIFEG, Orléans) summarised annual results of our members' research. Those books are extremely useful to the scientific community for obtaining quick (sometimes unpublished or in press) information upon current work in Paleoclimatology. A directory of members, with fax numbers, allows easy communication.

- CLIP also aims to provide modelers with *synthetic*, wide, regional results allowing to validate or improve their analyses in the continental areas.

In this scope, CLIP undertook, in 1994, to reconstruct maps of the Earth's environments at the extremes (cold / warm) of natural variability which occurred in the recent geological past (Last Glacial Maximum, Holocene Optimum). This project has the sponsorship of the Commission of the Geological map of the World (CGMW), another joint Programme of IUGS and UNESCO, and of ANDRA.

CLIP has grown steadily since its inception and has now 111 corresponding members from 28 countries. It supported by ANDRA, CIFEG, the French Ministry of Foreign Affairs, the French Geology Committee, IUGS, UNESCO and local Universities, research organisms and oil companies during the field workshops and excursions.

Nicole Petit-Maire
Project Leader

HOLOCENE TECTONIC UPLIFT OF LA VELA ANTICLINE RELATED TO THE ACTIVITY OF THE GUADALUPE THRUST, NORTHERN FALCON STATE (VENEZUELA)

F. Audemard[1], J. A. Rodríguez [1], and J.-C. Bousquet [2]

1 FUNVISIS. Apartado Postal 76880, Caracas 1070-A, Venezuela
2 Lab. Tectonophysique. Inst. des Sciences de la Terre, de l'Eau et de l'Espace, Univ. Montpellier II, Place Eugene Bataillon, 34095 Montpellier cedex 05, France

Abstract

The Falcón Basin in northwestern Venezuela has undergone an important tectonic inversion from Middle Miocene until Early Pleistocene times. However, it is difficult to tell whether this inversion is still going on today, but the Guadalupe thrust, responsible for the formation of La Vela anticline and its western prolongation, seems to be active, as the presence of an uplifted marine feature along the coast on the northern flank of this anticline suggests.

On the beach that surrounds the northern flank of La Vela anticline, a small patch (<15 m²) of beach-rock was found at ≃ 2.5 m above msl. It yielded a ^{14}C age of 2700 yr. B.P. from unreworked tests of Turritella sp. When compared to a set of marine features (beach-rock deposits, wave-cut benches and wave notches), observed at ≃ 1 m above msl along the northeastern coast of the Falcón State, between La Vela and San Juan de los Cayos, (believed to be associated with the maximum highstand of the Holocene transgression reported worlwide at about 4000 to 5000 B.P., thus implying that maximum Mid-Holocene sea level should be expected at ≃ 1 m above msl in the southern Caribbean region), this beach-rock deposit on the north flank of La Vela anticline seems to be uplifted of ≃ 1.5 m. Since this fold is genetically related to the Guadalupe thrust, this latter then seems to be moving coseismically. Considering a thrust plane dipping at 30°S, the coseismic slip can be roughly estimated at 3 m, capable of generating an Ms ≃ 7.0 earthquake.

Introduction

The Falcón region, during the Oligocene and Early Miocene, was mainly a marine basin, open to deep sea water to the east. In the Middle and Late Miocene, it was intensively folded and tectonically inverted by a NW-SE compression, forcing subsequent facies to deposit exclusively on the northern flank of the «newborn» Falcón anticlinorium (Audemard, 1993). This inversion had to be active until the Early Pleistocene, since the Pliocene La Vela formation (shallow marine deposits) is cropping out in perfect upright position to the northwest of La Vela anticline, and since the Plio-Pleistocene Coro Formation, whose upper part comprises mainly fan conglomerates, is tilted northward up to 65° (Audemard, 1993). However, it is difficult to tell whether this tectonic inversion of this Oligo-Miocene basin, located in northwestern Venezuela, is still going on. However, the Guadalupe thrust and its western prolongation, a tectonic feature responsible for both previously-mentioned tilting, seem to be active, as shown below.

Geological setting

La Vela anticline, in the northern Falcón basin located along the coast east of Coro (capital of the Falcón State) and nearby the town of La Vela de Coro (Fig. 1), is pretty well-known from the early 30's, because González de Juana carried out a thorough field work completed with borehole data. Recently, new seismic profiles have allowed to better describe this structure (Audemard and de Mena, 1985; Cabrera de Molina, 1985).

La Vela structure is a brachy-anticline (length and width are nearly the same) and its longest axis trends N 070° to N 080°. Due to its shape, it is also known as La Vela dome. This structure is bounded to the west by the Carrizal fault that strikes N 010° - N 015°, whereas it has a normal periclinal closure to the east, after González de Juana (1937) and Kavanagh (1959). However, we believe, with Cross (1952) and Tahal (1969), that this structure is equally bounded to the east by the NW-SE trending fault system that controls the eastern coast of the Falcón State, among which are La Soledad and Santa Rita faults (Fig. 1). González de Juana (1937,1972) and Kavanagh (1959) consider La Vela structure as a brachy-anticline, with two double-dipping anticlinal axes trending N 070° to N 080°, separated by a very narrow sub-parallel syncline. The flanks of the main anticline, located south, dip gently (Photo 1), whereas the northern fold presents a vertical-to-overturned northern flank. These folds are associated to the Guadalupe thrust (González de Juana, 1937; Cross, 1952; Kavanagh, 1959; Audemard and De Mena, 1985; Cabrera de Molina, 1985), also named Taima-Taima thrust by González de Juana (1972). This northvergent arcuated thrust is located offshore along the northern coast of La Vela anticline, but it can be observed on land east of El Muaco pier (González de Juana, 1937 and Kavanagh, 1959; Fig. 1). This brachy-anticlinal structure has been interpreted by Audemard (1993) in a different manner: the main gently-folded dome would be partially separated from the narrow overturned anticline by a sub-parallel secondary thrust fault of the major Guadalupe (TaimaTaima) thrust (Fig. 1). From several previously-interpreted seismic profiles (Audemard and De Mena, 1985; Cabrera de Molina, 1985), the dip of the thrust plane can be estimated at about 30° to the south, being very similar to the dip represented on a geological crosssection of La Vela anticline, interpreted by González de Juana (1937). The sedimentary sequence involved in this folding ranges in age between Middle to late Miocene (Socorro and Caujarao formations) and Pliocene (La Vela formation). The latter and younger formation is perfectly in upright position west of El Muaco pier and of the Carrizal fault, thus being the most remarkable evidence of Quaternary folding in this region (Photo 2).

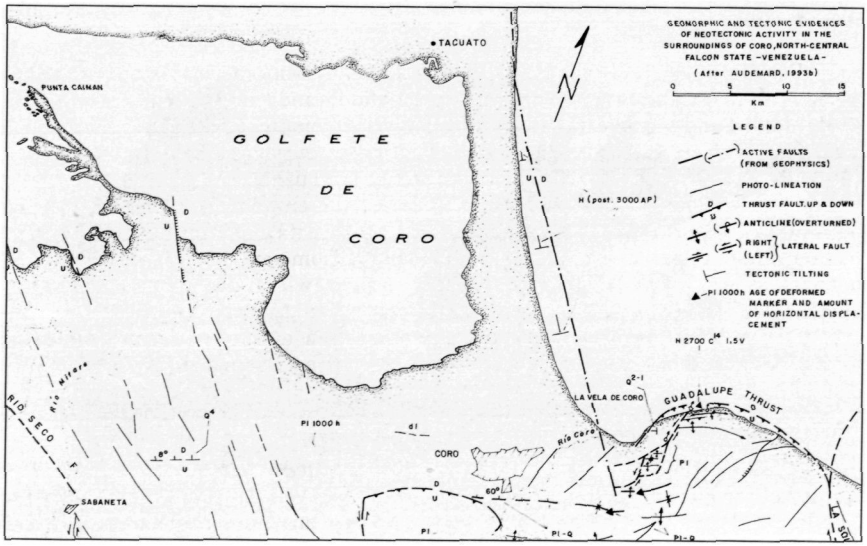

Figure 1. Neotectonic map of north-central Falcón State (Venezuela). Observe the irregular geometry of the frontal thrust system (Chuchure-Guadalupe thrust).

Photo 1. Morphological profile of La Vela anticline: bird-eye view of the gently dipping southern main anticline. Topography is perfectly adapted to the structure.

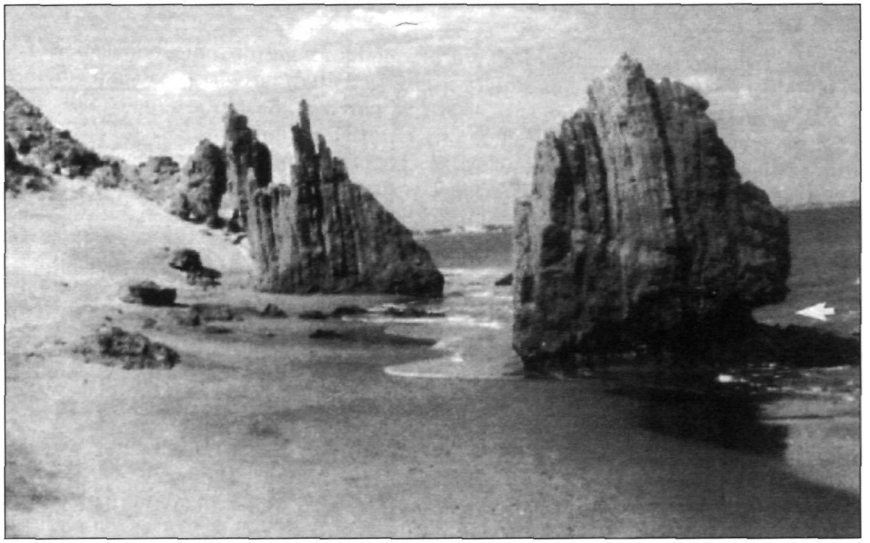

Photo 2. Vertical strata of La Vela formation of the Late Miocene-Early Pliocene, outcropping NW of La Vela anticline and west of El Muaco pier. Besides, observe the contemporary notch at the foot of the remnant block in the foreground, indicated by the white arrow.

Therefore, the north-vergent overthrusting of the Taratara block and the associated La Vela anticline take place along the Taima-Taima or Guadalupe thrust fault, bounded by the faults of Carrizal to the west (photo 3) and La Soledad to the east (Fig. 1). This deformation is Quaternary because the Pliocene La Vela formation is tilted. Moreover, it happens to be in upright position between the town of La Vela and El Muaco pier, on the northwestern tip of La Vela structure, implying that the amount of uplifl of this structure has been very important afler deposition of that shallow inner-shelf marine sequence (in the Plio-Pleistocene) .

The Guadalupe (or Taima-Taima) thrust constitutes the easternmost segment of a major thrust that extends westward for some sixty kilometers, from the town of Puerto Cumarebo to the village of Las Piedras (Audemard, 1993), located south of Sabaneta (Fig. 1), as it was also suggested by maps made by Smith (1962) and Cabrera de Molina (1985). Its vertical throw is estimated at 300 m (Ferrell et *al*, 1969). The thrust front is disrupted twice by short left-lateral (tear) faults or complex zones that can offset it southwards for a few to about ten kilometers, such as east of Coro. There, the front jumps south, between the villages of Caujarao and La Vela, from the southern Carrizal fault tip to a north steeply-dipping monocline affecting the fanglomerates of the Late Pliocene-Early Pleistocene Coro formation (Fig. 1 and Photos 4 and 5). In between, the thrust plane does not outcrop, but its presence is underlined by a set of NE-SW trending «en échelon» folds, that connects both segments (Audemard, 1993; Fig. 1). This geometry and the associated structures suggest the existence of a transfer zone, similar to those described by Baby *et al.* (1993) and Calassou *et al.* (1993). Analog modelling carried out by Audemard (1993) confirmed this possibility. Further west, this major

Photo 3. Fault-line scarp of the 10°-15° striking Carrizal fault at the Carrizal Cemetry.

Photo 4. North Steep north-dipping monocline affecting then Pliocene-Early Pleistocene Coro formation, south of Coro and nearby the village of Caujarao.

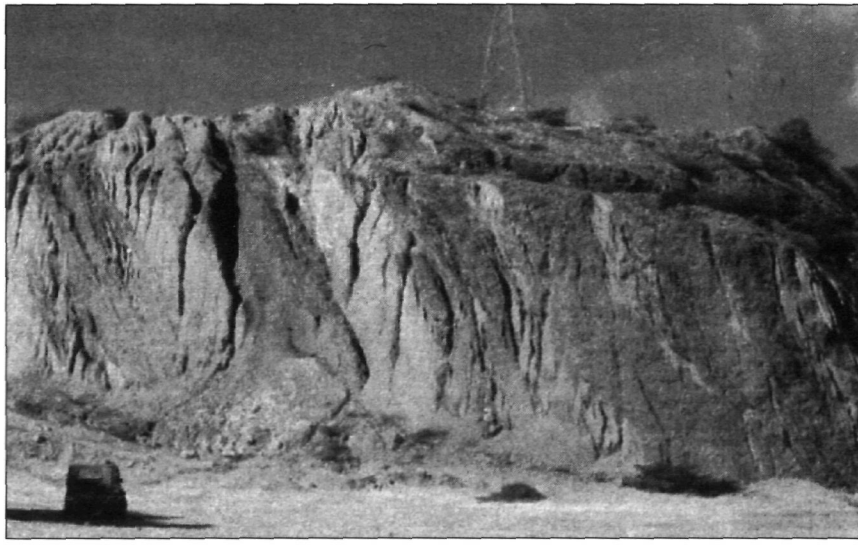

Photo 5. The Coro formation outcrops steeply, dipping north (65°) on a large road cut along the Coro-Caujarao-Churuguara road, south of the city of Coro.

thrust system has been identified by Wiedenmayer (1937) between Caujarao-El Isiro and San Antonio, SW of the city of Coro. At La Mina de Coro (ancient coal mine in the Cerro Pelado formation), this thrust is responsible for the overthrusting of the Middle Miocene Cerro Pelado formation onto the Late Miocene Caujarao formation. The second front disruption happens at the western end of this segment (Fig. 1). The San Antonio fault, after Wiedenmayer (1937), or Hatillo fault afler Cross (1952), offsets it 2.5 km left-laterally, but the post-Pliocene displacement is less than 1 km (post- La Vela formation). Even further west, between San Antonio and Sabaneta, the thrust fault is suggested on the Creole company map (Bellizzia, coord., 1971) and located south of La Fila Capote, within the mudstones of the Middle Miocene Querales formation. Cross (1952) had mapped the same thrust fault trace, which he named Chuchure, between Las Piedras (slightly south of the village of Sabaneta) and San Antonio (SW of Coro), along the valley of the small village of Chuchure (Fig. 1). This author also mentions that the northern compartment corresponds to a north dipping monocline, whereas the southern block is intensively deformed by faults and folds, some of which are overturned . Cross (1952) establishes that the Chuchure thrust is a north-vergent steeply-dipping reverse fault.

Audemard (1993) considers that the outer thrust front, that connects the Río Seco fault with the Guadalupe (Taima-Taima) thrust, may be developing in a more northern position than the previously-described thrust system, based on the following facts (Fig. 1):

- the tilted Q_4 alluvial deposits located NE of Sabaneta.
- ENE-WSW trending geomorphic evidences, such as line springs and aligned drainages, located west of Coro;

- eastward diversion of the Mitare river along its lower course, nearby the coast. It is relevant to mention that the alluvial plain cut by this river in its lower course is extremely young because it coincides with the still-prograding Holocene delta of the Mitare river.

As a matter of fact, due to its very modest surface expression (very slight geomorphic evidence), this thrust fault could very well correspond to an active blind thrust. Generation of this structure was well-reproduced during the analogue modeling performed by Audemard (1993).

Evidences of Late Quaternary tectonic activity

Before this work, the unique and indirect reference of a tectonic activity of La Vela anticline in Late Quaternary times probably corresponds to an observation made by Rohr (1945) and Danielo (1976), who report the tilt of a marine deposit, correlated to isotope stage 5, which is stronger nearby Puente de Piedra (eastern closure of La Vela anticline) and which decreases progressively eastward (in other words, when getting away from La Vela anticline).

However, a new evidence has been found on the present-day beach that surrounds the northern flank of La Vela anticline (Audemard, 1993). A small (less than 15 m^2) patch of beach-rock outcrops at $\approx$ +2.5 m msl on that beach (Fig. 2 and Photo 4). This deposit is rather thin, less than 10 cm thick, and dips gently to the north towards the Carribean sea (Fig. 2 and Photo 7). Its northern tip has dropped and dips 60° N, because wave action has eroded the tender underlying marls of the Miocene Caujarao Formation (Fig. 2 and Photos 6 and 7). ^{14}C age determinations were carried out on two samples: one on a beach-rock sample and another on a set of few unreworked tests of *Turritella sp.* sampled from it, yielding respectively an age of 5730 $\pm$ 85 yr. B.P. and 2705 $\pm$ 150 yr. B.P. Due to the good preservation of the gastropod shells, Audemard (1993) has considered the younger age to be more representative of the age of the beach-rock. At the northern foot of the tilted fragment, another beach-rock outcrops at $\approx$ + 0.50 m above msl and can be distinguished from the former one due to the lack of *Turritella sp* (Audemard, 1993). We believe that collapse of the northern tip of the older beach-rock and cementation of the younger beach-rock, have happened almost coevally in the last $\approx$ 2500 years, related to a sea level stand very similar to the present one, if not the same. As a matter of fact, we should mention that a 2.5 m elevated Holocene beach-rock then constitutes an anomaly, when compared to a set of marine-related features, such as: beach-rock deposits, wave-cut benches and wave notches, that can be observed at $\approx$ 1 m above msl, along the northeastern coast of the Falcón State, between La Vela and Punta Sauca (Photos 8 through 11). Besides, Audemard (1993) reports a dead coral reef in the intertidal zone at San Juan de los Cayos (eastern Falcón State) that has been truncated and levelled to present sea level. This author also considers that this reef, considering its state of preservation, might be sub-recent, but no age determination has been performed yet (Photos 12 through 15). Therefore, these seaside features might be associated to the maximum Holocene highstand reported worldwide at about 4000 to 5000 years ago by Fairbridge (1961), thus implying that a maximum sea level highstand in the Mid-Holocene should be expected at $\approx$1 m above msl in the southern Caribbean region (Audemard, 1993), as has been also reported in the western tropical Atlantic (Bahamas platform, slightly north of the Caribbean sea according to Bourrouilh-Le Jan, 1993).

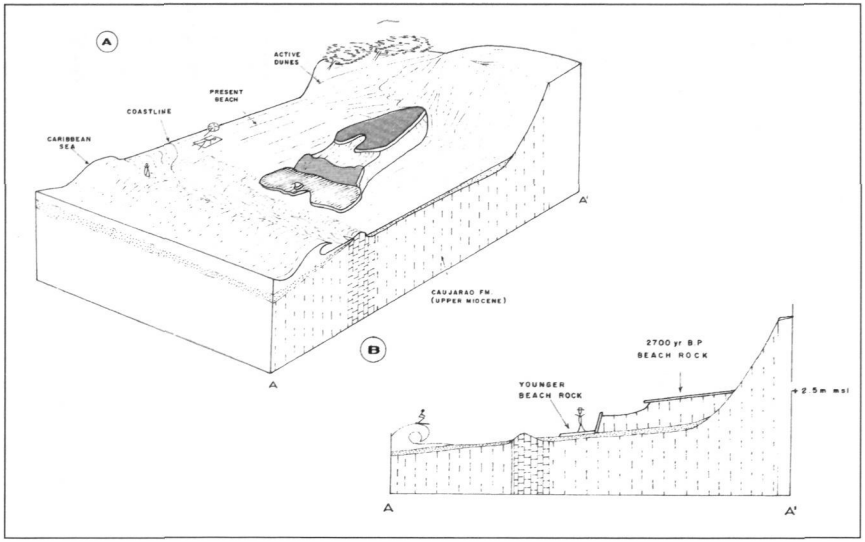

Figure 2. (**A**) Block diagram of uplifted beach-rock outcrop. (**B**) Schematic cross-section of Halocene beach-rock deposits (Audemard,1993).

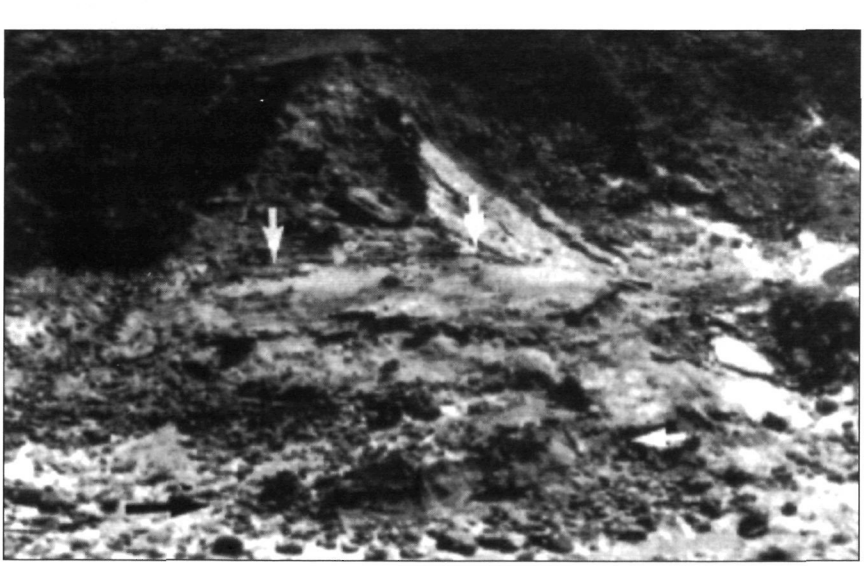

Photo 6. Bird-eye view of a patch of beach rock deposit elevated at + 2.5 m. above msl, on the beach east of El Muaco pier and north La Vela anticline.

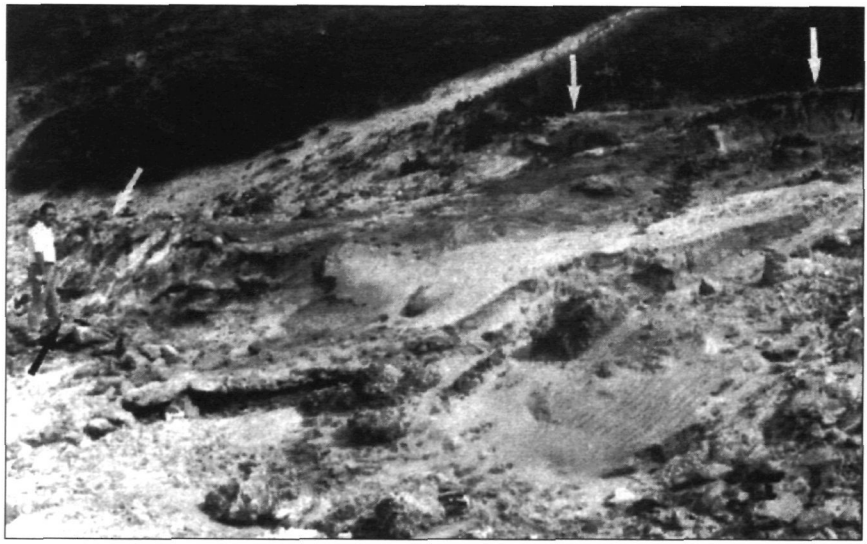

Photo 7. Ground view of an elevated beach rock located on the beach north of La Vela anticline. Its northern tip has collapsed due to wave erosion after the maximun Holocene highstand

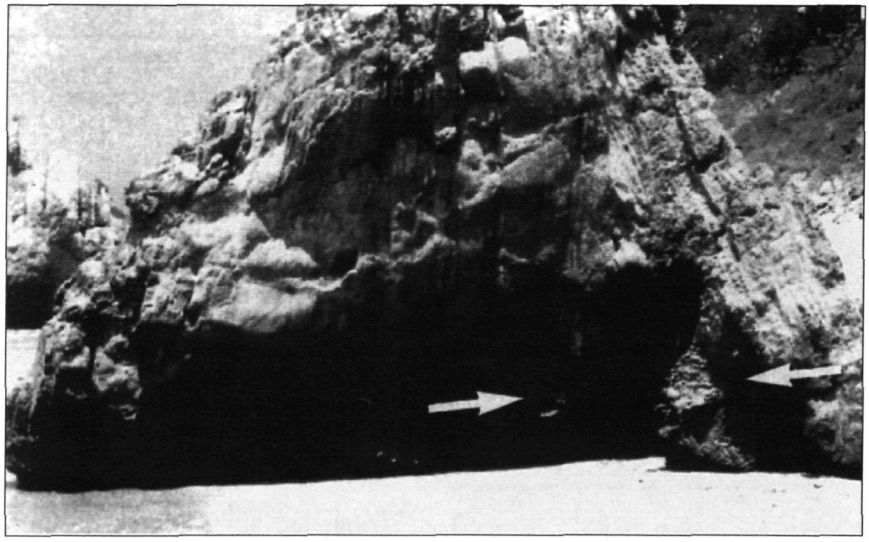

Photo 8. Slightly elevated beach-rock outcropping on the beach, west of El Muaco pier (evidence indicated by A. Singer) where the Pliocene La Vela formation is in a perfectly upright position. The beach-rock has been deposited on the sea-eroded vertical sandstones of La Vela formation.

Photo 9. Erosional benches at Sabanas Altas, northern coast of Falcón State. Two sets of benches are easily distinguishable: (1) a lower level under formation in the present intertidal zone and (2) a *c.* 1 m. elevated level correlated to the mid-Holocene highstand.

Photo 10. Erosional benches at El Pozo, between Sabanas Altas and San José de la Costa, farther east. Miocene formations of the Falcón basin at this site show two levels of marine erosion very similar to the Sabanas Altas outcrop.

Photo 11. Erosional notch at Punta Sauca, northeastern coast of Falcón State. It is obvious that this feature can not be produced by a present tidal range of about 35 cm.

Photo 12. Dead coral reef at the fishery village of San Juan de los Cayos, visible in the intertidal zone at low tide.

Photo 13. Truncated and levelled coral reef at present sea level on the beach of San Juan de los Cayos, eastern Falcón State. Its good state of preservation allows the identification of different coral species.

Photo 14. Dead *Porites* sp. corals emerged at about 0.5 m. amsl

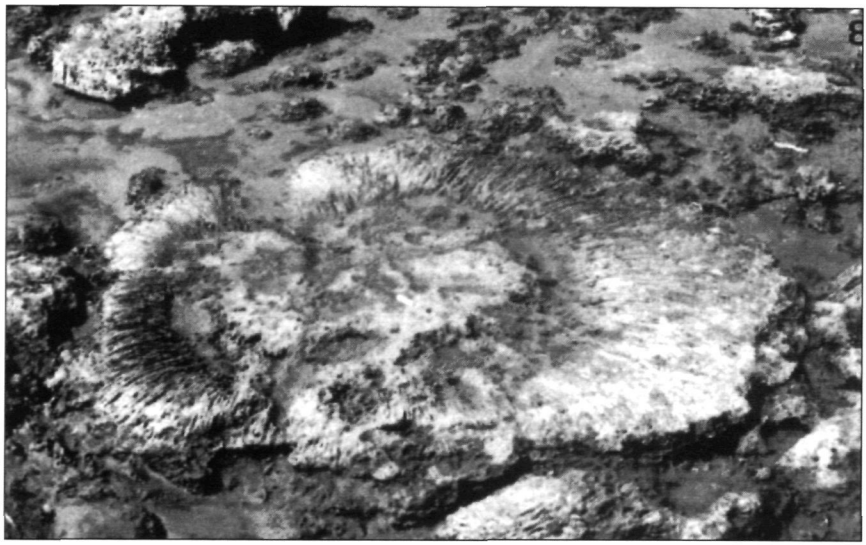

Photo 15. Truncated brain coral from the San Juan de los Cayos dead reef.

Besides, any other marine feature of the same age found on higher ground should be considered tectonically uplifted.

Neotectonic and seismo-tectonic implications

As mentioned above, the existence of the elevated beach-rock on the northern coast of La Vela anticline implies that this latter structure is being uplifted. Since the fold is genetically related to the Guadalupe thrust, this latter seems to be moving coseismically. Therefore, this is the only evidence of Holocene tectonic activity on the Guadalupe thrust up recorded to this day.

The amount of uplift undergone by the 2700 year old beach-rock can be estimated at 1.5 m. due to the upheaval of La Vela anticline. Considering a Guadalupe thrust fault plane dipping at 30° S (González de Juana, 1937), the coseismic slip can be roughly estimated at 3 m, if all the uplift happens coseismically. Such a slip is capable of generating an Ms ≈ 7.0 earthquake, based on a comparison with similar contemporary earthquakes which have occurred along reverse or thrust faults, such as the El Asnam october 10, 1980 earthquake (Ouyed *et al*, 1981; Bertero and Shah, 1983) and the Spitak December 7, 1988 earthquake (Philip *et al.*, 1992). This earthquake magnitude is in perfect agreement with the maximum credible earthquake that could be generated if the total length of the thrust fault trace (some 30 km long) broke at once.

Conclusions

The north-vergent overthrusting of the Taratara block and the associated La Vela brachy-anticline takes place along the Taima-Taima or Guadalupe thrust fault, bounded to the west and to the east respectively by the N 010° - N 015° striking, left-lateral

Carrizal fault and the NW-SE trending, right-lateral La Soledad fault. This thrust fault extends westward for some sixty kilometers from the town of Puerto Cumarebo to the village of Las Piedras, located south of Sabaneta. Its front is offsetted southward twice by left-lateral tear faults or complex zones, interpreted as transfer zones.

The tectonic activity of this thrust system can be easily established until the Early Pleistocene times, based on the two following facts: the Pliocene La Vela Formation (shallow marine deposits) is cropping out in perfect upright position NW of La Vela anticline and the Plio-Pleistocene Coro Formation is steeply tilted northward (65° N).

Nevertheless, the only evidence for a more recent activity is a small patch of beach-rock that was found at ≈ + 2.5 m above msl on the northern flank of the La Vela anticline. Unreworked tests of *Turritella sp* sampled from that deposit yielded a radiocarbon age of 2700 yr. B.P. Comparison with other marine features of the same age elevated about 1 m above msl suggests that this beach-rock deposit is uplifted, thus proving a late Holocene activity of the Guadalupe thrust, since this thrust, located north of the La Vela anticline, is responsible for the anticline formation.

If the recorded uplift (≈ 1.5 m) happens only coseismically (stick-slip), we can estimate the occurrence of Ms 7.0 earthquakes along the Guadalupe thrust. If not, less intense earthquakes are to be expected along this active tectonic feature.

Acknowledgements

We gratefully acknowledge financial support from CLIP and INTEVEP S.A. that allowed much of the field work. We also thank L. Ortlieb for the discussions held along the northern coast of eastern Falcón State, and our FUNVISIS colleague André Singer for the enlightening geomorphological discussions. Thanks also to Carlos Beltrán from the Earth Sciences Department of FUNVISIS.

References

Audemard, F.: (1993) *Néotectonique, Sismotectonique et Aléa Sismique du Nord-ouest du Vénézuéla (système de failles d'Oca-Ancón)* These Doctorat Université Montpellier II, 369 pp.

Audemard, F. and De Mena, J.: (1985) Falcón oriental, nueva interpretación estructural. *VI Cong Geol Venezolano, Caracas,* 6:2317-2329.

Baby, P., Spetch, M., Méndez, E., Guillier, B., Colleta, B. and Letouzey, J.: (1993). Development of transfer zones and location of oil and gas field in frontal part of Bolivian Andean fold-and thrust belt, *AAPG/SVG Int. Cong. and Exh., Caracas* 36 (Abstract).

Bellizia, A. (Coord.): (1971) Mapa geológico Capatárida-Paraguaná-Puerto Cumarebo-Río Tocuyo-Río Matícora, Hoja n°3. 1 :200.000, *M. M. H*

Bertero, V. and Shah, H. (Coord.): (1983) *El-Asnam, Algeria Earthquake of October 10, 1980: a Reconnaissance and Engineering Report,* Ed. Arline Leeds.

Bourrouilh-Le Jan, F.: (1993) A Mid-Holocene sea-level stand, higher than now, on the Bahamian platforms and the setting up of a hurricane regime on the North-American SE coast *2nd CLIP Meeting, Holetown, Barbados,* 7 (Abstract).

Cabrera de Molina, E.: (1985) *Evolución estructural de Falcón Central.* Tesis M.Sc., Esc. Geol. Min. y Geof., Univ. Central de Venezuela, 59p.

Calassou, S., Larroque, C. and Malavieille, J.: (1993) Transfer zones of deformation in thrust wedges: an experimental study, *Tectonophysics,* 221,3/4:325-344.

Cross, R.: (1952) Geology of North Central Falcón, *EPC10. 111 Unpubl. Co. Rpt. MARAVEN, S.A.,* 94 p.

Danielo, A.: (1976) Formes et dépots littoraux de la cote septentrionale du Vénézuéla, *Ann. Geogr.,* 85:68-97.

Fairbridge, R.: (1961) Eustatic changes in sea level *in Physics and Chemistry of Earth,* Pergamon Press, 4:99-185.

González de Juana, C.: (1937) Geología general y estratigrafía de la región de Cumarebo, estado Falcón, *Bol. Geol. y Min. (Venezuela),* 1,2-4:195-218.

González de Juana, C.: (1972) Guía de la excursión a la estructura de La Vela de Coro (Falcón), *IV Cong. Geol. Venez., Bol. Geol., Pub. Esp.* 5,1:317-327.

Kavanagh de Petzall, C.: (1959) Estudio de una sección de la Formación Caujarao en el anticlinal de La Vela, Estado Falcón. *Bol. Inf., Asoc. Venezolana Geol. Min. y Petrol.,* 2,10:269-318.

Ouyed, M., Meghraoui, M., Cisternas, A., Deschamps, A., Dorel, J., Frechet, J., Gaulon, R., Hatzfeld, D. and Philip H.: (1981) Seismotectonics of the El Asnam earthquake, *Nature* 292,5818:26-31.

Philip, H., Rogozhin, E., Cisternas, A., Bousquet, J.-C., Borisov, B. and Karakhanian, A.: (1992) The Armenian earthquake of 1988 December 7: faulting and folding, neotectonics and palaeoseismicity, *Geophys. J. Int.,* 110:141-158.

Rohr, K.: (1945) Morphological notes on the coastline between Boca de Gueque and La Vela, western Falcón, *Unpbl. Rpt. M M H., Caracas.*

Smith, F.: (1962) Mapa geológico-tectónico del Norte de Venezuela. I *Cong. Venezolano del Petról., Caracas.*

Tahal.: (1969) Mapa geológico región de Coro; Instituto Nacional de Obras sanitarias (INOS) *in Desarrollo de los Recursos de Aguas Subterráneas en las regiones de Valencia, Barquisimeto, Coro, Pedregal y Maracaibo.*

Wiedenmayer, C.: (1937) Informe geológico sobre los depósitos carboníferos de Coro,Distrito Miranda, Estado Falcón, *Bol. Geol. yMin. (Venezuela),* 1,1:1-65.

RECENT QUATERNARY SEDIMENTARY AND CLIMATIC CHANGES IN THE SALOUM DELTA (SENEGAL)

M. Bâ[1], J.-P. Barusseau[2], C. Descamps[2], and B. Diouf[1]

1 Université C.A.Diop, Département de Géologie, Dakar-Fann, Sénégal.
2 Laboratoire de Géochimie et Sédimentologie marine, Université, 66860 Perpignan Cedex, France.

Abstract

The Senegalese coast was modified by several transgressions during the recent Quaternary. The most important one, which determined the present-day landscape, is the Nouakchottian (7000-4000 y B.P.). However, sea level did not change significantly during the last 6000 years in the Saloum delta (southern coast of Senegal). The morphological and sedimentological changes observed in the late Holocene sequences were apparently induced by a constraining climabc background.

During the maximum of the Nouakchottian transgression (5500 B.P.) embayments formed. Towards 4000 B.P., the longshore drift induced the formation of beach barriers in the Saloum delta, which deposited an extensive thick green mud (dated 6130 to 3500 B.P.), and which deviated the Saloum river southwards.

Climatic changes modified the barriers development:

-phases of aridity corresponded to aeolian transport of silt and sand. These sediments were trapped behind the barriers,

-exceptional swells induced the breakage of the sand spits. The mouth was deplaced northwards, the beach barrier integrated the deltaic plain and the longshore drift constructed a new barrier to the front

The evoluhon of the present beach of the Sangomar spit and the formation of the fossil barriers in the Saloum delta are currently studied, in order to reconstitute the climatic and sedimentary changes during the late Quaternary. Alternation of north swell / south swell patterns and the modification of the fossil beach barriers are possibly correlated.

Introduction

In northwestern Africa, the Mauritanian coast is a key area in terms of regional marine evolution. The Holocene transgressive phase called «Nouakchottian» has been defined there by Elouard, (1968). Relative sea level curves have been proposed (Fig. 1; Einsele *et al.*,1974 a,b; Elouard *et al* 1977). The most recent one was proposed by Barusseau et *al.* (1989). According to those authors, the eustatic factor along the coasts of Mauritania and Senegal is often considerably overemphasized.

In the Saloum delta (Fig. 2), a negative oscillation seems certain during one millenium after the Nouackchottian maximum. The following sea level changes depended on the morpho-sedimentological evolution induced by climatic changes.

The aim of this paper is to describe the sedimentary and climatic evolution of the Saloum delta since the Nouakchottian transgression and to endeavour to reconstitute the climate from the study of the sand barriers formation.

The evolution of the Saloum delta during the Upper Quaternary

A diagram (Fig. 3) has been proposed by Ausseil-Badié *et al.* (1991): during the first phase, at around 5500 years B.P., the Saloum was an elongated gulf (estuarian phase). A second phase is the formation of sand barriers. It was shown that the sand barriers were formed by the littoral drift, although these barriers divide into a southern part (extending from the northern coast of the Gambia river mouth to the Diomboss river), and a northern part, strongly disturbed and almost obliterated by shifts of the Saloum river. Breaching of beach barriers induced a migration of the mouth of the Saloum river northwards, and an integration of the beach barriers into the deltaic plain. The Sangomar spit, in the Saloum delta, is the modern equivalent of these barriers.

On this diagram, only the second episode is dated, although some sand spits probably formed before. The most recent barriers were constructed during an episode of very dry climate, with strong changes in the hydrologic regime and the formation of a reverse estuary. In fact, during the late Holocene, the climate was more and more arid, but this arid climate was interrupted by wetter periods (2900-2500, 1200-750 years B.P.) and other not well defined periods.

Anyhow, it seems that the beach barriers have a uniform basement at the same level, thus without any eustatic variations.

The third stage is the deltaic formation. At the same time, silt and sand were transported by the wind and trapped behind the barriers. The fourth stage is approximately the same than the present-day one.

The swell action on the evolution of the Sangomar spit

The evolution of the Saloum delta is currently studied from the action of the swell on the erosion and the sedimentation of the Sangomar sand spit.

The spit extends about 20 km southwards: It extension in the twentieth century is about 60 m/y (Fig. 4). This sand spit was cut in 1987 due to a strong north-western swell. The breach is now 3,6 km long.

Our study has emphasized the relationship between the swell and the evolution of the spit (swell data from Meteo-France).

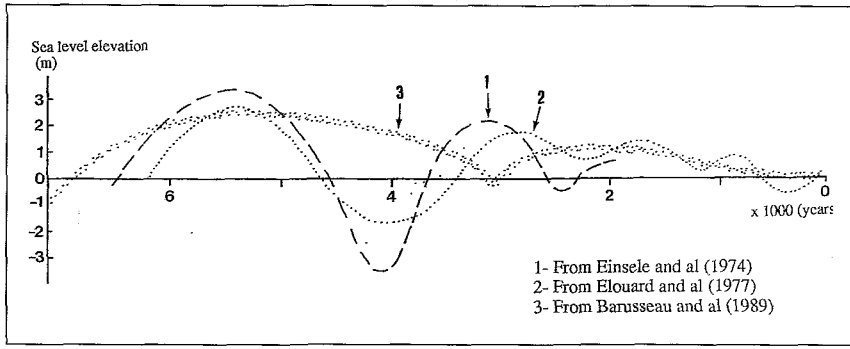

Figure 1. Proposed sea level curves for the last part of de Holocene (from Barusseau *et al.*, 1989).

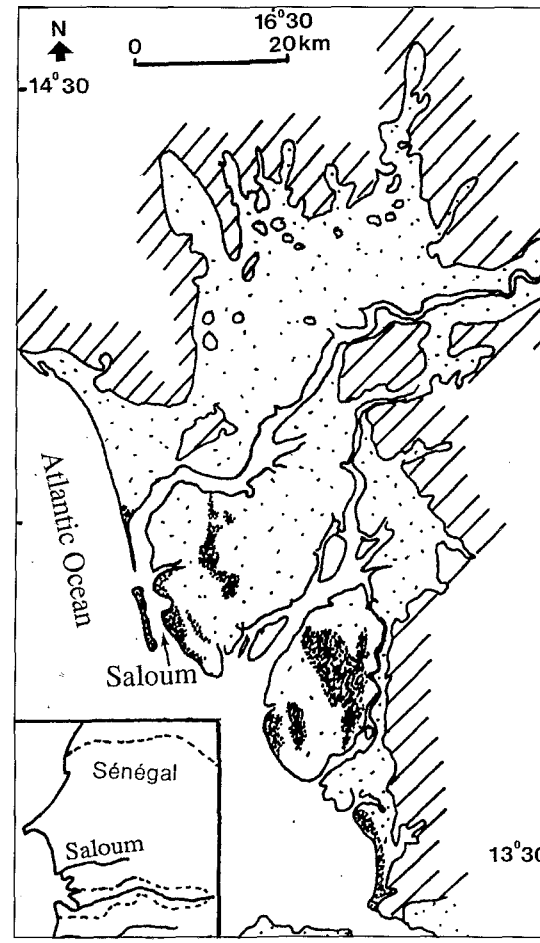

Figure 2. Location map of the Saloum delta.

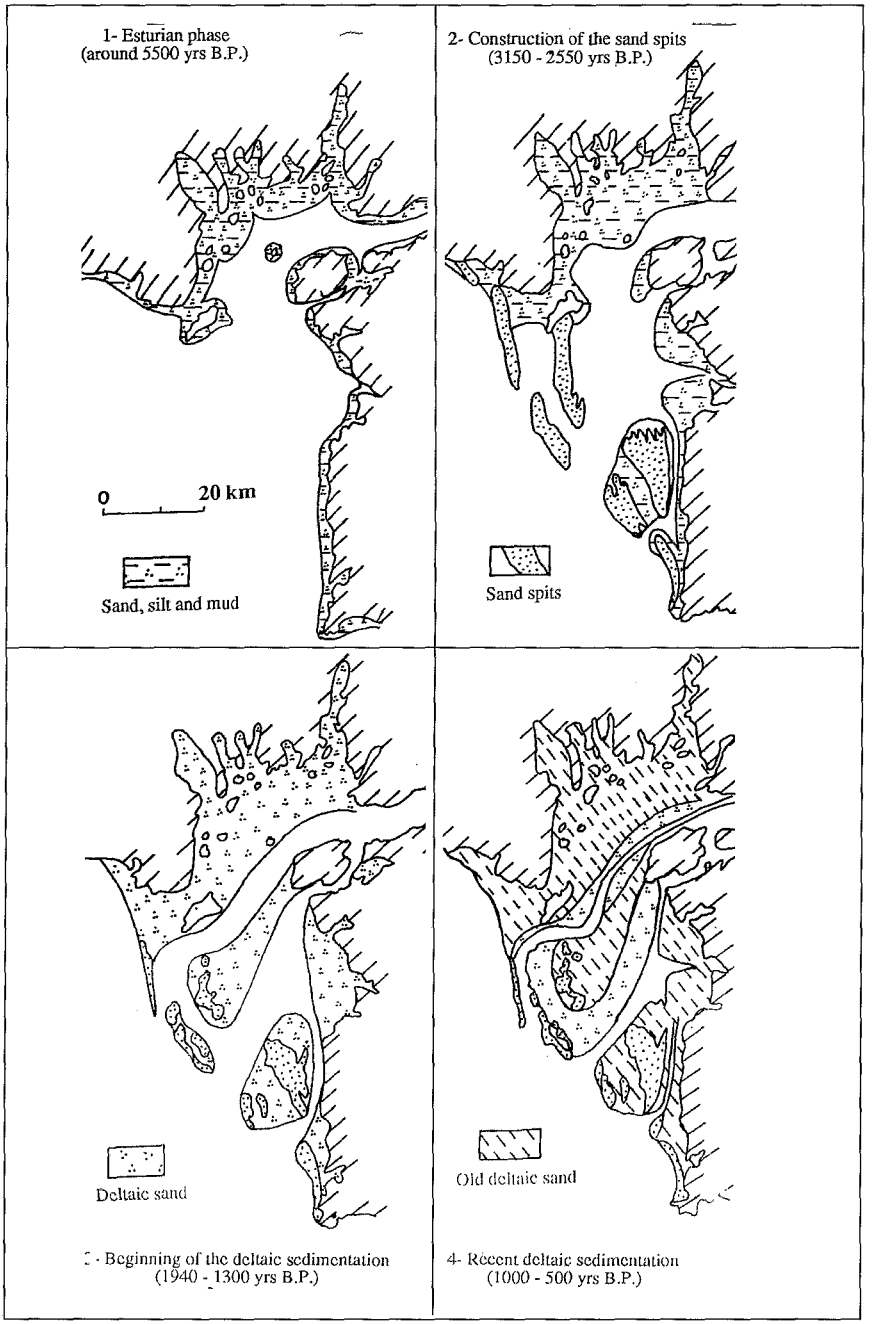

Figure 3. The evolution of the Saloum delta since 6,000 years (from Ausseil-Badié *et al.*, 1989)

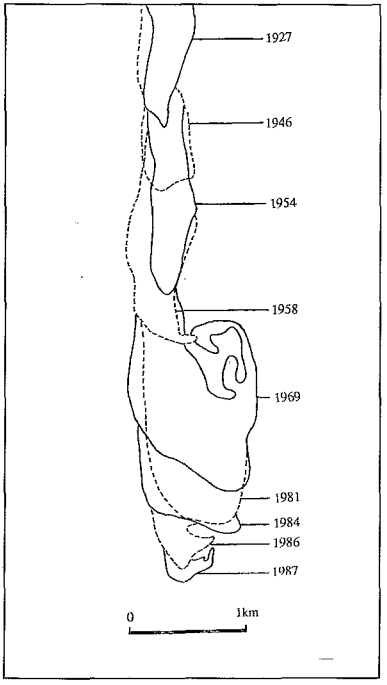

Figure 4. Morphological changes of the tip of the Sangomar spit betwen 1927 and 1987 (from Diaw *et al.*, 1991, modified).

During the dry season (from November to June) we observe only a north-north-west swell along the coast (Fig. 5) and a longshore drift from north to south. During the rainy season (from July to October), a northern swell and a southern swell alternate (Fig. 6). The swell is not the same along the coast: to the north it appears all the year round from the north. The swell from the south is rare (less than 10%) and there is no problem of erosion. On the contrary, to the south, during the rainy season, the same probability exists to get a north-western swell or a south-western swell.

We have plotted the shoreline of the Sangomar spit since 1991 (Fig. 7). The spit, to the north of the breach, is eroded during the dry season along the seaside between December and February. During the rainy season, there is an important erosion northwards to the north of the breach, when northern and southern swells alternate.

Discussion

The direction of the swell depends on the position of the Intertropical Zone of Convergence. This «line» moves during the year along the Senegalese coast, northwards during the rainy season, southwards during the dry season. It is possible that the position of the ITCZ changed during the Holocene for longer periods than a year, the longshore drift thus forming beach barriers from north to south, in the north of the delta, when the ITCZ was more to the south (arid climate). In the south beach barriers have been formed by a likely longshore drift from the south to the north, when the ITCZ was reaching further north (more humid climate). The present progression speed of these barriers shows that a few years are sufficient to build them (100 to 500 years).

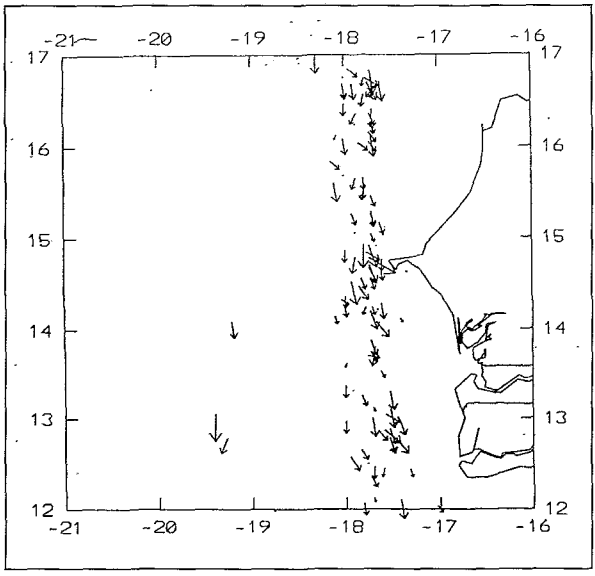

Figure 5. Direction and height of the swell (February 1987).

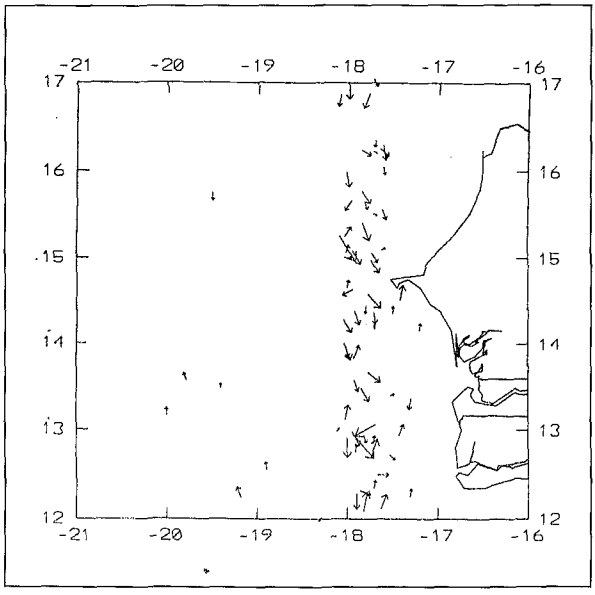

Figure 6. Direction and height of the swell (August 1992).

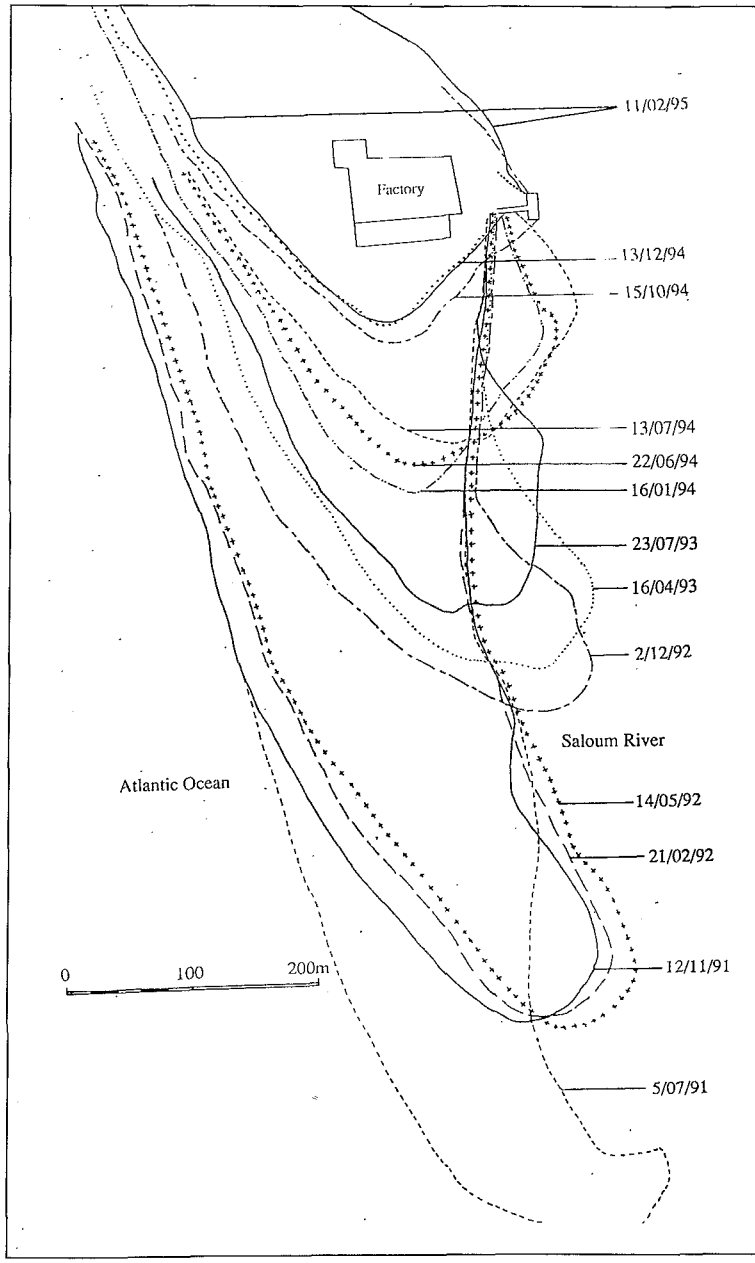

Figure 7. Shoreline evolution to the north of the breach (Sangomar spit).

The extension of a sand spit, to the north of the Senegalese coast, was shown to be 500 m/year and 60 m/year in the south (Barusseau et al.,1995). If the ITCZ had approximately the same reach during 100 years. In the late Quaternary, a beach barrier could be built.

It is possible, according to the position of the ITCZ and its mobility along the Senegalese coast, that all the sand barriers have not been formed only by the longshore drift from the north but by alternate wet and arid episodes. A more complete study of the sand barriers could provide information on those Holocene variations.

References

Ausseil-Badié, J., Barusseau, J.P., Descamps, C., Diop, S., Giresse, P. and Pazdur, M.:(1991). Holocene deltaic sequence in the Saloum estuary, Senegal. *Quaternary Research,* 36:178-194.

Barusseau, J.P., Descamps, C., Giresse, P., Monteillet, J. and Pazdur, M.: (1989). Nouvelle définition des niveaux marins le long de la cote nord-mauritanienne (Sud du Banc d'Arguin) pendant les cinq derniers millénaires. *C R Acad Sci Paris,* t. 309, Série II: 1019-1024.

Barusseau, J.P., Ba, M., Descamps, C., Diop, S., Giresse, P. and Saos, J.L.: (1995). *Coastal evolution in Senegal and Mauritania at 103 102, and 101 year scales: natural and human records. Quaternary International, 27.*

Diaw, A.T., Diop, S., Thiam, M.D., and Thomas, Y.F: (1991). Remote sensing of spit development: a case study of Sangomar spit, Senegal. Z. *Geomorph NF Berlin,* Suppl. 81: 115-124.

Einsele, G., Herm, D., and Schwarz, H.U.: (1974 a). Holocene eustatic (?) sea level fluctuation at the coast of Mauritania. «*Meteor*» *Forschung-Ergebnisse C,* 18:43-62.

Einsele, G., Herm, D., and Schwarz, H.U.: (1974 b). Sea level fluctuation during the *past 6000 years at the coast of Mauritania. Quaternary Research* 4:282-289.

Elouard, P., Faure, H., and Hébrard, L.: (1977). Variation du niveau de la mer au cours des 15000 derniéres années autour de la presqu'lle de Cap-Vert, Dakar, Sénégal. *Bull ASEQUA,* 50:29-49.

Elouard, P.: (1968). Le Nouakchottien, étage du Quaternaire de Mauritanie, *Annales de la Faculté des Sciences, Dakar,* (2):121-138.

GEOCHRONOLOGICAL FRAMEWORK FOR THE QUATERNARY PALEOCLIMATIC RECORD OF THE ROSA NEGRA SECTION. (FUERTEVENTURA-CANARY ISLANDS, SPAIN)

N.Bouab and M. Lamothe

GEOTERAP- Département des Sciences de la Terre. Université du Québec à Montréal. C.P. 8888, Succ. "Centre Ville" Montréal, H3C 3P8.- Canada.

Abstract

The Rosa Negra sedimentary sequence was dated by optically stimulated luminescence, using infrared stimulation of potassic feldspars (IRSL). The preliminary results for three samples are 181 ± 27 ka, 183 ± 27 ka and 318 ± 45 ka.

Introduction

This geochronological study was performed upon the Rosa Negra sedimentary sequence which exhibit a series of four paleosols in the Eastern Canary Islands (Fuerteventura). The sedimentological and paleontological aspects of this section are under study by Damnati, Meco and Petit-Maire. The chronological methodology is the luminescence dating method, using infrared stimulation of potassic feldspars (IRSL). The ages obtained should correspond to the time elapsed since the sediment was last exposed to sunlight, the *Age (ka) is Paleodose* (Gy)*/ dose-rate* (Gy. *ka-1)* The preparation of the samples for luminescence dating was already summarized elswhere (CLIP report 1993). Generally, the IRLS method is applied to potassic feldspars with a grain size of about 100-200 μm. On this volcanic island, the bedrock is essentially volcanic. However, the eolian sands are mostly constituted by detrital biogenic carbonate fragments (bioclasts) originating from the coastal environment. A minute component is of minerals eroded from the local volcanic rocks. Quartz and feldspars were extracted from a somewhat smaller grain size fraction (45-90 μm) than the one generally used, since none were found in sufficient abundance for measurements in the 100-200 μm range. These silt-sized grains are presumed to be carried from the Sahara by wind.

Measurement of the paleodose:

For each sample, several aliquots are separated. Each natural aliquot is exposed to a very short optical stimulation, which is called a short shine (SS_0), for normalization. Then, some aliquots are irradiated with increasing gamma doses. After a preheat of 160°C for 3 to 9 hours, which is necessary to remove the unstable luminescent signal, a growth curve is built up in order to determine the paleodose (*cf.* CLIP Report 1993, p. 17). For homogeneous samples like those of the Tah section in Morocco (Bouab and Lamothe, 1994) this growth curve shows a very high reproductibility between the aliquots (Fig. 1). Unfortunately, the samples from the Rosa Negra section in Fuerteventura have a much lower reproductibility. This may result from undetected sensitivity changes in luminescence upon preheat. The luminescent response to the short shine was used to normalize each point of the curve. In some cases, this normalization was unsuccessful (Fig. 2). We tried to normalize with a method known as «second glow normalisation» (SS_1). In this method, the luminescent signal is completely removed by light («bleached») and an equal beta or gamma radiation dose is given to all the aliquots. They should have the same relative luminescent signal as SS_0. The fact that in several cases SS_0 was different from SS_1 suggests that there is a problem of change of sensitivity during preheat and/or bleaching (Fig. 3). All the aliquots that showed a variation of their sensitivity during preheat were then removed from the analyses and the remaining aliquots only have been used for the growth curve.

Measurements of the dose-rate:

The second part of the age equation, the dose-rate or the «annual dose», is determined with the measurement of the contents of natural radioactive elements in the environment (Table 1). In this volcanic environment, the annual alpha, beta and gamma doses are very low. The environmental dose was determined directly in the field with a gamma spectrometer, and indirectly by neutron activation analyses in the laboratory, and alpha counting. Direct and indirect measurements yielded equivalent results for the doserate. For potassic feldspars, there is a significant beta contribution from the internal potassium. In the case of the Rosa Negra section, we cannot yet establish this internal dose for the grains, since the yield of material is very low. The analyses will be performed on the grains that were used for IRSL. This internal beta dose was estimated at 0.11 Gy/ka. The total annual dose is low, around 1Gy/ka.

Preliminary IRSL ages:

For three samples of the Rosa Negra section (Fig. 4 and Photo 1), we have the following preliminary results:

RND4: Age= 181 ± 27 ka.
RNC3: Age= 183 ± 27 ka.
RNB1: Age= 318 ± 45 ka.

The ^{14}C ages of gastropods extracted from paleosols of this section are ≥ 33.8 ka, ≥ 33.8 ka, 28.4 ka and 32.5 ka BP (Meco *et al;* this volume). It is common for luminescence ages to be overestimated, such as in the case of sediments which are badly zeroed

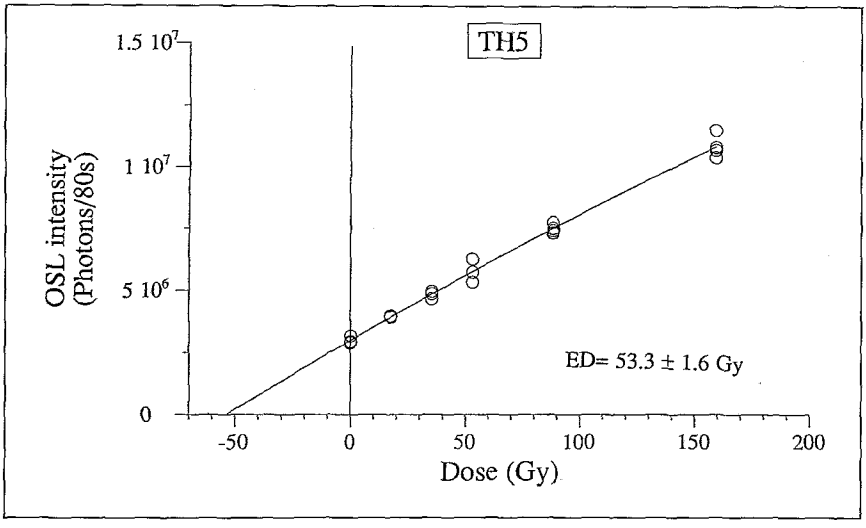

Figure 1. Growth curve showing good reproductibility. Sample extracted from the Tah section (TH5).

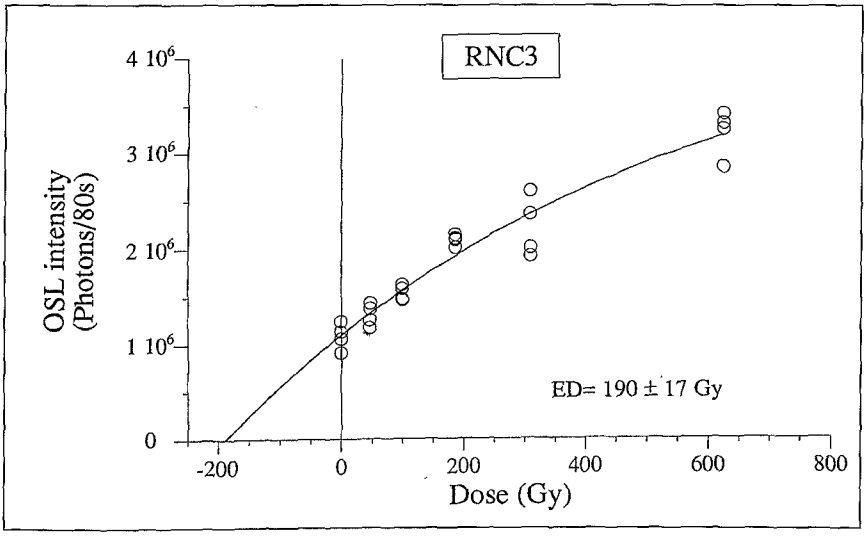

Figure 2. Growth curve showing poor reproductibility even after natural normalization (i.e. SS_O). Sample extracted from the Rosa Negra section (RNC3).

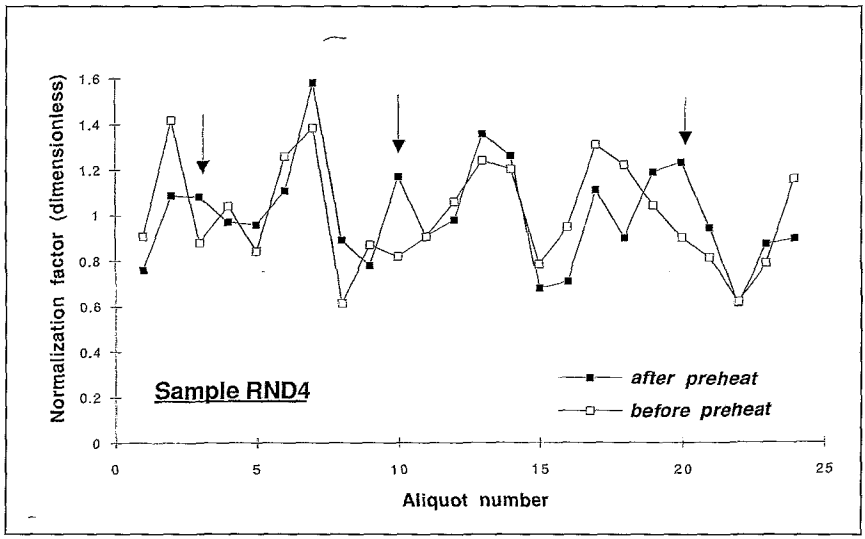

Figure 3. Normalization factors of each aliquot before and after preheat and measurements. The arrows show examples of aliquots that exhibit a change of sensitivity (Sample RND4).

Samples (ppm)	U (ppm)	Th (ppm)	K %	Water content in situ (%)	Water content saturation (%)	Water content average (%)	Dose-rate (Gy/ka)
RNB1	1.4±0.1	1.5±0.1	0.34±0.01	14	36.6	19.65	1.05±0.1
RNC3	1.6±0.2	1.9±0.01	0.44±0.01	17.3	41.4	23.4	1.02±0.1
RND4	1.9±0.2	1.4±0.1	0.34±0.01	9.4	46.8	18.75	1.02±0.1

Table 1. Dose-rate data.

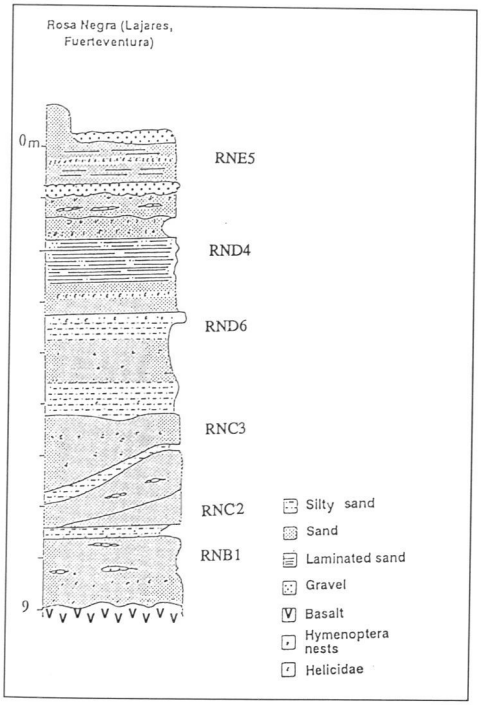

Figure 4. The Rosa Negra section (modified from Damnati *et. al.*, 1996). The letters correspond to the luminescence samples (e.g. RNB1).

during their transport. In this eolian and much insulated environments, this is very unlikely and zeroing is confidently assumed. It could be concluded that these sediments were fossilized at Rosa Negra much earlier than presumed. It must be emphasized that the assessment of the dose-rates is still in progress and the ages presented above are based on several assumptions that are now being tested in the laboratory.

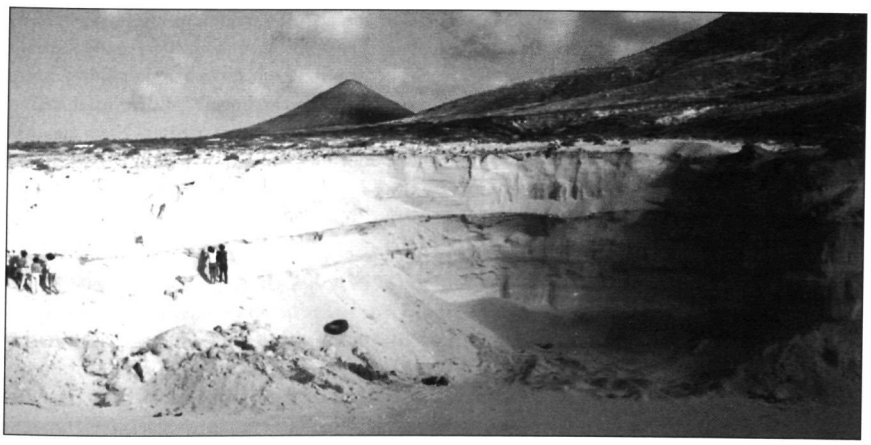

Photo 1. Paleosols interbedded into the dunes. Rosa Negra quarry (Fuerteventura).

References

Bouab, N. and Lamothe, M.: (1993) Optical dating of eolian sediments from the Western Sahara and Eastern Canary Islands: a 1993 progress report. *UNESCO-IUGS-EPGC-CLIP Report 1993,* 16-17.

Bouab, N. and Lamothe, M.: (1994) Optical dating of eolian sediments from the Western Sahara: 1993 progress report *UNESCO-IUGS-EPGC-CLIP Report 1994,* 28.

Damnati, B., Petit-Maire, N., Fontugne, M., Meco, J. and Williamson, D.: (1996) Quaternary Paleoclimates in the Eastern Canary Islands, *Quaternary International,* 31:37-46.

PEDOGENESIS AND PALEOCLIMATIC IMPLICATIONS OF LATE PLEISTOCENE PALEOSOLS IN THE YANGTZE DELTA (CHINA)

Q. Chen and C.X. Li

Department of Marine Geology and Geophysics, Tongji University, Shanghai, 200092, P.R. China

Abstract

The paleosol dated 15,000 - 25,000 yr B.P., with a burial depth of 3-28 m, is a major soil stratigraphic unit occurring across a large portion of the Yangtze Delta. The late Pleistocene paleosol possesses a sharp boundary with overlying Holocene marine deposits; it gradually turns into underlying strata. Plant roots and debris, cracks filled with clays are found in the paleosol, and distinct paleosol features have been revealed by micromorphological examinations. Sporopollen and phytolith analyses suggest that a colder and drier climate than at present predominated during the paleosol formation. Contents of CaO are compared between the late Pleistocene paleosol, yellow brown earth developed from Xiashu loess and yellow mian soil developed from loess of northwestern China. The results suggest that, during the paleosol formation, the mean annual precipitation was about 500 - 800 mm. The wet and dry seasons were distinct, the groundwater level altered greatly, the winter monsoon was stronger than present, and the summer monsoon was intense.

Introduction

Recent studies (Li *et al.*, 1991,1992) demonstrate that the terrestrial stratum, common in the late Pleistocene strata of the Yangtze Delta, is a paleosol. Paleosols possesses great importance in the studies on stratigraphic division and correlation and on land-ocean interaction of the late Quaternary in the Yangtze Delta. The paleosol formed on the past landscape contains information of its forming factors, including climate, vegetation, landscape, parent material and time. It is superior to strata, fossils and other single indicators in the paleoclimatic reconstruction. Therefore, the late Pleistocene

paleosol in the Yangtze Delta is an ideal material for the study of paleoclimates. In this paper, paleoclimatic data are inferred based on paleosol data from more than ten cores in the Yangtze Delta.

Distribution and stratohorizon of the paleosol

The late Pleistocene paleosol is preserved on the northern and southern flanks of the Yangtze Delta. The paleosol, 3 -28 meters deep, is shallow in the west and deep in the east. It slopes from west to east, although its burial depth locally changes. In the western part of the Delta, the thickness of the paleosol averages 7.2m, with maximum of 9.0 m, and the paleosol turns thinner in the eastern part, the mean thickness in Shanghai district is 2.9 m, with a maximum of 5.7 m (Li *et al.*, 1996). The upper part of the paleosol is grayish olive (7.5Y 4/2), and gradually turns downwards to yellowish brown (10YR 5/6), light yellow orange (10YR 8/4). The paleosol possesses a sharp boundary with the overlying Holocene mud sediment of littoral and neritic facies (East), or limnetic facies (West). It gradually turns into underlying grayish yellow littoral or fluvial silt and sandy clay (Fig. 1 and 2).

Characteristics of the paleosol

The paleosol from the Yangtze Delta contains distinct soil features which indicate a long period of subaerial exposure and pedogenesis.

Argillans

One of the most convincing indicators of soil formation is provided by the build-up of clay as coatings and, in particular, as void linings (Fenwick, 1985). Argillans are common in the paleosol of the Yangtze Delta, and occur mainly as coatings of peds and crack linings. Multiple-layered argillans, which can be found in the dendritic cracks, are the result of long period eluviation and illuviation. The argillans exhibit waxy luster on the natural sections of the paleosol, and most of such sections are slickensides. Argillans are brown yellow color, which indicates the translocation of ferrugineous materials.

Cracks

Cracks in the paleosols, 2 - 20 cm long and 3 - 10 mm wide, are vertical and wedge out downwards. They are filled with gray clay, which contrasts sharply with the yellow orange matrix. Microcracks, 30 - 50 μm wide, are filled by brownish yellow cutans. Craks resulted from the desiccation during subaerial exposure, and the inner fillings indicate clay translocation during wet seasons.

Peds

2 - 7 mm grained peds are clear in the middle part of the paleosol and turn obscure upwards or downwards. They are divided by cutan - filled cracks, and the micropeds are also distributed commonly between microcracks and pores.

Plant roots and debris

Plant roots and debris are commonly concentrated in the upper part of the paleosol. Roots are vertical, some of them coated with calcareous materials form long calcareous nodules. Others appear to be long, ferrugineous nodules. The nodules are 1 -2 cm in

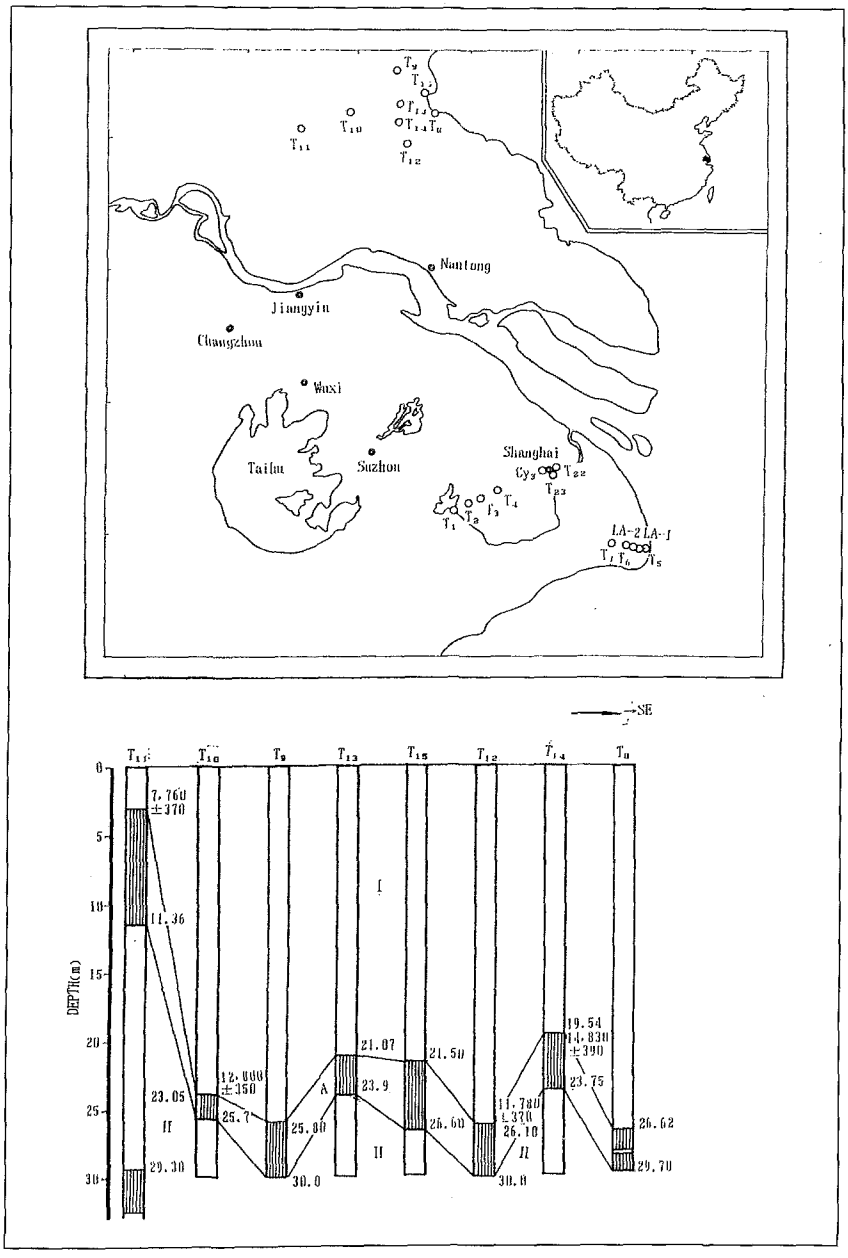

Figure 1. Location of Drilling cores (up), and section in the northern flank of the Yangtze Delta (down) A. First palaeosol horizon, B. second palaeosol horizon, I. First marine stratum (including fresh water marsh deposits in the West), II. Second marine stratum.

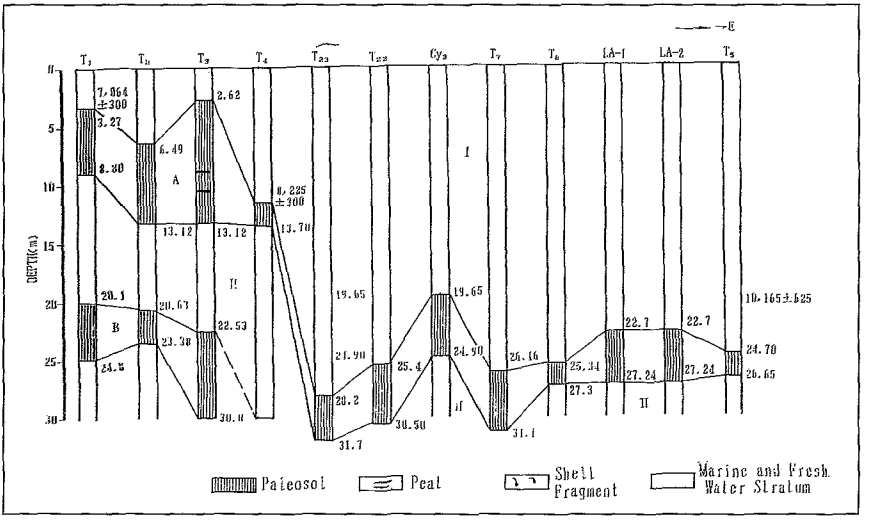

Figure 2. Section in the southern flank of the Yangtze Delta. (See Figure 1 for indication of A, B, I, and II).

diameter, 20 -30 cm long, with a maximum of 50 cm. Plant debris, usually 2 -4 mm long, cover 50% in the coarse-fraction (>0.063 mm) of the paleosol, and most of them are carbonized. The coincident occurrence of plant roots and debris suggests plant debris come from plants *in situ*. This suggests that herbaceous plants were flourishing during the paleosol formation. Besides, the paleosol contains abundant phytoliths (more than 200 - 300 grains in each 40 g sample: Liu *et al.*, 1995), the herbaceous ones predominate. Therefore, the plants indicated a herbaceous environment in the Yangtze Delta during the paleosol formation.

Ferrugineous and manganous nodules

Nodules are small (< 1 mm) and rare in the upper part of the paleosol, most of them are round siderite and rhodochrosite, the content of which decreases downwards. The contents of limonite and hematite are high in the middle part of the paleosol, and decrease upwards and downwards. The content of pyrolusite increases downwards, and almost all the nodules are pyrolusite at the lower part of the paleosol. The distribution of the nodules in the paleosol suggests that the conditions changed from reduction to oxydation downwards, and Fe^{2+}, Mn^{2+} have translocated vertically.

Therefore, the paleosols in the Yangze Delta have experienced distinct pedogenesis. They are a key record of climatic conditions during the late Pleistocene, for which little depositional record exists.

Paleoclimatic implications of the paleosol

Temperature

Phytolith analysis shows that the herbal vegetation predominated during the paleosol formation (Fig. 3). There are Elong, Point, Pipe shape, Spine shape, Fest, Cube Sphere plant opals, originated from *Gramineae* and *Chenopodiaceae* vegetated in relatively colder and drier environments of northern China, which cover a large percentage in the phytolith

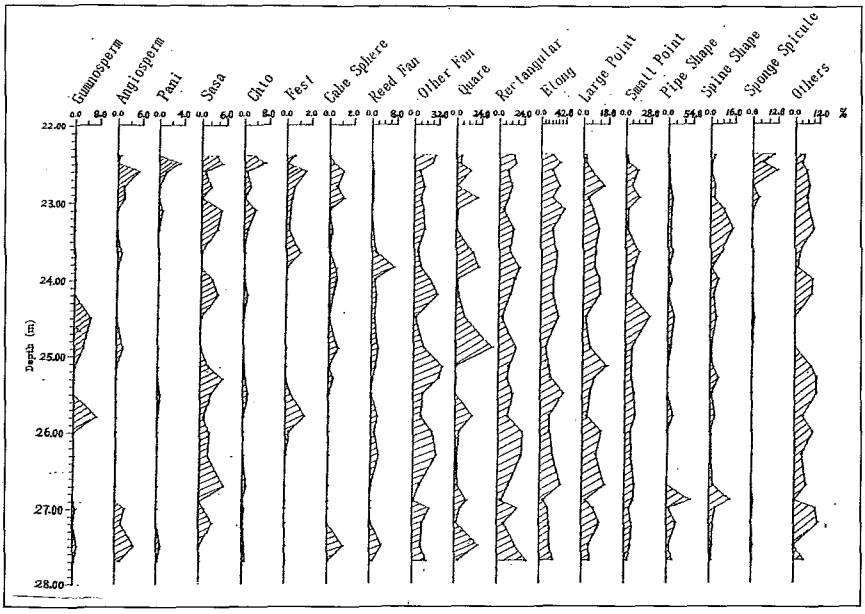

Figure 3. Phytolith spectrum of LA-1 core in the Yangtze Delta.

assemblage of the paleosols. The climate of the late Pleistocene in the Yangtze Delta was colder and drier than at present and was similar to the one in the temperate climate zone in northern China. A sporopollen study suggests that during the paleosol formation, the temperature was 6 - 8.4 degrees centigrade lower than at present. The climate was cold and dry (Wang *et al.*, 1984), which coincides with the result of phytolith analysis. However, the paleosols also contain some layers with a large percentage of Chlo, Pan, Sasa, Fan plant opals, which originated from *Gramineae* vegetated in the subtropical zones of southern China. It is inferred that a warm and humid climate existed during some periods of the paleosol formation, which can also be indicated by the argillans filling the cracks.

Precipitation

CaO content of soil and precipitation

A yellow brown soil developed from Xiashu loess in Nanjing district and a yellow mian soil originated from the loess of northwestern China have similar parent materials (Wu, 1985; Xiong *et al., 1990).* Although both of them have formation durations of about 10,000 yrs., their CaO contents are different. The average CaO content of the yellow brown soil is 0.96%, and that of the yellow mian soil is 7.43% (Xiong *et al.*, 1990). The mean annual precipitation at Lanzhou, where the typical yellow mian soil develops, is about 330 mm. At Nanjing, where yellow brown soil occurs, it is more than 1,000 mm (Hou *et al.*, 1985). The differences in CaO content between the soils with similar parent material and formation durations mainly result from precipitation of the two regions.

Loess, with longer exposure durations, possess higher CaO contents than paleosols in Louchuan sections in the Shaanxi Province of China. For example, the forming

durations of L1 and S1 are 60,000 - 85,000 yrs., and 45,000 - 70,000 yrs., respectively. However, the mean CaO content of L1 is 7.72%, and that of S1 is only 1.71% (initial data after Liu *et* al.,1985). This results from the warmer and wetter climate during the pedogenesis.

According to the above analyses, it is inferred that the leaching rate of CaO content ($1 - CaO_{soil} / CaO_{parent\ material}$) can be applied to the correlation of eluviation degrees between soils with similar forming durations, and different parent materials, and such correlation can further indicates the difference of mean annual precipitation between various regions.

Deduction of precipitation

A recent study shows that the parent materials of the paleosols in the Yangtze Delta are flood plain deposits (Li *et al.*, 1996; Chen *et al.*, 1996a). Using the mean CaO content of flood plain deposits of the modern Yangtze River (about 4.1%), it is calculated that the leaching rate of CaO is 82.92% for the paleosol. However, the rate of yellow mian soil, whose forming duration is similar to the paleosol, is 3.75% (initial data after Liu *et al.*, 1985; Xiong *et al., 1990).* Thus, the mean annual precipitation of the Yangtze Delta during the paleosol formation was more than that of Lanzhou (about 330 mm) where a typical yellow mian soil exists. The leaching rate of CaO in the yellow brown soil in Nanjing, where mean annual precipitation is more than 1,000 mm, is 87.88% (initial data after Liu, *et al.*, 1985; Xiong *et al., 1990),* slightly higher than that of the paleosol in the Yangtze Delta. The low relief of the flood plain during the paleosol formation in the Yangtze Delta (Li *et al.*, 1986; Chen *et* al.,1996b) is favourable to the leaching out of CaO. The high leaching rate in CaO of the paleosol is partially due to the high water content of the wetlands. It can be inferred that the mean annual precipitation during the paleosol formation was lower than that of Nanjing. Therefore, the mean annual precipitation of the Yangtze Delta may have been 500 - 800 mm during the paleosol formation.

Seasonal variability

The high leaching rate of CaO, the ferrugineous concretions and the distribution of pyrolusite at the lower part of the paleosol suggest that the grounwater level greatly fluctuated during the paleosol formation (Chen *et al.*, 1996b), which indicates that wet and dry seasons sharply contrasted, winter and summer monsoons being both active. Based on the above inference that the climate was colder and drier than at present, the winter monsoon was stronger. Although the precipitation was lower than nowadays, the wet and dry seasons were distinct, and the summer monsoon was of high intensity during the paleosol formation.

Conclusions

The late Pleistocene paleosols in the Yangtze Delta had experienced distinct pedogenesis, and are the ideal tools for paleoclimatic reconstruction. Phytolith and sporopollen analyses suggest that, during the paleosol formation, the climate was cold and dry, and the temperature was lower than at present. There also existed some warm and humid episodes. The annual precipitation was about 500 - 800 mm, wet and dry seasons were distinct, winter monsoon (northwestern wind) was stronger than at present, and the summer monsoon (southeastern wind) was also of a certain intensity.

Acknowledgements

This study was supported by the National Natural Science Foundation of China. We are very grateful to Li Ping and Sun Heping for assisting in the laboratory work and providing valuable ideas during the study.

References

Chen, Q.Q. and Li, C.X.: (1996a) Preliminary study on late Quaternary paleosols and paleoenvironments of the Yangtze Delta, *Acta Sedimentologica Sinica, 13 (supp.): 79-87. (in* Chinese).
Chen, Q.Q., Sun, H.P. and Li, C.X. : (1996b) The late Quaternary paleosols and sea level fluctuation in the Shanghai area, *Tongji University Jour., 24,1: 33-37.* (in Chinese).
Fenwick, I.: (1985) Paleosols: Problems of recognition and interpretation *In* J. Boardman (ed.) *Soils and Quaternary Landscape evolution,* John Wiley and Sons. New York,: 3-21.
Hou, R.Z.: (1985) *Comprehensive Atlas of China,* China map press, Beijing, 190.
Li C.X., Min Q.B. and Sun H.P. (1986). Holocene strata and transgression at the southern flank of the Yangtze River Delta, *Science Bulletin,* 21:1650-1653. (in Chinese).
Li, C.X., Chen, Q.Q., Li, P. and Cong, Y.Z.: (1996) The late Quaternary paleosols and their parent materials in the Yangtze Delta area, *Tongji University Jour, 24,4:439-444. (in* Chinese).
Li, P. and Sun, H.P.: (1991) The characteristics of paleosol in the late Pleistocene strata in the Changjian Delta, *Shanghai Geology,* 1:16-20. (in Chinese).
Li, P. and Tian, W.J.: (1992) Late Quaternary paleosol formation in the Yangtze Delta area *in* Z.T. Gong (ed) *Environmental Change of Soils,* China Science and Technology Press, Beijing, 79-85. (in Chinese).
Liu, B.Z., Li, C.X. and Ye, Z.Z.: (1995) Phytoliths and their paleoenvironmental significance in the studies of late Quaternary paleosols in the Yangtze Delta area, *Marine Geology and Quaternary Geology,* 15,2:17-24. (in Chinese).
Liu, D.S., et al.: (1985) *Loess and the Environment,* Science Press, Beijing, 481 p. (in Chinese) .
Wang, K.F., Zhang, Y.L., Jiang, H. and Han, X.B.: (1984) The assemblage of late Quaternary spore-pollen and its stratigraphic and paleogeographic significance in the Yangtze Delta area, *Acta Oceanologica Sinica,* 6,4:485-498. (in Chinese).
Wu, B.Y.: (1985) Studies on the sedimentological characteristics of Xiashu loess in Nanjing, *Marine Geology and Quaternary Geology,* 5,2:113-123. (in Chinese).
Xiong, Y. and Li, Q.K.: (ed) (1990) *Soils of China* (second edition), Science Press, Beijing, 746 p. (in Chinese).

QUATERNARY CLIMATES RECORDS ALONG THE EGYPTIAN RED SEA COAST

O. Conchon and F. Baltzer

Département Sciences de la Terre, Université Paris-Sud, F 91405 Orsay. France

Abstract

The Quaternary sedimentary sequence and the geomorphological features characterizing the piedmont of the East Egyptian coastal range (presently hyper-arid) indicate significant past climatic changes.

The quantitative chronostratigraphical scale is based on the isotopic dating of reefal complexes. Littoral marine sediments, 1m above present mean sea level (PSL), were dated as Holocene. The littoral terrace, 6 to 8 m above PSL, was dated as stage 5e, and at places as stage 7 and even 9. The datations of an inland reef complex, up to 42 m above PSL, is in progress. Six units of continental accumulation are organized in four terraces F'/F.

Relatively humid climatic conditions occurred, at least occasionally, during the Last Interglacial, followed by an arid episode. Semi-arid periods, with sometimes tropical conditions, took place during the transitional phases between the glacial maximum and the interglacial stages.

Introduction

The region studied along the Red Sea coast of Egypt is a Mio-Plio-Pleistocene piedmont below a coastal chain in Proterozoic rocks, 1000 -1400 m high (Fig. 1 A, B).

The present climate of this region is hyper arid: mean annual rainfall 4 mm (over 25 years), annual maximum 34 mm (over 35 years; an exceptional rainfall of 34 mm in 24 hours was once measured).

Quaternary continental sediments

Quaternary continental sediments are organized in fans or terraces (Fig. 1C, and Fig. 2A; Photo 4) (Freytet *et al.*, 1993, Baltzer *et al.*, 1993), built with four main types of sediments: fluvial sediments in braided rivers (Photo 2 and 3), or rarely in straight channels, debris flow deposits (Photo 6) and sheet floods deposits (Baltzer and Conchon, 1987; Conchon *et al.*, 1994). Most of them consist of poorly rounded boulders and pebbles, in a silty-sandy matrix.

Along the lower course of Wadi Nahari, a travertinous limestone overlie fluvial deposits. It is micritic, with algal (stromatolitic) laminations and concretions, at places perforated by reed prints (Photo 1) (Freytet *et al.*, 1994).

Quaternary marine sediments

Quaternary marine sediments are essentially coral reefs (Photo 5) and pebble beaches which built a littoral terrace (6 m to 8 m above present mean sea level) and inland complex reefs (Photo 4) uplifted at 42 m above present sea level in Wadi Igla, at 41 m in Wadi Khalilat el Bahri (Fig. 1C, Fig. 2B; Photo 4; Plaziat *et al.*,1989).

Stratigraphy

The stratigraphy of the continental deposits is based on the topographical relationships and on the relationships between continental deposits and marine formations (Fig. 2, Fig. 3).

The chronostratiaraphy is based on two types of arguments: radiochronology and climatic arguments, in correlation with neighbouring regions. It is known that the Last Glacial Maximum was arid in the Sahara (for ex, Pachur *et al.*, 1987, Petit-Maire *et al.*, 1991), and the alluviation implying humid conditions (see below) cannot take place during this period, which is also a period of low sea level. *The fluvial sedimentation occurred during transitional phases between glacial and interglacial maxima*

First datations of reefs along the Egyptian Red Sea coast were published by Butzer and Hansen (1968), Veeh and Giegengack (1970). New coral samples were U/Th dated (Choukri, 1994). Among 45 coral samples which were chemically analysed, 27 were not recristallised and could be used for dating (Reyss *et al.*,1993; Table 1). The average value is 121.8 ± 3.5 ka, included in substage 5e. U/Th datations were tested with new materials: sea-urchin spines, entirely in primary calcite, coupled with U/Th datation of non recristallised corals, at the same places. Seven sea-urchin spines had the same 5e ages as coral samples; this agreement showns sea-urchin spines are good material for dating, and can be used when coral samples are recristallised (Choukri *et al.*,1995).

In two sites, it was demonstrated that the littoral terrace was built in a substage 5e reef and a stage 7 reef (Table 1, Fig. 2B). The same organisation was recognised along the southeastern coast of Sinai (Gvirtzman *et al.*,1992). In another site of the Egyptian coast, an age older than 350 ka seems to correspond to stage 9. New samples will be analysed to validate the old ages. Stage 7 coral reefs were also dated along the Red Sea coast of Sudan (Hoang *et al.*,1986), and stages 7 and 8 (or older) were recognised ($\delta^{18}O$) in a core in the central Red Sea, at the same latitude as our own samples (Almogi-Labin *et*

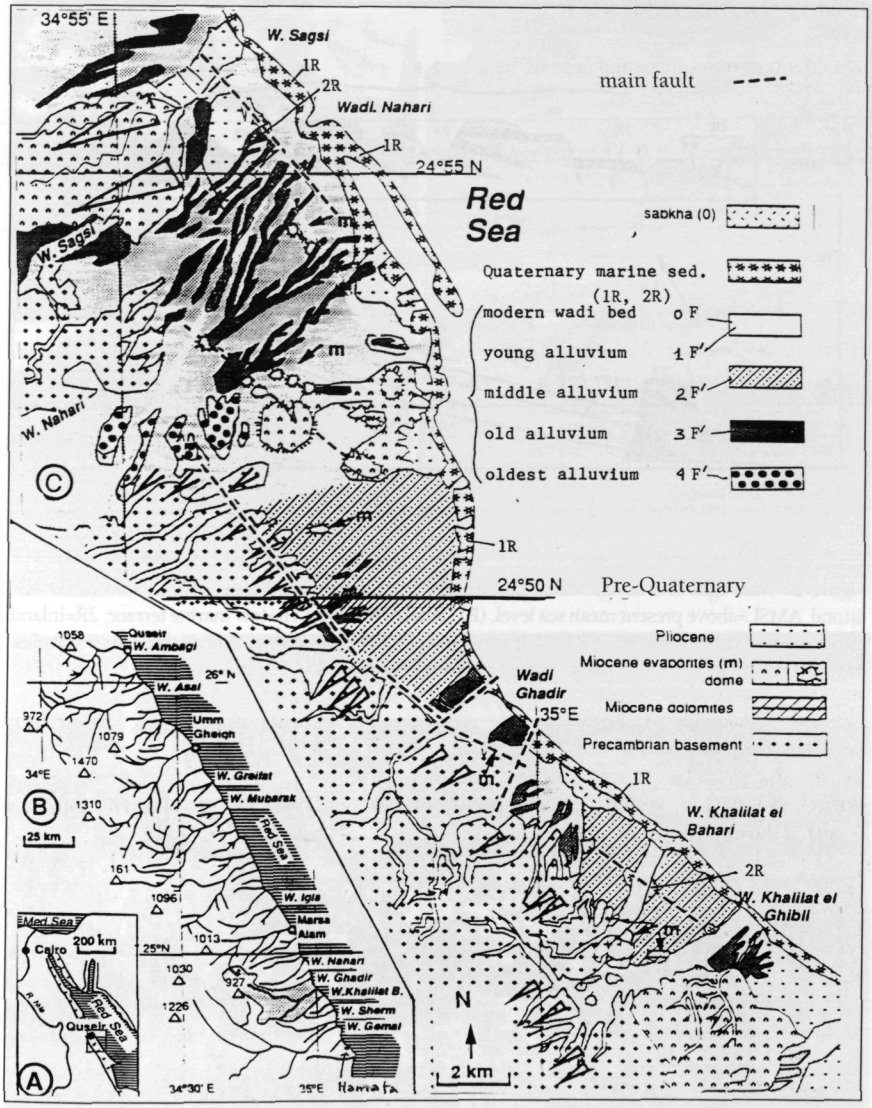

Figure 1. (A) Location map. (B) Drainage pattern: temporary rivers (wadis) in the area studied. (C) Geological map of the southern part of the area studied.

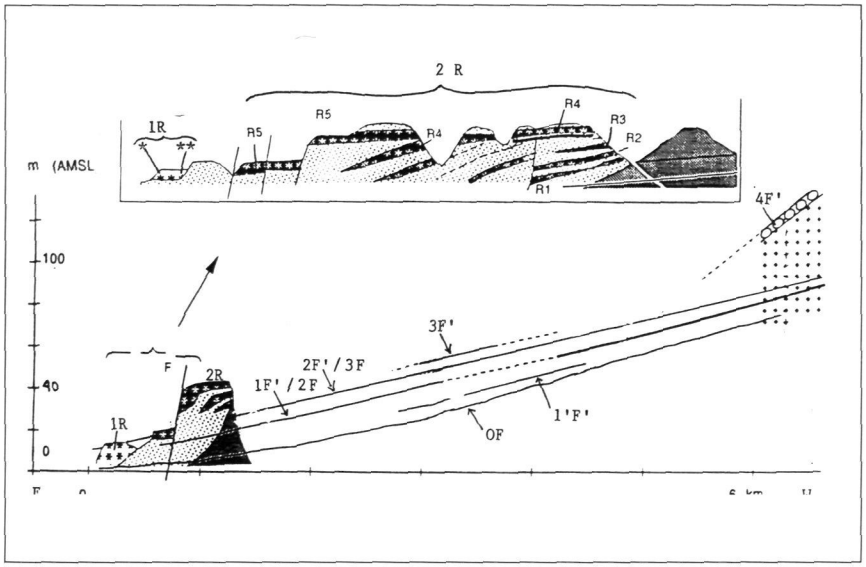

Figure 2. Wadi Igla. (A) Longitudinal profiles of fluvial terraces and transverse section across the littoral. AMSL=above present mean sea level. (B) Detail of the reefs: 1R=low marine terrace, 2R=inland reef complex, with 5 reefs (R1 to R5). The present reef (OR) is not drawn. *mean value for 4 samples, +6m., 117.2 ± 3 ky (st. 5e). **mean value for 3 samples, +8m., 252.7 ± 25 ky (st. 7).

Photo 1. Right side of Wadi Nahari, *cf.* **Photos 2 and 3.** Travertinous limestone with cylindrical concretions around reed stems (stems were not fossilized and remain as voids). Scale (ballpoint)=13 cm.

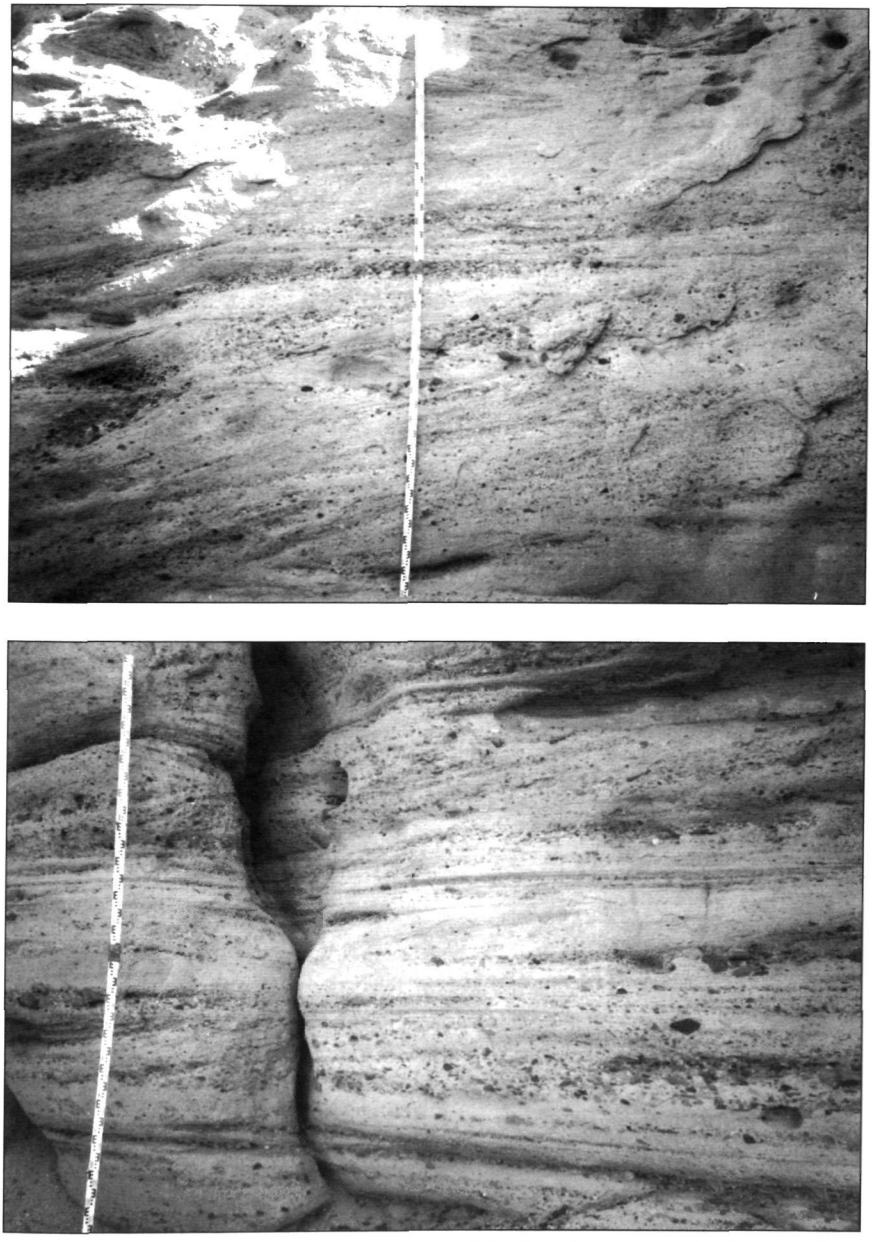

Photos 2 and 3. Right side of Wadi Nahari, downstream (2 km from the pesent sea-shore). Two sections across cemented braided river deposits (below travertinous limestone). Large-scale cross bedding in the sections perpendicular to the main stream (ph.2) and in the sections parallel to the stram (ph.3). Pebbles in a sandy matrix.

Photo 4. Left side of Wadi Khalilat el Bahri, about 2 km from the present sea-shore. **a**, upper fan 2F′ (sheet flood and d ebris flow deposits); **b**, beach pebble s over the inland reef complex, 41m. above the mean present sea-level; **c**, inland coral reef complex 2R (4 reef units); **d**, lower fan 3F′(debris flow deposits); **e**, present wadi bed (OF).

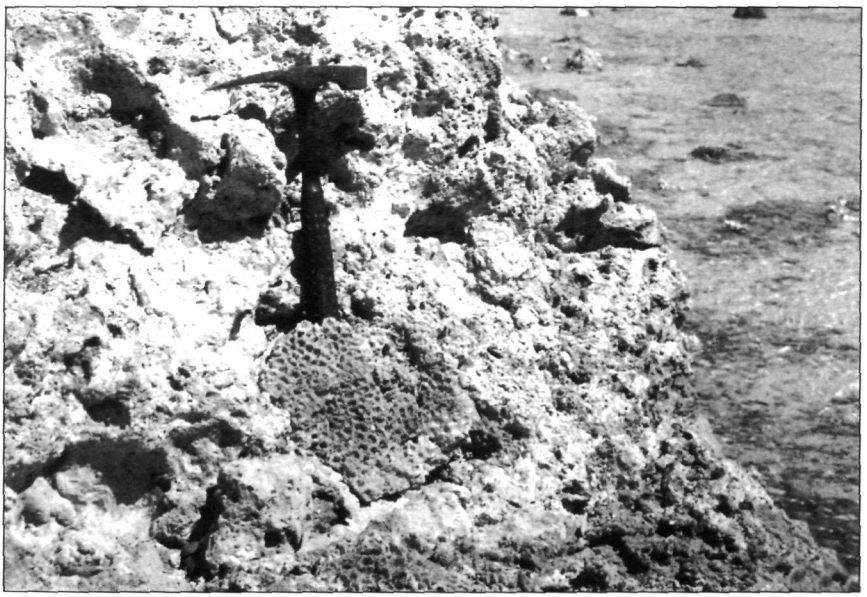

Photo 5. Shore cliff in the coral reef 1R (stage 5e), North of Wadi Nahari.

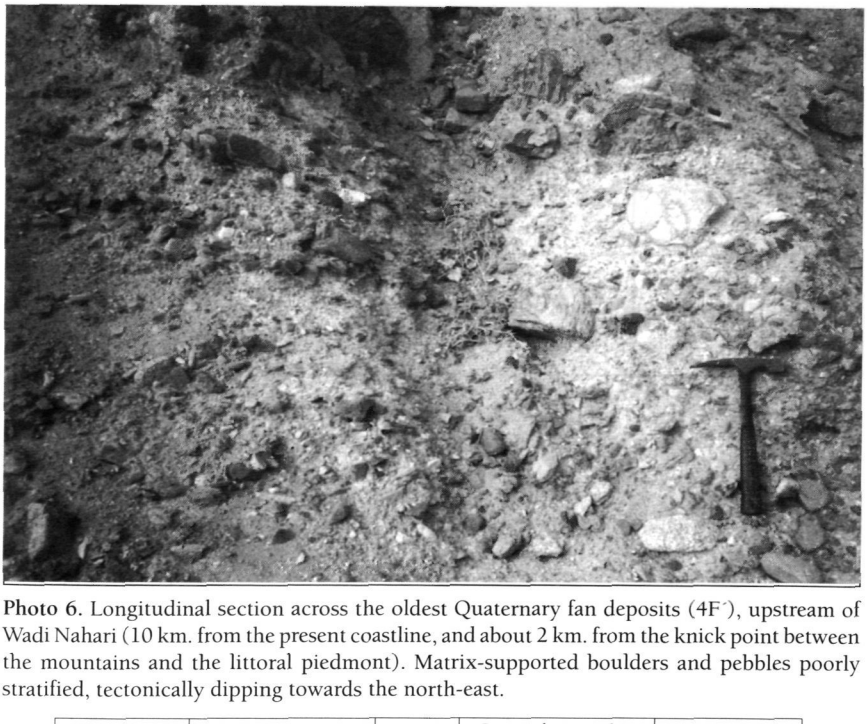

Photo 6. Longitudinal section across the oldest Quaternary fan deposits (4F´), upstream of Wadi Nahari (10 km. from the present coastline, and about 2 km. from the knick point between the mountains and the littoral piedmont). Matrix-supported boulders and pebbles poorly stratified, tectonically dipping towards the north-east.

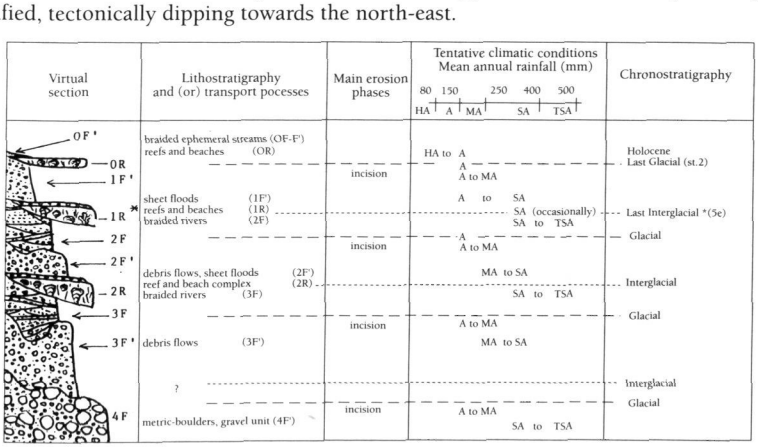

Figure 3. Stratigraphic virtual section representing the succession of Quaternary deposits between Quseir and Wadi Gemal, the correlative climatic conditions, and a tentative chronostratigraphic scale. *Isotopic stage 5e was based on 9 coral samples dated in 5 places in the area studied. On the schematic section, the oldest fan deposits (4F´) are figured below the younger ones, albeit (4F') are topographically higher; deposits (3F´) succeed to (4F´) after a deep incision; deposits (2F´) succeed in the same way to (3F´) after incision, and (1F´) after incision of (2F´). The oldest reefs (2R) are also situated higher than the youngers (1R and 0R), being elevated by tectonism. HA=hyperarid, A=arid, MA=moderately arid, SA=semiarid, TSA=tropical semi-arid conditions.

location	sample number*	altitude (m)	230 Th age (x *10^3years)*
Wadí Igla	C 8(1)	2-3	117.5 +4.4 / -4.2
W. Igla	C 8(2)	5	115.6 +5.8 / -5.5.
W. Igla	C 8(3)	6	118.0 +5.6 /-5.3
W. Igla	C 8a	2.5	117.6 +4.4/-4.2
W. Igla	C 8b	8	258 +30/-24
W. Igla	R 8a	8	252 +38 / -28
W. Igla	R 8b	8	248 +53 / -36
W. Khalilat el Bahri	C11 (1)	2-3	119.9+5.8/-5.5
W. Khalilat el Bahri	C11 (3)	5	124.2+4.9/-6.2
W. Khalilat el Bahri	C11 (4)	6	115.7 +6.5 / -6.2

*from Reyss *et al.*, 1993, and Choukri *et al.*, 1995

Table 1. Ages of coral samples C (*Porites*, Faviidae) and sea-urchin spines R, along the Red Sea coast of Egypt, at places where relationship with detrital sediments are studied.

al., 1986). Stages 7 and 9 coral reefs were determined on the southeastern coast of Sinai (Gvirtzman *et al.*, 1992).

At places where ancient coral reefs (stages 7 and 9) are situated in the same littoral terrace as stage 5e reefs, no tectonism (or very weak) affected the region since stage 7 or 9. Along the Egyptian Red Sea coast, there are probably non-uplifted regions, at least since 260 ka, and possibly since 360 ka, while other blocks were faulted and uplifted (Baltzer *et al.*, 1992).

Plaziat and Choukri, as Hoang *et al.* (1996) in Sudan, have never found samples with ages of substages 5c or 5a, contrary to the results of El Moursi (1992) who found two samples for stage 5a (mean value 87,1 ± 2,4 ka), and one sample for 108,5 ± 3,7 ka, evaluated as st. 5c, the others belonging to stage 5e. Datings of 81 ka and 98 ka for two coral samples on the eastern coast of Gulf of Suez were critically interpreted as stage 5e by Gvirtzman *et al.*, (1992).

Detailed studies by Plaziat, with precise levelling, demonstrate a small lowering of sea level during the 5e highstand (Plaziat et *al*, 1995).

A few samples of corals near the present sea level had Holocene ages (Table II).

Paleoclimatic interpretation of the Quaternary piedmont deposits.

In the southern Sinai, fossil corals *Porites* in terraces dated 108 -140 ka, 140 - 200 ka and terraces older than 250 ka, show a fluorescence characteristic of humid conditions on the adjacent land (Klein et *al*, 1990) Except by this analytic method, coral reefs do not give out information upon paleorainfall. Detrital sediments and their cementation are rarely used, nevertheless they are indicators of climatic changes, albeit with little precision. We emphasised the climatic interpretation of continental sediments.

The *algo-bacterial laminations* in tuffaceous limestone were built below water, suffering only very short periods of desiccation (Freytet *et al*, 1994), indicating a more humid climate than nowadays.

Mangrove oysters in middens, N. of Hurghada (S. of Suez Gulf):
5 645 ± 84 y BP
5 675 ± 115
6073 ± 84
Corals of a marine erosion surface, between present mean sea level and mean low sea level,
N. of Wadi Gemal: 7 670 ± 206 BP
S. of Hamata: 6 410 ± 84

Table II Holocene ^{230}Th datings, years BP (from Plaziat *et. al.*, 1995).

The *cementation* of the braided channel deposits (Figs. 5, 6) in the lower course of several wadis implies shallow phreatic waters, which are absent in arid regions, deep waters only being present (Freytet *et al.*, 1994)

A calcrete on the surface of the Last Interglacial emerged reefs is a *«laminar horizon»* (Freytet *et al,* 1994) developed under quite arid conditions (Verrecchia, 1994). This arid phase occurred since the reefal construction, possibly during the Last Glacial Maximum (st.2).

In order to deduce the climatic conditions prevailing during the Pleistocene *detritical sedimentation* we have compared the Pleistocene detritus with the modern sedimentation, after floods: modern floods removed some pebbles, but the longest were 50 cm, and the sediments deposited were mainly silty and sandy. Although a few quantitative data exist for modern river and fan deposits in arid areas (Laronne and Reid, 1993), some observations and experiments conclude that strong rains moved pebbles smaller than 21 cm (rainfall of 20,6 mm during 24 hours in the Death Valley of California, Beaumont and Oberlander, 1971), or lighter than 10 kg (South Negev, Shick, 1987). Rainfalls of 50 to 70 mm per hour are necessary to trigger off debris flows (Beaty, 1974); these rainfalls can occur in moderately arid regions, with 150 mm mean annual rainfall.

The abundance of boulders 50 - 100 cm long (60 - 400 kg or more) in many exposures of Egyptian detrital sediments indicates high hydrodynamics. It seems that higher rainfalls than at present are necessary to trigger off floods which can transport and deposit big boulders, as long as 1 meter, and to trigger off debris flows (Fig. 3; Conchon *et al.*, 1994).

These inferred climatic conditions are in good agreement with those of Dorn *et al*, (1987), who deduced from $\delta^{13}C$ in the pebble desert varnish that sedimentation in the fans of Death Valley (California) occurred during «humid» periods (semi-arid).

In the Central Sahara, during Quaternary humid phases, permanent rivers existed with estimations of 250 to 400 mm mean annual rainfall (Flohn and Nicholson, 1980, Petit-Maire *et al.*, 1991).

In eastern Egypt, debris flow deposits overlying braided deposits form a couple, which is cut as a terrace during an incision phase preceeding the maximum of each glacial period (Fig. 3). Sanlaville (1992) assumed that erosion occurred on the Sudanese coastal plain during the regression at the beginning of stage 4.

Other evidences of a humid climate are related with interstadials:

- a limestone with *Charophytes and fresh water shells (Lymnea, Hydrobia...,* mixed with more saline shells, *Melanoides, Potamides,* indicating highly fluctuating salinity) was found between a marine layer and a gypsum bed, assumed as stage 5e (Plaziat *et al.*, 1995).

- Neolithic middens in the Gulf of Suez have mangrove oysters (encrusting *Avicennia* roots) dated 6000 to 5600 BP (Table II). Detailed studies of fossil mangroves, with typical shells of *Terebralia palustris,* demonstrate that this type of mangrove disappeared from the Egyptian shores at c. 5000 BP, when aridity increased (Plaziat *et* al., 1995). The presence of *Terebralia palustris* mangal species demonstrates a humid phase during the Holocene, at about 6000 BP. It is in agreement with an Holocene humid phase throughout the Sahara, estimated with a mean annual rainfall of 200-300 mm at 22°N (Petit-Maire, 1992), with a humid phase between 8.5 and 6 ka BP deduced from the interpretation of Pteropod assemblages in the Central Red Sea, and the inferred climate on the adjacent land (Almogi - Labin *et al.*, 1991). The characteristics of cementation and dissolution in the quaternary reefs give evidence for a humid phase (dissolution), before an arid one (gypsous cement; M'Rabet and Purser, 1988).

Humidity during the interglacial stages 5 and 7 is known in desertic neighbouring regions: for instance, it was a determined by pollen in the travertines South of the Dead Sea (Israel), presently hyperarid (Weinstein-Evron, 1987), and by detrital sediments along the Sudanese coast (Hoang et *al.*, 1995). Large freshwater lakes in the Sahara were evidenced during the 5e and 1 interglacials (Petit-Maire, 1982,1992, Petit-Maire et al.,1995). In contrast, arid phases along the Mediterranean coast of Egypt, are deduced from eolianites during one period of the Holocene, and during substages 5a,5c,5e and stage 9 (Elasmar, 1994).

Conclusion

Humid phases are recognized during several Quaternary periods on the Egyptian coast of the Red Sea, as in other regions of the north-African tropical belt (Petit-Maire,1986, 1992; Petit-Maire et al., 1995). The last humid phase is dated around 9,5 to 4,000 BP. The 5e one is dated 125-130 ka (Yan and Petit-Maire, 1994; Petit-Maire et al., 1995).

The correlations between continental and marine sedimentation on the eastern Egyptian piedmont allow to correlate climatic phases with sea level changes (glacial or interglacial global phases). At least *moderately arid conditions* seem to have prevailed during the post-interglacial lowering of sea level, with deposition of debris flow or sheet flood sediments, and *semi-arid conditions* during the post-glacial sea level rise, with the deposition of braided river sediments and their cementation.

Four terraces resulted from humid periods of sedimentation intercalated with four incision phases. Fan F' over river F type deposits form a couple in one terrace, but they are separated downstream by an interglacial coral reef, observed respectively between 3F and 2F', 2F and 1F'. When the old inland reefs will be dated -if permitted by new methods as UTh dating of sea-urchin spines -, their complexity (several coral units) might modify and complicate the scheme.

The semi-arid conditions during Quaternary periods in eastern Egypt are probably close to those which presently occur in southeastern Zagros, Iran (200-300 mm mean annual rainfall) where vegetation covers not only the modern river bed of the Mehran,

with phreatic waters, but also the valley slopes, while many cobbles and pebbles lie in the modem wadis (Baltzer *et al.*,1982).

References

Almogi-Labin, A., Luz, B. and DUPLESSY, J.C.: (1986) Quaternary paleo-oceanography, Pteropod preservation and stable-isotope record of the Red Sea. *Palaeogeography Palaeoclimatology, Palaeoecology,* 57 2-4: 195-211.

Baltzer, F., Conchon, O., Freytet, P. and Purser, B.H.: (1982) Un complexe fluvio-deltaique sursalé et son contexte: originalité du Mehran (SE Iran). *Mém. Soc. géol Fr, N.S.,* 144:43-52.

Baltzer, F. and Conchon, O.: (1987). La dynamique de la sédimentation détritique continentale sur le piémont de la chalne côtière sud-égyptienne (Mer Rouge) *1er Congrès Fr. Sédim.,* Paris, rés.: 40-41.

Baltzer, F., Conchon, O., Freytet, P., Plaziat, J. C. and Purser, B.H.: (1992) Déformations néotectoniques des terrasses quaternaires - rocheuses, alluviales et marines - de la côte NW delaMerRouge(Egypte). *C.R.Acad. Sci.* Paris315,11:1717-1724.

Baltzer, F., Conchon, O., Freytet, P. and Purser, B.H.: (1993) Climatic and tectonic evolution recorded by Plio-Quaternary sedimentary terraces and fans along the Egyptian coast of the Red Sea. *Geol. Soc. Egyt, Sp. Publ.* 1:321-342.

Beaty, C.B.: (1974) Debris flows, alluvial fans, and a revitalized catastrophism. *Zeitschr. Geomorph.,* n.f., 21:39-51.

Beaumont, P. and Oberlander, T.M.: (1971) Observations on Stream Discharge and Competence at Mosaic Canyon, Death Valley, California *Bull. Geol. Surv. America* 82: 1695-1698.

Butzer, K.W. and Hansen, C.L.: (1968) *Desert and River in Nubia* Univ. Wisconsin Press, 562 p.

Choukri, A.: (1994) *Application des méthodes de datation par les séries de l'uranium a l'identifcation des hauts niveaux marins sur la cote égyptienne de la Mer Rouge au moyen de coraux, radioles d'oursins et coquilles, et sur la cote atlantique du Haut-Atlas au Maroc, au moyen de coquilles.* These Univ. Rabat, 192 pp.

Choukri, A., Reyss, J.L., and Plaziat, J.C.: (1995) Datations radiochimiques des hauts niveaux marins de la rive occidentale du Nord de la Mer Rouge au moyen de radioles d'oursin. *C.R. Acad. Sci. Paris,* 321:25-30.

Conchon, O., Baltzer, F. and Purser, B.H.: (1994) Enregistrement sédimentaire des variations climatiques quaternaires sur la bordure NW du Rift de la Mer Rouge (Egypte). *Quaternaire* 5 3/4: 181 -188.

Dorn, R.I., De Niro, M.J. and Ajie, H.O.: (1987) Isotopic evidence for climatic influence on alluvial fan development in Death Valley, California. *Geology* 15:108-110.

El Moursi, M.E.E.: (1993) Pleistocene evolution of the reef terraces of the Red Sea coastal plain between Hurghada and Marsa Alam, Egypt. Journ. *Afr. Earth Sc.,* 17, 1: 125-127.

Flohn, H., and Nicholson, S.: (1980) Climatic fluctuations in the arid belt of the «Old World» since the Last Glacial maximum; possible causes and future implications, *Palaeoecology of Africa and the surrounding islands,* Balkema, Rotterdam. 12: 3-21.

Freytet, P., Baltzer, F. and Conchon, O.: (1993) A Quaternary piedmont on an active rift margin: the Egyptian coast of the NW Red Sea. *Zeit. Geomorph.* N.F, Berlin-Stuttgart, 37, 2:215-236.

Freytet, P., Baltzer, F., Conchon, O., Plaziat, J.C. and Purser, B.H.: (1994) Signification hydrologique et climatique des carbonates continentaux quaternaires de la bordure du désert oriental égyptien (cóte de la Mer Rouge). *Bull. Soc. géol. Fr.* 165,6:593-601.

Gvirtzman, G., Kronfeld, J. and Buchbinder, B.: (1992) Dated coral reefs of southern Sinai (Red Sea) and their implication to late Quaternary sea levels. *Marine Geol.*, 108:29-37.
Hoang, C.T1., Dalongeville, R. and Sanlanville, P.: (1996) Stratigraphy, Tectonics and Palaeoclimatic implications of uranium-series-dated coral reefs from the Sudanese coast of the Red Sea. *Quatern. Internat.*, 31 :47-51.
Klein, R., Loya, Y., Gvirtzman, G., Isdale, P.J. and Susic M.: (1990) Seasonal rainfall in the Sinai Desert during the late Quaternary inferred from fluorescent bands in fossil corals. *Nature*, 345:145-147.
Laronne, J.B. and Reid, I.: (1993) Very high rates of bedload sediment transport by ephemeral desert rivers. *Nature*, 366: 148-150.
M'Rabet, A. and Purser, B.H.: (1988) Diagenese de récifs actuels et plio-quaternaires le long de la côte égyptienne de la Mer Rouge. *Coll. Sédim. Récifs*, Tunis, rés.:55-58.
Pachur, H.J., Roper, H.P., Kropelin, S. and Goschin, M.: (1987). Late Quaternary hydrography of the Eastern Sahara. *Berliner geowiss. Abh.*, Berlin (A), 75,2:331-384.
Petit-Maire, N.: (1982) *Le Shati, lac Pleistocene du Fezzan.* Ed. CNRS, Marseille - Paris, 118 pp.
Petit-Maire, N.: (1986) Paleoclimates in the Sahara of Mali, *Episodes*, 9,1 :7-16.
Petit-Maire, N.: (1992) Environnements et climats de la ceinture tropicale nord-africaine depuis 140 000 ans. Mém. *Soc. géol. Fr*, n.s., 160:27-34.
Petit-Maire, N., Fontugne, M. and Rouland, C.: (1991). Atmospheric methane ratio and environmental changes in the Sahara and Sahel during the last 130 kyrs. *Palaeogeography, Palaeoclimatology, Palaeoecology*, 86:197-206.
Petit-Maire, N., Sanlaville, P. and Yan, Z.: (1995). Oscillations de la limite nord du domaine des moussons africaine, indienne et asiatique, au cours du dernier cycle climatique. *Bull. Soc. géol. Fr*, 166,2:213-220.
Plaziat, J.C., Purser, B.H. and Soliman, M.: (1989) Localisation et organisation interne de récifs coralliens immatures sur un cône alluvial du Quaternaire ancien de la Mer Rouge (Sud de l'Egypte). *Géol. médit.*, 16, 2-3:41-59.
Plaziat, J.C., Baltzer, F., Choukri, A., Conchon, O., Freytet, P., Orszag-Sperber, F., Purser, B., Raguideau, A. and Reyss, J.L.: (1995) Quaternary changes in the Egyptian shoreline of the Northwestern Red Sea and Gulf of Suez. Quatern. *Internat.* 29/30:11 -22.
Reyss, J.L., Choukri, A., Plaziat, J.C. and Purser, B.H.: (1993) Datations radiochimiques des récifs coralliens de la rive occidentale du Nord de la Mer Rouge, premières implications stratigraphiques et tectoniques. *C.R. Acad. Sci. Paris*, 317,11:487-492.
Sanlaville, P.: (1992) Changements climatiques dans la péninsule arabique durant le Pléistocène supérieur et l'Holocène. *Paléorient*, 18,1 :5-26.
Schick, A. P.: (ed) (1987) *Erosion, Transport and Deposition Processes with emphasis on Semi-arid and Arid areas.* Field guidebook: main excursion. The Hebrew Univ. Jerusalem, 169 p.
Veeh, H.H. and Giegengack, R.: (1970). Uranium series ages of corals from the Red Sea. *Nature*, 226:155-156.
Verrecchia, E.P.: (1994). L'origine biologique et superficielle des croûtes zonaires. *Bull. Soc.* géol. Fr., 165, 6:583-592.
Weinstein-Evron, M.: (1987) Palynology of Pleistocene Travertines from the Arava valley, Israel. *Quaternary Research*, 27:82-88.
Yan, Z. W. and Petit-Maire, N.: (1994) The last 140 ka in the Afro-Asian arid/semi-arid transitional zone, *Palaeogeography, Palaeoclimatology, Palaeoecology*, 110:217-233.

PALEOCLIMATIC OBSERVATIONS AT SALAR DE PUNTA NEGRA, NORTHERN CHILE

A. Craig

Department of Geography, Florida Atlantic University, Boca Raton, Florida 33431, USA.

Abstract

The combination of physical, biological and anthropogenic evidence shows that the paleoclimatic factors resulting in hyperarid conditions at Salar de Punta Negra (Chile) have been essentially static during the Holocene.

Introduction

Interesting comparisons can be made between the climatic regimes of the Canary Islands and the Andean salares of northern Chile. Both areas occupy equivalent latitudinal positions, are influenced by cool oceanic currents, have extensive volcanic deposits, and arid climates with high evaporation rates. A radical change in elevation accounts for much of the environmental differences.

This research in the Salar de Punta Negra began as a result of articles by the North American archaeologist Thomas F. Lynch (1984, 1986, 1990). Over the past 25 years, Lynch has established a sound reputation as a South American paleo-Indian specialist. His basic premise for the Andean and Salar de Punta Negra areas requires a more benign paleoclimatologic environment during the early Holocene when paleo-Indians first entered this now extremely inhospitable zone.

The Salar de Punta Negra is a high altitude (3000 m), hypersaline, bolson located in northern Chile (Fig. 1). It is a fault controlled, graben-like Tertiary basin that has always had centripetal drainage similar to that found on many other nearby salares in this part of the Andes. Lynch (1990) postulates at least one very high former lake level creating an overflow of fresh (?) water northward into the adjacent Salar de Imilac and possibly from there into the mighty Salar de Atacama (2,400 m).

Figure 1. Study area location map.

This potentially important paleoclimatic environmental scenario is inconsistent with the geological observations presented here, together with biological evidence that support a hypothesis of long term hyperaridity, punctuated by brief, highly localized catastrophic rainfall events of undetermined origin. These mobilize the accumulated products of mass wasting from higher Andean elevations, and channel them into wadis as flash flood bedload. Only two such events can be detected in the last 500 years.

Geomorphic Indicators

The Punta Negra salar derives its name from a conspicuous eruption of jet black diorite lava that issued from a fissure along the eastern boundary fault. The flow moved in three coalescing lobes down to the salar's maximum level shoreline. Lack of any oxidation products on the leading edge indicates it did not enter the water. Stratigraphic relationships place this outpouring of lava in late Pleistocene or early Holocene time because it overlies the extensive colluvial pediment (Fig. 2 and Photo 2) seen to the north. However, the Punta Negra Lava is itself onlapped by a younger late Pleistocene (?) alluvial terrace (Fig. 2,2) on the south side that was formed by deposits discharged from a steep gradient quebrada draining the Central Andean Massif, indicated in the lower right corner of Figure 2.

A characteristic broad (3 -4 m) trace of the famous Inca Highway crosses the Punta Negra lava flow near the fissure from which it erupted (Fig. 2). This military pathway was constructed ca. 1485 AD to facilitate the conquest and domination of northern Chile by armies of Tupac Yupanqui, before the arrival of Spaniards. The highway constitutes an important time-line allowing us to establish the comparative chronology of several extensive alluvial fans and terraces. By this means, we can determine those features shown in Figure 2 as the Colluvial Pediment (4), the Punta Negra Lava (3), and the Pleistocene Terrace (2) are, as we may well anticipate, pre-highway in age; incised into this surface are the Highest Holocene Terrace (1) and the Historic Flash Flood Deposit which both obliterate the road and must be younger than the highway. The high terrace is obviously older than the flash flood deposits.

No geomorphic evidence exists of former lake levels higher than what is shown in Figure 2. From that maximum lake level to the 1964 shoreline, an evaporite crust of chlorides and sulphates has developed. Today this is even more extensive, resulting in a great reduction in the hypersaline brine evaporation surface shown in Figure 2. In other words, the area of evaporite crust is now much greater than shown, extending entirely across the salar over most of its area.

Biogenic Indicators

Extensive observations have been made by staff biological scientists of the La Escondida company, in a commendable effort to achieve overall environmental compatibility with their open pit mining operations in a fragile desert location. These efforts include in depth studies of the resident flamingo population of the salar, quarterly reconnaissance expeditions into remote high altitude (4,500-5,200 m) salares to gather baseline data on lake levels, snowpack, vegetational responses and animal censuses. From these studies, we can extract some useful biogenic indicators of paleoclimatic conditions in the study area.

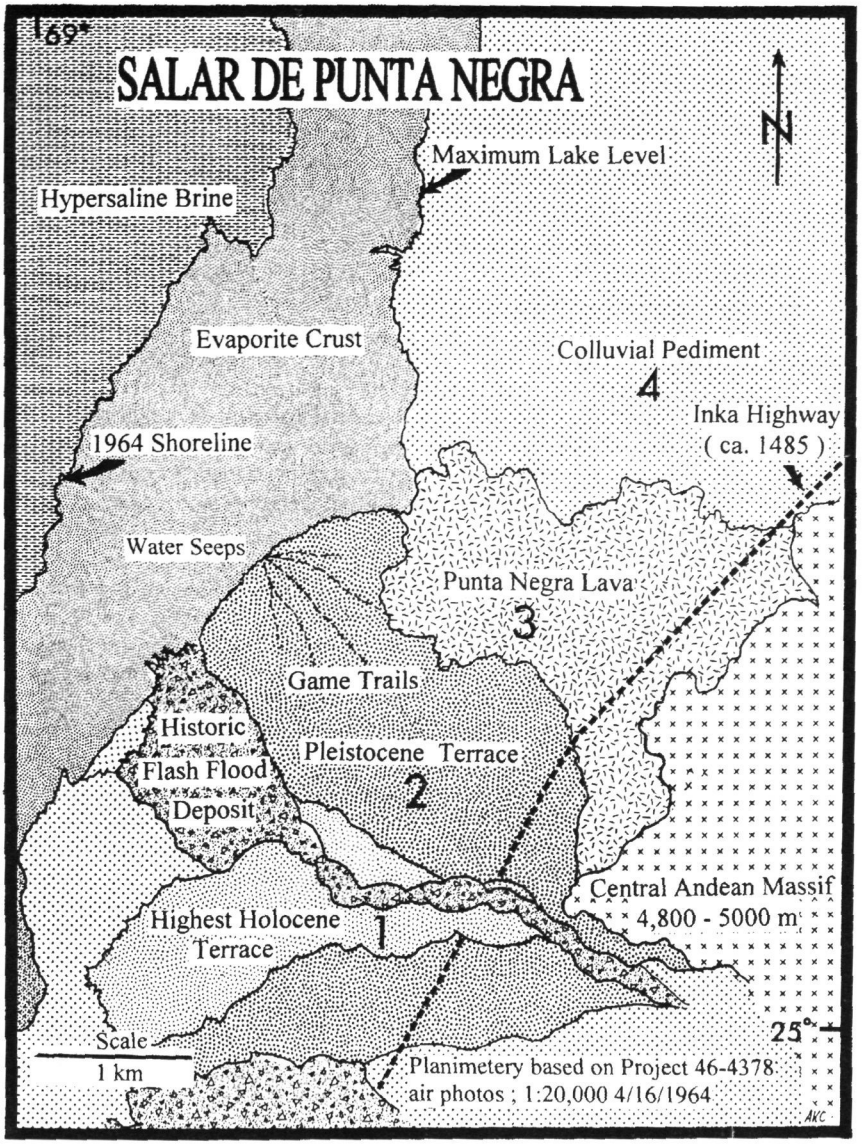

Figure 2. Geomorphic map of Salar de Punta Negra, southeastern section.

Parada (1990) has determined flamingos breeding in the shallow, hypersaline open waters of Salar de Punta Negra have adapted to feed exclusively on diatoms in the absence of the constituents of their usual diet of small crustacea and gasteropods. Artificial concrete nest platforms have been placed as a kind of seawall to protect the nesting area from wave erosion caused by strong nigttime katabatic winds. This unusual arrangement has been accepted by these birds and the population seems to remain stable. Long term paleoclimatic data may eventually result from a detailed study of diatoms in sediment cores from this salar.

Vicuña territorial dungheaps *(defecaderos)* are another interesting bioindicator of paleoclimatic conditions in the study area. These strange mounds (Photo 1) are conspicuous markers used by Andean camelids to define their boundaries around feeding grounds which the dominant male defends vigorously. They have grown to remarkable size on the evaporite crust surface where they surround pastures of *Deyeuxia breviaristata,* a halophilic brown grass irrigated from below by capillary action.

Anthropogenic Indicators

Evidence of aboriginal hunting activities can be seen adjacent to every active spring and water seep, along the eastern shoreline of the salar. These prehistoric artifacts are especially noticeable near the terminus of the Punta Negra lava flow. Here, there are dense scatters of silex debitage surrounding several small circular placements of head-sized stones (Fig. 4) where archaic hunters erected temporary shelters or concealments close to the vicuña trails leading to the watering holes.

At these locations, some projectile points have been found (Lynch, 1990) and a bifacial scraper/knife consistent in appearance with lithics of the Formative period (7-5000 BP). These artifacts establish the earliest human presence in the study area. Several nineteenth century brass ammunition casings were found in the same locality, left behind by modern camelid hunters. This points to animal ecology and hunting relationships indicative of overall climatic stasis have been in place over the salar throughout much of the Holocene.

Discussion and conclusion

Before mining of the La Escondida copper deposits began, more than 40 deep (avg. 350 m) water wells were drilled along the eastern flank of the salar with varying results. Company geologists report (pers. comm.) subsurface stratigraphy of the salar consists of intercalated volcanic ash, evaporites, lava and alluvial fan deposits. The latter produce connate groundwater with a wide range of salinities. Certain intervals produce high quality potable water used to support some 1200 company workers. Other wells yield brine used to transport a copper concentrate in slurry form a distance of 180 km to an ocean loading dock near Antofagasta.

Although these data are proprietary, we conclude wells producing potable water are bottomed in buried alluvial fan deposits containing flash flood water. By analogy, we see this is the same source for the seeps that now allow sparse growth of the vicuña pastures at the base of the Pleistocene terrace.

From a combination of the physical, biological and anthropogenic evidence, it seems the paleoclimatic factors producing hyperarid conditions at Salar de Punta Negra have been essentially static during the Holocene.

Photo 1. Vicuña territoral dungheap. "Pasto vicuñero" grasses in background.

Photo 2. Prehistoric shelter or hunting blind with abundant debitage. Note backpack for scale.

References

Lynch, T.F.: (1984) The Salar de Punta Negra: Late and postglacial climate change, water budgets, and settlement around a former freshwater lake, *American Quaternary Association Programs and Abstracts. 8th Biennial Meeting, Boulder, Colorado,* 73.

Lynch, T.F.: (1986) Climate change and human settlement around the late Glacial Laguna de Punta Negra, Northern Chile: The preliminary results, *Geoarchaeology,* 1:145-162.

Lynch, T.F.: (1990) Quaternary climate, environment, and the human occupation of the southcentral Andes, *Geoarchaeology,* S,3:199-288.

Parada, M.: (1990) Flamencos en el Norte de Chile; Distribución, abundancia y fluctuaciones estacionales del número, *ler Taller Internacional de Especialistas en Flamencos Sudamericanos,* Corporación Nacional Forestal (Chile), Sociedad Zoológica de Nueva York, 52-79.

MINERALOGICAL AND SEDIMENTOLOGICAL CHARACTERIZATION OF QUATERNARY EOLIAN FORMATIONS AND PALEOSOLS IN FUERTEVENTURA AND LANZAROTE (CANARY ISLANDS,SPAIN)

B. Damnati

Abdelmalek Essaadi University. FST - Tanger. Department of Geology B. P. 416., Tanger, Morocco

Absbract

Lanzarote, a volcanic island, is located 125 km to the west of the Moroccan coast of the Sahara. Its climate is arid to semi-arid. The mean annual precipitation is 105 mm. The important eolian formations in this island are interbedded with paleosols. A quarry cutting into those formations («Mala»), in the north of the island, has been sampled and some sedimentological and mineralogical parameters (granulometry, carbonates, clay mineral) were studied. The preliminary results show that:

- In the lowest unit, between +0 and +2m., the sediment is rich in the > 125 µm fraction. However, the silt fraction (<63 µm) is important (about 30% of the total sediment). The carbonates are abundant in the coarser fraction (>125 µm). This unit is enriched in illite and kaolinite in its lowest part, and in smectite in its upper part.

-The middle unit, between +2 and +16 m, is composed of sand (ca. 100%). The carbonates are abundant (ca. 90%). The illite and kaolinite content is high.

-The upper unit, between +16 and +22 m is intercalated between evolved soils and poorly evolved soils. The evolved soils are marked by more silt, less carbonate and more smectite. The poorly evolved soils are characterised by more sand, more carbonate and more illite and kaolinite.

Those three lithostratigraphical units are related with three climatic periods.

In Fuerteventura island, Rosa Negra section shows, from the bottom to the top, a basaltic substratum, four red paleosols interbedded with yellowish and whitish sand (stratified or not). At the top, some layers are enriched in Hymenoptera and Helicidae shells.

Introduction

In the Canarian Archipelago, Fuerteventura and Lanzarote islands are the closest to the coast of Africa about 125 km at Cape Juby, at c. 28°N-14°W. The climate is complex, with differences both between islands and between directions in slope facing within the same island (Magaritz and Jahn, 1992). It is influenced by the cold Canary Current, which reduces precipitation and causes arid temperatures equivalent to those in the Western Sahara. Rainfall averages 105 mm, varying from 53 mm to 220 mm in the winter time. The mean temperature of the islands is 20°C, with extremes of 40 and 5.4°C. Ocasionally, wind suspended dust particles from Sahara.

In these volcanic islands volcanic, since 1985, preliminary research have been performed on important geological paleoclimatic records: marine terraces, carbonates deposits and eolian formations, interbedded with fossiliferous paleosols (Meco and Stearns,1981; Petit-Maire et *al,* 1987, Meco et *al,* 1992; Magaritz and Jahn, 1992). The alternating sequences of eolian deposits and paleosols represent climatic oscillations between arid and relatively humid conditions (Damnati et al., 1996).

Sampling expeditions on Fuerteventura and Lanzarote were undertaken in 1993. Sections in three quarries were observed and sampled: Rosa Negra and Cañada Melián in Fuerteventura and Mala in Lanzarote. A multidisciplinary study of those formations has been performed by a CLIP scientific team covering geology, sedimentology isotope studies, paleomagnetism, OSL,^{14}C and U/th dating and paleontology.

In this paper, we shall give some sedimentological (granulometry) and mineralogical (carbonates and clay minerals) results of Mala and Rosa Negra sections.

Methods

The granulometry was measured by sifting, separating the fractions superior and inferior to 63 um. Helicidae shells fragments were eliminated to avoid errors.

A Bernard calcimeter was used, the average error being 5%.

All samples were subjected to X-ray diffraction analysis of the >2 μm decalcified particles, as follows. The samples were dissociated under water, decarbonized in 5 N hydrochloric acid, and then dispersed in distilled water. The defloculation was carried out by repeated centrigugation and microhomogenization after mixing. The particles inferior to 2 μm were selected by decantation, using Stokes law in 50 μm, and then prepared in oriented pastes on calibrated glass slides. The X-ray investigation dealed with passages between 1° and 16° teta: natural condition, ethylenic glycol saturation, heating during 2 hours at 500°C, hydrazin hydrate saturation. The quantitative estimations took into account the area of basal peaks, with is diminished for the low cristallized minerals (smectite) and enlarged for the well organized minerals (Kaolinite) (Chamley, 1971,1979).

Results

Rosa Negra section was obtained by caving through an ancient quarry site (Figure 1).It rests upon a basaltic substratum. The section is 9 m thick and subdivided in two units A and B.

* Unit A: *c.* 6m thick; four red paleosols are interbedded with yellowish or whitish sand layers.

* The unit B is characterized by the Hymenoptera nests, Helicidae shells and laminated sand. At the top of the section two gravel layers are observed (Fig. 1).

The sediments of Rosa Negra section is rich in calcium carbonate and/or magnesium (between 50 and 90%). Granulometry analyses show that the coarser fraction (> 63 μm) is the important one. The clayey fraction consists of smectite, illite and kaolinite. Smectite is the most frequent (40-85%), followed by illite (10-50%) and kaolinite (5-20%). The unit A is characterized by highly variable content of clay minerals. In unit B the smectite is clearly dominant (Fig. 1).

Mala profile is 22 m thick. It may be subdivided into three distinct units (Fig. 2):

* Unit A: 2 m thick with reddish and yellowish silty sand and Helicidae shells;

* Unit B: 14 m thick, with crossbedded sands evolving into horizontal layers and ending in unstratified sand;

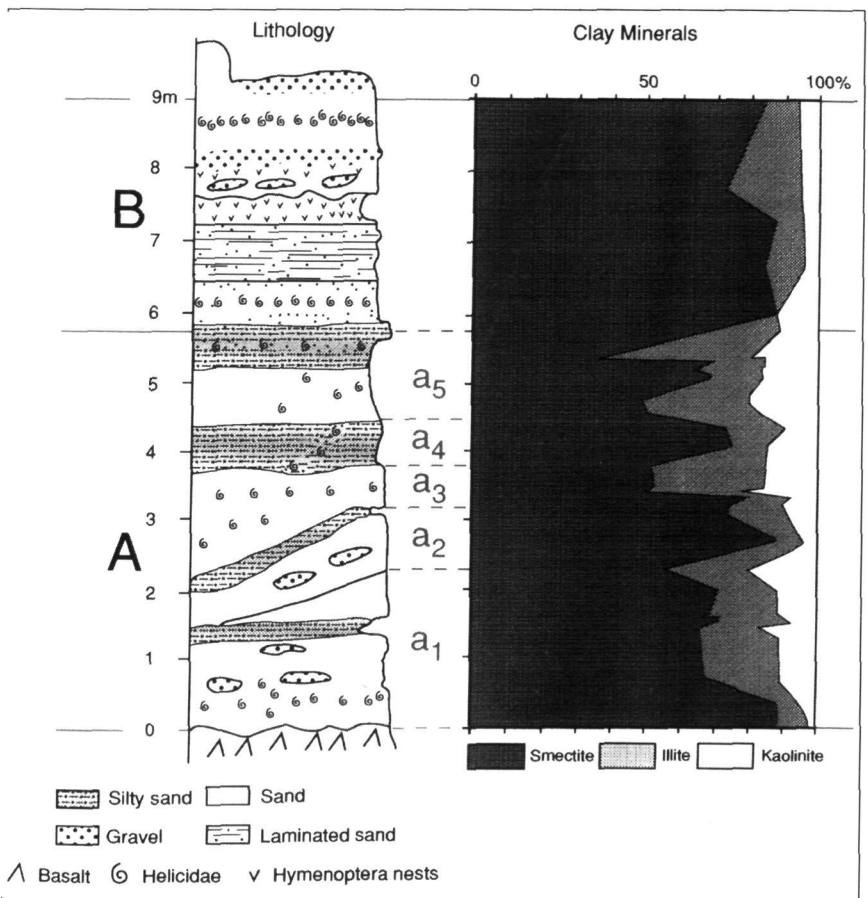

Figure 1. Lithostratigraphy of Rosa Negra section and clay minerals repartition.

* Unit C: 6 m thick, with three reddish evolved paleosols (C_1, C_3 and C_5) interbedded with greyish poorly evolved paleosols (C_2 and C_4 Fig. 2).

The granulometry shows that the coarser fraction (>125 μm) is the most important (70 to 100%) particularly in the middle unit (B) . The percentage of the silty fraction (> 63 μm) increases in the lower and upper units (A and C). The $CaCO_3$ content of the sediment follow the same repartition of granulometry. Carbonate content in the coarser fraction is between 90 to 100%. The carbonate content in silty fraction is between 60 and 90 5 (Fig. 2). The clayey fraction consists of smectite, illite and kaolinite. Smectite is the most abundant (50-90%), followed by illite (20-80 %) and kaolinite (0-40 %). The lower unit and the upper unit (A and C) show a high variation of the three clay minerals. The middle unit or paleodune (B) shows a high content of illite (Fig. 3).

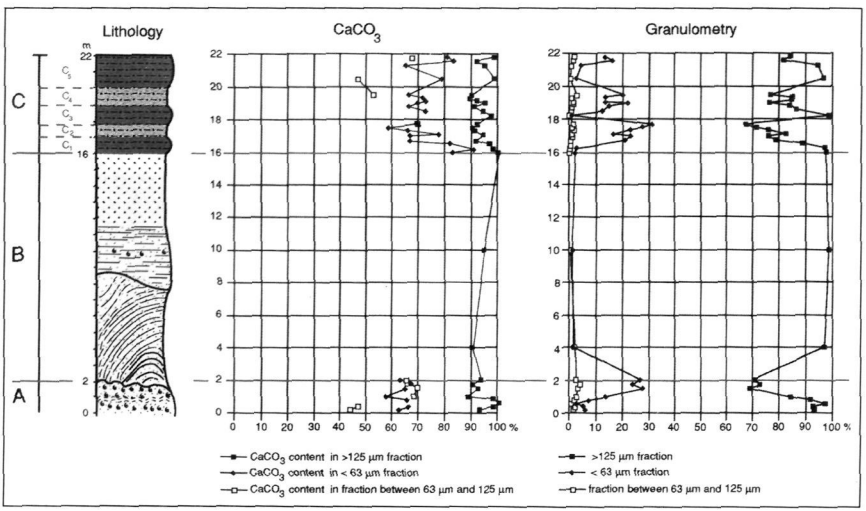

Figure 2. Lithostratigraphy of Mala section and calcium carbonate and granulometry variations

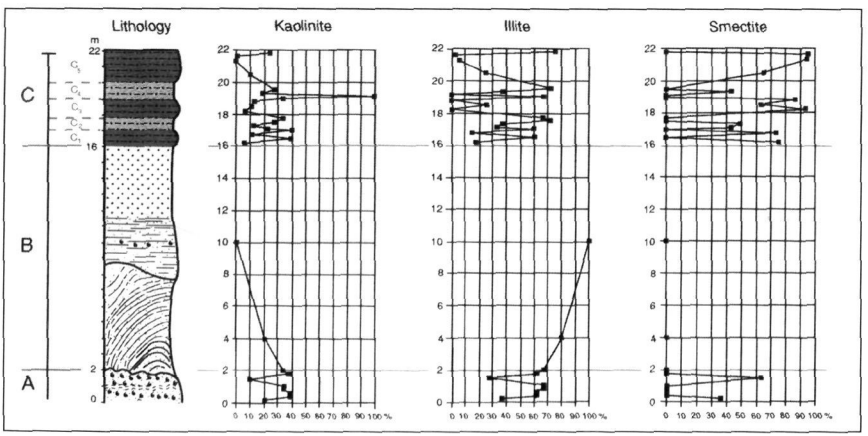

Figure 3. Clay minerals in Mala profile.

Discussion

Those results show that granulometry and lithology are well correlated. In the paleosols, the percentage of the silty fraction is relatively high. The paleodunes are composed by 80 to 100% of coarser sands.

The sediments are enriched in calcium carbonate ($CaCO_3$). The silty layers present a lower carbonate content than the sandy ones.

Various origins and formation may explain the mineralogical diversity of clays. Illite forms in cold and / or dry climates through alteration of the silicate rocks (Millot, 1964, Paquet, 1969, Chamley, 1971). Kaolinite is related with a warm-wet climate, when run-off results into drainage of ions. Smectite is also related with an alteration of wet and dry episodes in warm climatic conditions (Millot, 1964, Paquet, 1969, Chamley, 1971).

The present day eolian Saharian sediments have the same micromorphological and mineralogical characteristics (Lange, 1982) . We thus suggest that western Sahara is the main origin of those sediments, which fits the known processes of eolian transport in those areas (Whalley and Smith, 1981; Mc Tainsh and Walker, 1982; Chamley et al., 1987). We use the kaolinite and illite content of sediments as an indicator or relative *in situ* clay genesis (Chamley et *al,* 1987; Damnati *et al.,* 1996). The illite and kaolinite group is a good marker or remote eolian transport, in contrast with smectite which is also linked to local processes.

In this way, a clear Saharian influence thus appears in unit A of Rosa Negra section with high variation of illite and kaolinite percentage. The unit B is rich in smectite and is correlated with local processes.

The three lithostratigraphical units of Mala section are related with three climatic periods. The lowest one corresponds to a transitional period of climatic instability, with mixed eolian sediments (from the Sahara and local sources) and clays (high variation of illite and kaolinite percentage). The middle unit is a typical fossil dune with essentially illite, a witness for a very dry climate. The upper unit is a new transitional period, the wetter conditions being more accentuated than during the lowest unit phase.

The chronological data show that all the ages will be separated in three paleoclimatic stages:

* > 25 ka with a wet period;
* until 14 ka with a dry period;
* a return to wetter climatic conditions in the Holocene.

These three stages are correlated with paleoclimate records in northern Africa (Petit-Maire *et al,* 1987, 1989, 1993, 1994; Street-Perrot *et al,* 1989; Petit-Maire, 1991; Magritz and Jahn, 1992). However, many chronological problems (material and method) exist, particularly for Rosa Negra and Mala sections, for dating exactly the paleosols and paleodunes.

Conclusions

The late Quaternary deposits at Rosa Negra (in Fuerteventura island) and Mala (in Lanzarote island) essentially consist of alternating sequences of eolian deposits and paleosols. These sequences represent climatic oscillations. During the wet episodes, alteration of the basaltic substratum produces smectite and favoured pedogenesis. During

the dry (colder ?) episodes, eolian action is important (rise of the kaolinite and illite content). Dust is brought over from the Sahara, testifying to a dominant wind direction.

In Rosa Negra section, two periods are distinguished. A first one with alternating allochtonous and autochtonous contributions (climatic instability), a second one with only autochtonous contributions.

In Mala section, three periods were observed. The first one corresponds to a transitional period of climatic instabilily (unit A). The second one with a fossil dune (unit B) deposited probably during very dry climatic conditions. The third one represents an alternating period of allochtonous and autochtonous transport correlated, with climatic instability.

In order to better understand these deposits, it is important to have a greater and more reliable set of ages (Bouab and Lamothe, in progress).

References

Chamley, H.: (1971). Recherche sur la sédimentation argileuse en Mediterranée. *Sci.* Géol. Starsbourg. France. Mém. 35.

Chamley, H., Diester-Haass, L. and Lange, H.: (1977). Terrigeous material in East Atlantic sediments cores as an indicator of NW Africa climates. *«Meteor» Forsh-Ergebnisse,* Berlin, Reihe C, n° 26: 44-59.

Chamley, H.: (1979). North Atlantic clay sedimentation and paleoenvironment since the late Jurassic. *In* Talwani, M., Hay, W., Ryan, W., B.F. (eds). Deep Drilling Research Atlantic Ocean: Continental Margins and Paleoenvironment. *Am Geophys Union Maurice Ewing* Ser, 3:342-361.

Chamley, H., Coudé-Gaussen, G ., Debrabant, P., and Rognon, P.: (1987) . Contribution autochtone et allochtone a la sédimentation Quaternaire de l'Ile de Fuerteventura (Canaries): altération ou apports éoliens ?. *Bull. Soc Géol France* (8), t.III, 5:939-952.

Damnati, B., Petit-Maire, N. Fontugne, M., Meco, J., and Williamson, D.: (1996) Quaternary paleoclimates in the eastern Canary Islands. *Quaternary International,* 31 :37-46.

Lange, H.: (1982) Distribution of chlorite and kaolinite in eastem Atlantic sediments of North Africa. *Sedimentology,* 29: 427-431.

Magaritz, M., and Jahn, R.: (1992) Pleistocene and Holocene soil carbonates from Lanzarote, Canary Islands, Spain: Palaeoclimatic implications. *Catena* 19:511-519.

Mc Tainsh, G.H., and Walker, P.H.: (1982)Nature and distribution of Harmattan dust. *Zeitschf.* für Geol. *NE,* Berlin 26,4:417-435.

Meco, J. and Stearns, C.E.: (1981) Emergent littoral deposits in the eastern Canary Islands. *Quaternary Research* 15: 199-208.

Meco, J., Petit-Maire, N., and Reyss, J.L.: (1992). Le Courant des Canaries pendant le stade isotopique 5, d'apres la composition faunistique d'un haut niveau marin a Fuerteventura (28°N). *C R Acad. Sci. Paris,* 314. Série 11:203-308.

Millot, G.: (1964) *Géologie des argiles.* Masson ed. Paris. 499 p.

Paquet, H.: (1969) Evolution géochimique des minéraux argileux dans les altérations et les sols des climats méditerraneens et tropicaux a saisons contrastées. Mém. Ser. *carte géol .Alsace-Lorraine,* Strasbourg, n° 30.

Petit-Maire, N., Delibrias, G., Meco, J., Pomel, S., Rosso, J.C.: 1986. Paléoclimatologie des Canaries orientales (Fuerteventura) *C R Acad. Sci. Paris* (2), 303:1241-1246.

Petit-Maire, N., Rosso, J.C., Delibrias, G., Meco, J., and Pomel, S.: (1987). Paléoclimats

de l'Ile de Fuerteventura (Archipel Canarien) *Palaeoecology of Africa and the surrounding Islands* 18:351-356.

Petit-Maire, N.: (Ed) (1991) Paléoenvironnement du Sahara. Lacs holocenes a Taoudeni (Mali).Editions CNRS. Marseille/Paris. 239 p.

Whalley, W.B., and Smith, B.J.: (1981). Mineral content of Harmatan dust from northern Nigeria examined by scanning electron microscopy. *J. Arid Environments* 4:21-29.

GLOBAL SEA LEVEL CHANGES AS INDICATED BY ^{14}C AND $^{230}Th/^{234}U$ DATING OF MARINE TERRACES IN THE PERSIAN GULF AND ALONG THE MAKRAN COAST (IRAN)

Fontugne[1] M., Reyss[1] J.L., Hatté[1] C., Pirazzoli[2] P.A. and Haghipour[3] A.

1 Centre des Faibles Radioactivités, Laboratoire Mixte CNRS-CEA, Avenue de la Terrasse, F91198-Gif-sur-Yvette cedex, France
2 Laboratoire de Géographie Physique, CNRS-URA 141, 1, Place A. Briand, 92190-Meudon Bellevue, France
3 Geological Survey of Iran, PO BOX 13185-1494, Teheran, Iran

Abstract

Recent tectonic activity along the Iranian coasts of the Persian Gulf and the Arabian Sea has caused uplift of shorelines and coral terraces. This paper deals with the tectonic trends that can be deduced from the Holocene and upper Pleistocene raised terraces, along a 1500 km long sector from Busheir to Gwater, at the Pakistan border. Sequences of up to 20 superimposed shorelines have been identified. ^{14}C and $^{230}Th/^{234}U$ dates of these terraces have allowed us to calculate upliff rates that are considerablely lower than those estimated previously by Vita-Finzi (1979, 1982) and to estimate the relative variations of sea level during the last two climatic cycles.

Introduction

Sequences of raised marine terraces have been reported from many coastal areas in the world. The best known are Huon Peninsula, Barbados, New Hebrides, Sumba and Alor Islands (Chapell and Veeh, 1978; Bloom *et al*,1974; Pirazzoli *et al.*, 1993; Hantoro *et al*, 1994). As described previously by Vita-Finzi (1979,1982) and Snead (1993), well developed coral reef terraces are also found along the Iranian coasts. Preliminary results from the first author give uplift rates as high as 6.6 mm/year. If these uplift rates are correct, these terraces could provide an excellent opportunity to date high sea levels, but also intermediate sea levels, during the late Pleistocene.

Coastal areas of the northern Persian Gulf and the northern Oman/Makran Sea have been surveyed and we have sampled the main formations along about 1,500 km (from 30°N50°E to 25°N-62°E). The tectonic complexity of the Iran plate can be summarized as follows (Fig. 1). The northern Persian Gulf forms the southeastern part of the Zagros structural province, characterized by NW-SE trending fold-thrust belts, which results from the PlioPleistocene Alpine orogeny. These regions consist of Paleozoic/Mesozoic and Tertiary stratigraphic sequences, including salt diapirs related to early Paleozoic Hormoz series. The southeastern Zagros structure has been tectonically active since the late Tertiary, as part of the southern deformational front or convergence belt (Mesopotamian foreland/Persian Gulf basin) and the Arabian-Iranian continent-continent collisional plate margins. Eastward, from the Zagros to the southeast and farther east beyond the Oman/Minab line, the E-W structure of the Makran accretionary complex results from the active ocean continent subduction zone between the Oceanic Oman Sea plate and Makran province of the Iranian plate. This province is bordered by two faults at its eastern and western edges: they are influenced by the continent-continent collision system (Arabian/Iranian and Indian and Asian plates).

Qeshm Island, at the mouth of the Persian Gulf, was also studied. Qeshm is the largest island (1600 km2) in the Persian Gulf and the most populated island of Iran. It is located in the Strait of Hormuz (Fig. 2) and extends from 26°30' to 27°00'N and from 55°15' to 56°17'E. The shortest distance by sea to Bandar Abbas city (center of Hormozgan province) is 25 km and the nearest point of the Iranian mainland lies at 2.5 km. The Qeshm area, lying on the southern coasts of Iran constitutes the eastern termination of the Zagros Province, and is characterised by the same geological, sedimentary and structural features. The emergence of Tertiary sediments, partly associated with younger or Quaternary deposits, resulted from the compressive tectonic forces related to the latest phase of the Alpine orogeny. This phase has been the most important folding phase affecting the entire Zagros structural Province after the late Tertiary. A preliminary study (Haghipour and Fontugne, 1993) indicates local uplift rates for marine terraces ranging from 1.1 to 2.6 mm lyr.

Sampling and determination of absolute ages and uplifting rate

Along the coastal areas of the northern Persian Gulf and Makran province, the Quaternary marine terraces (usually a few meters to about 10 m each) are well developed, forming steep-like elevated cap rocks. More than 25 levels were found in the Qeshm Island and up to 16 levels in Chah Bahar area, in the eastern Makran. Only few terraces could have been displaced as the result of faulting. These terraces consist of coral lumachelle limestone/ grindstone and sandstone deposits. All of them unconformably overly the older Miocene and Pliocene bedrock formations. The maximum inland extension of the marine terraces is in the Sedij area (Makran province), about 10 km from the present shoreline.

Locations of sampling of the 102 terraces are reported in Table 1 and Figure 2-3. Samples were collected for a preliminary estimation of recent coastal movements as deduced from ^{14}C (lowest terraces) and Th/U (highest terraces) age determination methods. The samples selected from the Quaternary terraces for age determination consisted of lime shells and corals, previously analyzed by X-ray diffraction. Only aragonite coral samples (the primary phase at the time of formation) were chosen to determine the age of

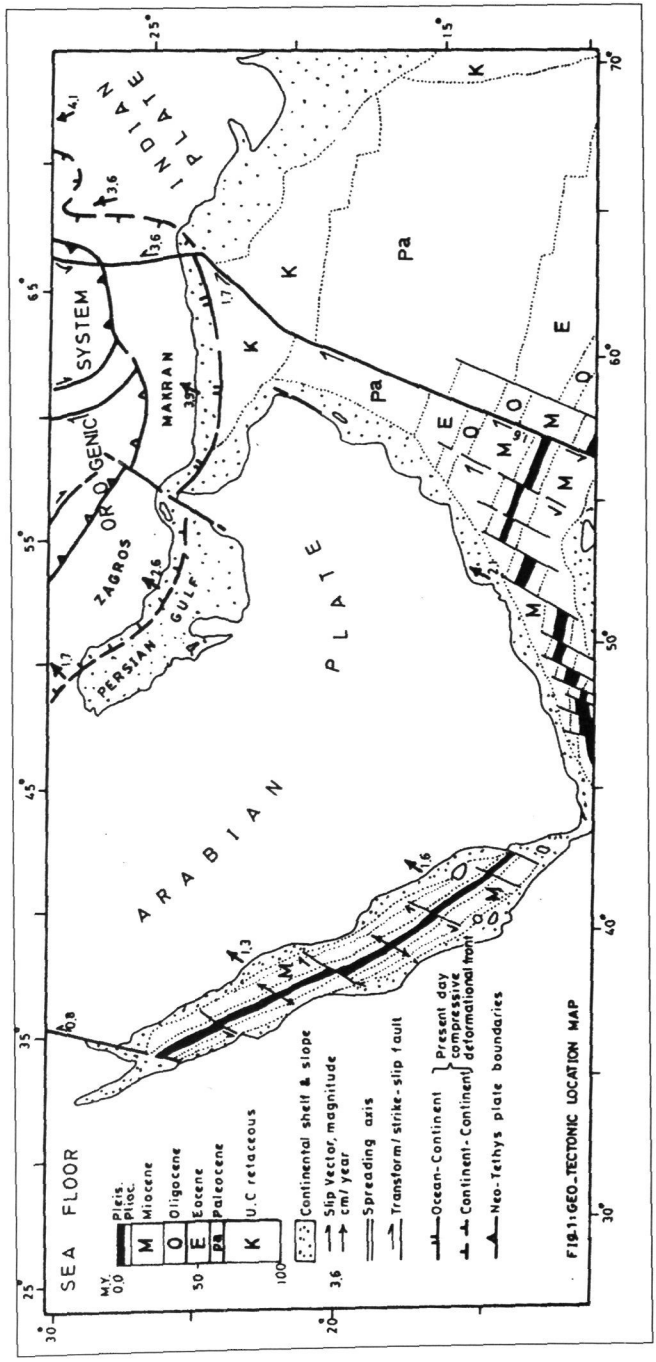

Figure 1. Geotectonic location map.

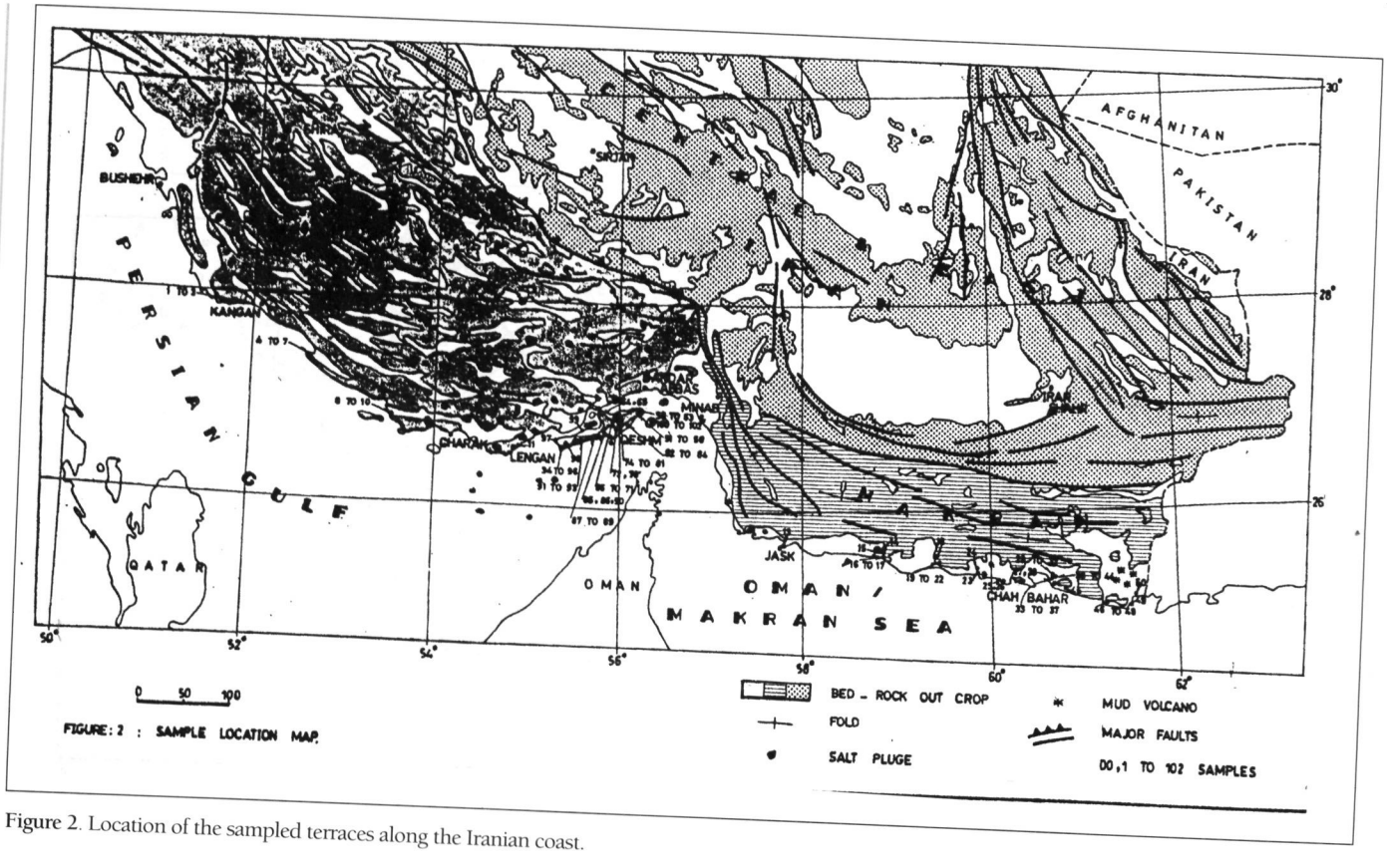

Figure 2. Location of the sampled terraces along the Iranian coast.

LOCATION	N°	LATITUDE	LONGITUDE	ALTITUDE	SAMPLE
QESHM	QE 51	26°55'40"	56°15'00"	1	2
	QE 52	26°55'40"	56°15'00"	6	1+2
	QE 53	26°55'30"	56°11'59"	13	1+2
	QE 54	26°55'36"	56°11'52"	26	1+2
	QE 55	26°55'49"	56°11'46"	43-48	1+2
	QE 56	26°56'46"	56°13'57"	90	1
	QE 57	26°56'46"	56°13'57"	100	1
	QE 58	26°56'21"	56°13'28"	70	1+2
	QE 59	26°59'33"	56°09'26"	9	1
	QE 60	26°59'59"	56°09'06"	70-60	1
	QE 61	26°57'56"	56°13'57"	132±15	1
	QE 62	26°58'08"	56°14'18"	100	2
	QE 63	26°58'21"	56°15'08"	25? 15	1+2
	QE 64	26°57'05"	55°45'10"	1PM	1
	QE 65	26°56'42"	56°45'10"	27	1
	QE 66	26°56'57"	55°59'14"	1,5PM	1
	QE 67	26°56'57"	55°59'14"	1,5PM	1
	QE 68	26°56'57"	55°59'14"	15-25	1
	QE 69	26°56'35"	55°59'08"	45	1
	QE 70	26°56'35"	55°59'08"	51	1
	QE 71	26°56'41"	55°59'17"	70-80	1
	QE 72	26°55'57"	56°01'55"	120-160	1+2
	QE 73	26°55'06"	56°02'06"	112	1
	QE 74	26°52'44"	56°04'55"	140	1+2
	QE 75	26°52'14"	56°05'18"	160-145	1+2
	QE 76	26°52'43"	56°04'54"	125	1
	QE 77	26°53'01"	56°04'47"	110	1
	QE 78	26°53'00"	56°04'45"	96	1
	QE 79	26°52'54"	56°04'12"	90	1
	QE 80	26°51'32"	56°03'25"	45	1
	QE 81	26°50'10"	56°04'05"	25-35	1
	QE 82	26°46'45"	56°04'22"	6	1
	QE 83	26°46'45"	56°04'22"	0,5PM	1
	QE 84	26°46'45"	56°04'22"	1,5	1
	QE 85	26°43'12"	56°49'15"	14	1+2
	QE 86	26°43'21"	55°49'12"	20-50	1+2
	QE 87	26°43'10"	55°41'09"	220*206	1+2
	QE 88	26°43'34"	55°42'37"	180	2
	QE 89	26°43'14"	55°43'52"	155	1
	QE 90	26°46'56"	55°49'19"	20	1
	QE 91	26°36'51"	55°31'41"	6,5PM	1
	QE 92	26°36'51"	55°31'12"	15-18	1
	QE 93	26°36'47"	55°31'12"	13	1
	QE 94	26°32'20"	55°17'24"	4pm	1+2
	QE 95	26°34'10"	55°16'36"	20	1
	QE 96	26°33'10"	55°16'47"	12	1+2
	QE 97	26°39'22"	55°15'42"	4,5PM	1
	QE 98	26°35'42"	55°20'53"	145	1
	QE 99	26°44'35"	55°38'11"	27	1
	QE 100	26°59'44"	56°12'40"	10PM	1+2
	QE 101	26°59'26"	56°13'00"	30	1+2
	QE 102	26°59'26"	56°13'00"	21	1+2

Table 1. Location, origin and altitude of the samples collected along the Iranian and Qeshm island coast.

LOCATION	N°	LATITUDE	LONGITUDE	ALTITUDE	SAMPLE
DAYER	DA 1	27°49'59"	51°54'23"	msl 1,5±0,5	1
	DA 2	27°49'59"	51°54'23"	msl 1,5±0,5	2
	DA 3	27°49'59"	51°54'23"	9	1+2
HALEH	HA 4	27°23'49"	52°35'38"	2,5PM	1+2
	HA 5	27°23'49"	52°35'38"	100	1+2
	HA 6	27°23'49"	52°35'38"	30	1
	HA 7	27°23'49"	52°35'38"	23	2
JAZEH	JA 8	26°49'36"	53°31'31"	9-6	1+2
	JA 9	26°49'36"	53°31'31"	20-21	2
	JA 10	26°49'36"	53°31'31"	38	1
LENGEH	LE 11	26°46'12"	53°37'06"	7	2
POL	PO 12	26°58'21"	55°44'42"	2,5	1
JASK	JA 13	25°38'11"	57°45'59"	2PM	1
SEDICH	SE 14	25°37'19"	58°52'46"	70-75	1
	SE 15	25°34'28"	58°53'24"	35-45	1
	SE 16	25°32'08"	58°53'04"	13	1+2
	SE 17	25°32'08"	58°53'04"	3	1+2
ZARABAD	ZA 18	25°32'50"	59°24'48"	40	1
	ZA 19	25°29'27"	59°27'41"	50	1
	ZA 20	25°29'27"	59°27'41"	38	1
	ZA 21	25°29'27"	59°27'41"	32	1
	ZA 22	25°29'27"	59°27'41"	25	1
TANG	TA 23	25°23'20"	59°52'26"	25-30	1
	TA 24	25°24'12"	59°53'05"	55-60	1
GORDIM	GO 25	25°21'19"	60°07'15"	70	1
	GO 26	25°21'19"	60°07'15"	60	1
KONARAK	KO 27	25°21'16"	60°21'18"	70	1
	KO 28	25°21'16"	60°21'18"	33	1
CHABAHAR	CH 29	25°23'02"	60°38'17"	200	1
	CH 30	25°23'02"	60°38'17"	180	1
	CH 31	25°23'02"	60°38'17"	160	1
	CH 32	25°23'02"	60°38'17"	137	1
	CH 33	25°20'17"	60°37'47"	140	1
	CH 34	25°20'17"	60°37'47"	133	1
	CH 35	25°20'17"	60°37'47"	130	1
	CH 36	25°20'17"	60°37'47"	125	1
	CH 37	25°20'17"	60°37'47"	110	1
	CH 38	25°20'25"	60°37'02"	80	1
	CH 39	25°20'25"	60°37'02"	60	1
	CH 40	25°20'46"	60°36'55"	53	1
	CH 41	25°19'25"	60°37'26"	36	1
	CH 42	25°19'18"	60°37'21"	28	1
	CH 43	25°19'18"	60°37'21"	20	1
	CH 44	25°19'10"	60°37'13"	4	1
LIPAR	LI 45	25°15'33"	60°49'20"	52	1
BERIS	BR 46	25°07'16"	60°12'06"	40	1
	BR 47	25°07'16"	60°12'06"	49	1
	BR 48	25°07'14"	61°13'52"	53	1
PASA-BANDAR	PA 49	25°05'36"	61°26'01"	40	1
GWATER	GW 50	25°09'55"	61°30'07"	3	1
					Shell=1
					Coral=2

Table 1. Location, origin and altitude of the samples collected along the Iranian and Qeshm island coast.

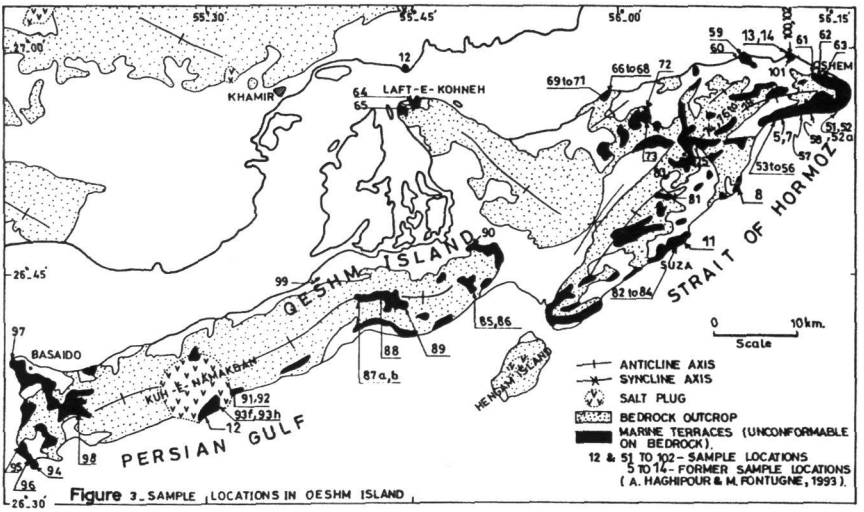

Figure 3. Location of the sampled terraces in Qeshm Island.

Location	Sample	N°	emersion	GIF-N°	Age BP	$\partial^{13}C$	AGE Cal BP
DAYER	1	DA 1	1.5 ± 0.5	9840	3,270 ± 45	1.8	2950-2740
POL	1	PO 12	2.5 ± 2	9841	3,610 ± 35	1.42	3371-3172
JASK	1	JA 13	>2	9842	24,800 ± 800	1.52	
CHABAHAR	1	CH 44	2±2	9843	3,670 ± 50	-1,34	3466-3213
GWATER	1	GW 50	3±1,5	9844	25,970 ± 300	0.49	
QESHM	2	QE 51	2.5±1	9845	calcite		
QESHM	1+2	QE 52	6±2/2±1	9846	calcite		
QESHM	1	QE 64	4 ±2.5	9847	5,650 ± 50	2.15	5934-5700
QESHM	1	QE 66	3 ±0.5	9848	6,210 ± 50	2.04	6556-6297
QESHM	1	QE 67	2.5±0.5	9849	4.400 ± 50	2.27	4420-4125
QESHM	1	QE 83	1,5 ±1.5	9850	>30,000	0.92	
QESHM	1	QE 84	0,5 ±1.5	9851	38,300 ± 300	-0,73	
QESHM	1	QE 93	13	9852	5,680 ± 70	1.96	6026-5681
QESHM	1+2	QE 94	≥8	9853	>31,000	2.86	
QESHM	1	QE 97	≥4.5	9854	>33,000	2.56	
QESHM	1	QE 91	8.0 ±2	9855	5,040 ± 50	1.33	5283-4970
	Shell=1						
	Coral= 2						

Table 2. Radiocarbon dating of marine terraces.

terrace formation. Fourteen ^{14}C dates were determined by ß-counting, from shells samples in the lower terraces. Calibrated ages were obtained using the marine calibration curve of the model proposed by Stuiver and Braziunas (1993) with a $\Delta R=190 \pm 25$ years for the Persian Gulf (Southon and Fontugne unpublished data). Because of the large number of the recrystallized coral samples, only six samples, all containing less than 1-2% calcite, were suitable for $^{230}Th/^{234}U$ dating of the upper terraces (10-25 m versus present mean sea level).

Results and discussion

Results are reported in table 2 (^{14}C dating) and table 3 ($^{230}Th/^{234}U$ dating). Holocene ages correspond to only three formations along the coast of the Persian Gulf and Makran Province, and five in Qeshm Island. The ages of these formations range between 3,270 and 6,210 years BP. Older terraces (>26,000 years BP) were found at elevations lower than 4 metres at Jask, Gwater and Qeshm Island.

The Holocene data from Iran, compared with the mean sea-level curve reported from other areas of the Persian Gulf and the northern Indian Ocean (Pirazzoli, 1991), suggest a relatively minor uplift. The precise uplift rate, or the differential uplift rate between the different tectonic provinces, cannot be deduced from our Holocene data. However, such results show that previous estimates (Haghipour and Fontugne, 1993) have overestimated the water depth for deposition of the dated samples, and suggest that the uplift rate outside the salt dome areas is less than 1.1 mm/year.

The older terraces, at altitudes ranging from 10 to 26 metres a.s.l. have yielded $^{230}Th/^{234}U$ U/Th ages between 104 and 139 ka (Table 3). However, the six coral samples analyzed contained calcite, and their $^{238}U/^{234}U$ ratios are not strictly representative of the sea water one (1,149). Such a pattern could provide an explanation for the large scattering in age values, often encountered in such studies. Nevertheless, all these formations are representative of isotopic stage 5e, with the exception of sample QE-54, which may be associated with isotopic stage 5c.

The average rate of annual uplift in the Qeshm Island and along the coast of the Persian Gulf can be estimated by using those absolute ages to estimate the sea-level position at the time of formation of each terrace. The most likely mean uplift rate in this area would be 0.2 mm/yr, since the last interglacial period (125 ka). Such an estimate is consistent with those determined from Holocene terraces, but is much lower (more than one order of magnitude) than the 6.6 mm uplift rates claimed by Vita-Finzi (1979).

Conclusion

Elevations of Holocene raised terraces are of the same order as those reported from other areas in the Persian Gulf and the northern Indian Ocean. They indicate that no important uplift occured since 6.2 ka. The long term uplift rate is low, as deduced from dating of isotopic stage 5e terraces. Results obtained for Holocene and late Pleistocene periods desagree with those proposed by previous authors. However, this study should be considered as preliminary. Other suitable samples for dating are needed to confirm the trends. In addition, further estimates of the relative variations of sea level during the two last climatic cycles will soon be obtained using ESR dating.

Sample	altitude	%Calcite	^{238}U ppm	$^{234}U/^{238}U$	$^{230}Th/^{234}U$ to	$^{230}Th/^{232}Th$	Age ka	1sigma ka
QE 54B	26m	1,5	2,66 ±0,05	1.16±0.02	0.624 ±0.018	>500	104	108-99
QE 100	10m	1	2,67±0,03	1.14±0.01	0.734 ±0.017	402	139	145-133
QE 102	21m	1,5	2,66 ±0.05	1.14±0.02	0.700 + 0.018	296	127	133-121
HA 7	23m	0	2.59 ± 0.04	1.21 ± 0.02	0.654 + 0.013	544	111	115-107
JA 8	6-9m	1	2.97 ± 0.06	1.20 ± 0.03	0.714 ± 0.038	210	130	144-118
JA 9	21m	0	3.08 ± 0.08	1.21. ± 0.03	0.676 ± 0.031	>500	118	128-109

Table 3. $^{230}Th/^{234}U$ ages of marine terraces.

Acknowledgements

We are very grateful to G. Haddad for his suggestions and his help in editing the manuscript. We thanks Qeshm Free Area authorities for their logistical and financial support.

References

Bloom, A.L., Broecker, W.S., Chappel, J., Matthews, R.K., and Mesolella, K.J.: (1974) Quaternary sea level fluctuation on a tectonic coast: new 230Th/234U dates from the Huon Peninsula, New Guinea, *QuaternaryResearch,* 4:185-205.

Chapell, J. and Veeh, H.H.: (1978) 230Th/234U age support of an interstadial sea level of -40 m at 30,000 years BP, *Nature,* 276:602-603.

Haghipour, A. and Fontugne, M.: (1993) Quaternary upiift of Qeshm Island, *C.R. Acad. Sci. Paris* 317, II: 419-424.

Pirazzoli, P.A.: (1991) *World atlas of Holocene sea level changes,* Elseviers Oceanography series 58, 300 pp.

Snead, R.J.: (1993) Uplifted marine terraces along the coasts of Pakistan and Iran *in* J.F. Shroder (ed) *Himalaya to the sea,* Routledge, London.

Stuiver, M. and Braziunas, T.F.: (1993) Modeling atmospheric 14C influences and 14C ages of marine samples to 10,000 BC., *Radiocarbon,* 35: 137-189.

Vita-Finzi, C.: (1979) Rates of Holocene folding in the coastal Zagros near Bandar Abbas, Iran, *Nature,* 278:632-633.

Vita-Finzi, C.: (1979) Recent crustal deformation near the strait of Hormoz, *Proc. R. Soc.,* 382:441-457.

TOWARD NEAR-WEEKLY CLIMATIC HISTORIES FROM LATE QUATERNARY CORALS

M.K.Gagan [1], L.K. Ayliffe [1], A.R. Chivas [1], M.T. McCulloch [1], P.J. Isdale [2], S. Anker [3], D. Hopley [3], W.S. Hantoro [4], and J.M.A. Chappell [5].

1 Research School of Earth Sciences, The Australian National University, Canberra, ACT 0200, Australia
2 Australian Institute of Marine Science, P.M.B. No.3, Townsville M.C., Qld. 4810, Australia
3 Sir George Fischer Centre, James Cook University, Townsville, Qld. 4810, Australia
4 Research and Development Centre for Geotechnology, Indonesian Institute of Sciences, Jl. Cisitu Sangkuriang, 21/154D, Bandung 40135, Indonesia
5 Research School of Pacific and Asian Studies, The Australian National University, Canberra, ACT 0200, Australia

Abstract

Natural climate variability in the tropics is poorly understood because high quality instrumental records from low laUtudes are generally limited to the past several decades and to isolated sites. Coral-based research is designed to provide long-term perspectives of the dynamics of the monsoon, El Niño-Southern Oscillation (ENSO), and climate-linked surface ocean currents. Long-lived massive corals from modern reefs may be uniquely capable of providing accurate proxy records of these important climatic systems over the past several centuries (Dunbar and Cole, 1993). Such records are essential for establishing a lengthy baseline of natural climate variation agaist which any man-induced climate change should be detectable.

Summarised in this paper are some recent research highlights including: (1) documentation of the dynamics of the Leeuwin Current; (2) new evidence for skeletal ^{13}C enrichments driven by synchronised coral spawning; (3) documentation of the magnitude of Pinatubo-induced sea-surface cooling in the Western Pacific Warm Pool; and (4) evidence for a weaker ENSO and monsoon in the southwest Pacific during the mid-Holocene «climatic optimum».

Leeuwin Current Dynamics

Ningaloo Reef, Western Australia, is a good site at which to test the sensitivity of the Leeuwin Current to sea-surface temperatures (SSTs) and tradewind strength (Southern Oscillation) in the area of the Western Pacific Warm Pool (WPWP). Such information is important for understanding the dynamics of the Indonesian Throughflow (Fig. 1) which is suspected to have an effect on global ocean circulation that is disproportionate to its size. Highlights of the 15-year-long (1978-1993), near-weekly Ningaloo Reef oxygen isotope ($\partial^{13}O$) and carbon isotope ratio ($\partial^{13}C$) record are summarised in Figure 2. Winter SSTs (derived from coral $\partial^{18}O$ values) respond to the phase and strength of the ENSO cycle. During anti-ENSO years, enhanced winter southeast tradewinds set-up sea levels north of Australia which strengthen the Leeuwin Current (warmer winter SSTs). The opposite occurs during ENSO years when the tradewinds relax or reverse (cooler winter SSTs). This mechanism appears to be operating during the very strong ENSO of 1982 (coolest winter) and during the strong anti-ENSO of 1988 (warmest winter).

Three metre-high coral colonies growing at Ningaloo Reef have now been drilled and the longest of these cores should yield a continuous history of Leeuwin Current variation spanning at least 200 years. Considerable information can be gained about the dynamics of the Indonesian Throughflow via this record, particularly if the magnitude of thermal and windforcing in the Throughflow region are known, in addition to the response of the Leeuwin Current. Multi-century SST records for the WPWP region are being prepared by colleagues overseas which can be used to estimate the magnitude of temperature-induced fluctuations in sea-level gradients between the Pacific and Indian Oceans. It may be possible to document winter tradewind strength using corals fringing southern Java (Fig. 1), where the magnitude of winter upwelling is driven by tradewind velocity. A pilot study is under way to evaluate the potential for using Javan winter SSTs as a proxy for tradewind strength in the region south of Indonesia. A similar approach to the Ningaloo Reef project is being tested in the western Indian Ocean (Kenyan reefs) where the flow velocity of the Somali Current is linked to the strength of the Southwest Monsoon, which brings seasonal rain to much of central Asia.

Synchronised Spawning Chronologies

Previous work at Pandora Reef, Great Barrier Reef (Figure 1) revealed a carbon isotope signature closely corresponding to the annual October/November coral spawning event (Gagan et al., 1994). Such a signal would be particularly useful because the timing of spawning is brief and very predictable thus making it possible to construct precise chronologies for coral-based data (Harrison and Wallace, 1990). Ningaloo Reef is a good site at which to validate the carbon isotope-spawning link because the timing of synchronised spawning at Ningaloo is exactly 4 months later than in the Great Barrier Reef.

Maximum ^{13}C enrichments (highest $\partial^{13}C$ values) are thought to mark the times of coral spawning (Figure 2). It is important to note, however, that prior to 1984 there are no substantial ^{13}C enrichments which is interesting because it generally takes 4-8 years for a massive coral to reach sexual maturity. This «quiet zone» in the coral $\partial^{13}C$ record (1978-83) seems to reflect what for this coral specimen would be the first 6 non-repro-

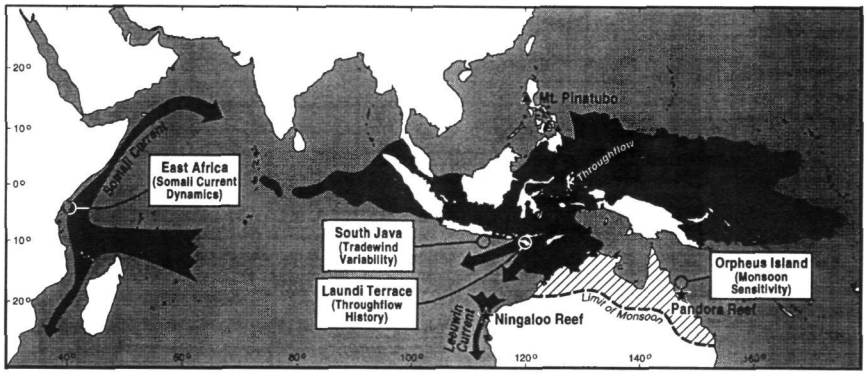

Figure 1. Physiographic map showing the location of reef study sites, the Western Pacific Warm Pool (WPWP, mean SST>28° C), and schematic ocean circulation patterns.

ductive years and provides new-found evidence for a connection between skeletal $\partial^{13}C$ and coral spawning. The ^{13}C enrichment in 1984, therefore, probably marks the onset of spawning which is repeated every year thereafter.

From 1984 to 1990, there is a remarkable coincidence between the time of the maximum ^{13}C enrichments and the known spawning dates for Ningaloo Reef (Fig. 2). The spawning signal for all 7 years matches the known spawn dates within the error of the timeseries (± 30 days) which was plotted assuming the minimum SST arrives near October 1. The utility of the mass spawning signal is well illustrated during the years of 1988-89 when the maximum summer SSTs arrived about 2 months later than normal. The fact that the spawning signal occurs at the expected time during these years, regardless of changes in the timing of the SST cycle, testifies to its usefulness as a «built-in» time-clock that is independent of SST. The ^{13}C-response to spawning should provide an accurate chronometer since the annual spawn-times are separated by exactly 12 or 13 lunar months and can be forecasted to within ± 3 days. Synchronised spawning is common for long-lived massive corals and, to date, has been documented in the Great Barrier Reef, eastern Indian Ocean, Caribbean, Red Sea, Japan, and elsewhere (Harrison and Wallace, 1990), so it may provide a widely applicable coral chronometer.

Pinatubo Aerosol-induced Cooling

The stratospheric aerosol cloud produced b y the major volcanic eruption of Mt. Pinatubo (June 1991) in the Philippines (Fig. 1) produced an estimated 0.3°C cooling of the lower atmosphere in 1992-93. Yet it is the distribution and magnitude of sea-surface cooling, particularly in the tropics, which may be crucial for understanding volcano-induced climate change. Documenting the magnitude of cooling in the WPWP may be particularly important since equatorial gradients in Indo-Pacific SSTs drive the Walker circulation. The magnitude of sea-surface cooling in the WPWP has not been documented because it is difficult to correct satellite retrievals of SST which show negative biases exceeding 1°C in the aerosol contaminated tropical regions.

Alternatively, we produced a 12-year (1981-93) near-weekly oxygen-isotope record from a Western Australian (Ningaloo Reef) *Porites lobata* coral precisely positioned to

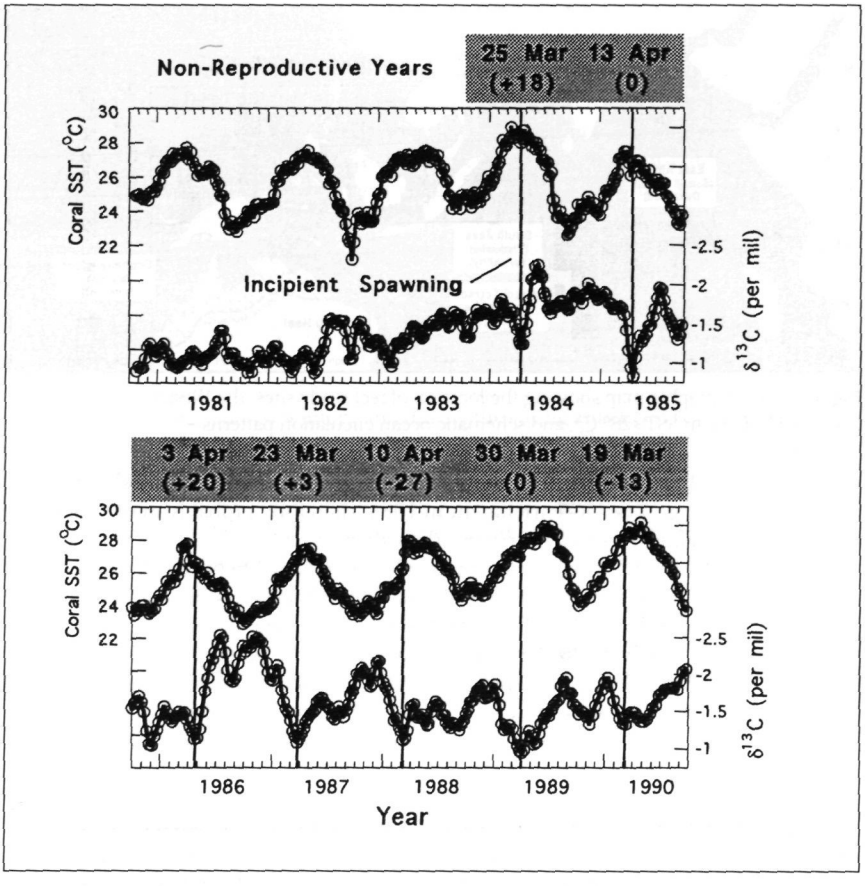

Figure 2. Near-weekly time-series of $\partial^{18}O$ (converted to equivalent SSTs) and $\partial^{13}C$ values from the Ningaloo Reef *Porites lobata* coral. The timing of maximun ^{13}C enrichment (shown by vertical lines) is compared with the documented timing of coral spanwing at Ningaloo Reef. Numbers in brackets indicate the difference (no. of days) between the knwon spawn dates and the spwan times given by the timing of the maximun ^{13}C enrichments.

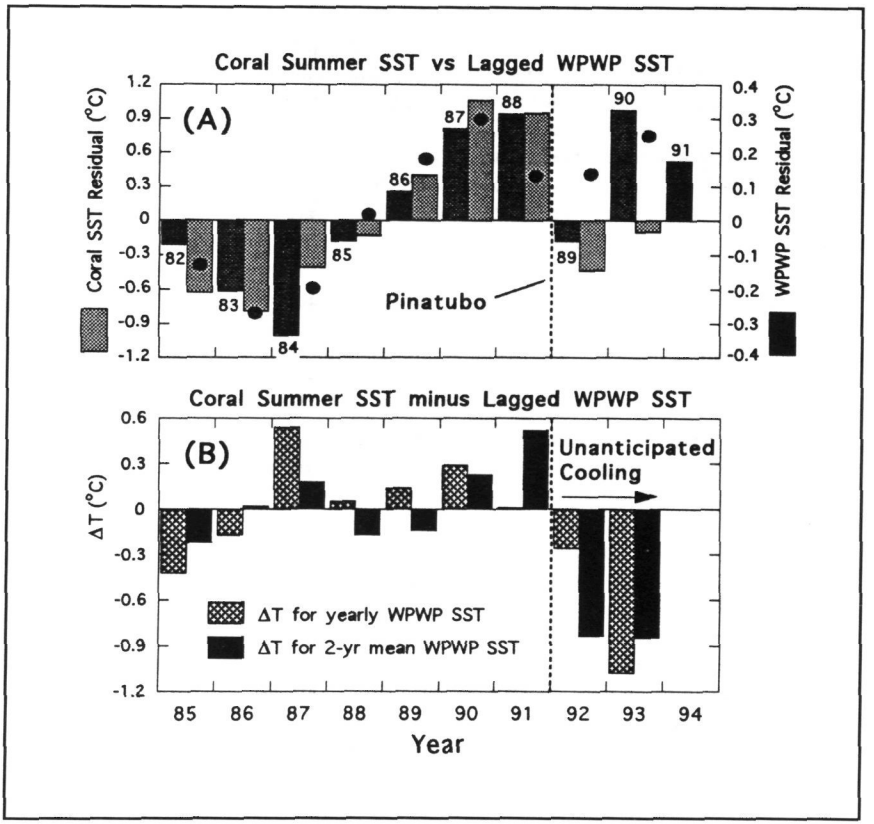

Figure 3. (A) Comparison of Ningaloo coral summer (January-April) SST residuals (light stippled bars) with 32-month lagged yearly SST residuals for the WPWP (Yan *et. al.*, 1992; dark stippled bars). Numbers adjacent to dark stippled bars indicate the calendar year of each WPWP residual. Black dots show the 2-yr running mean for the WPWP residuals (26 month lag). See text for data-fitting technique. (B) Difference between coral summer SST residuals and lagged WPWP SST residuals (ΔT) shown in (A). The magnitude of unanticipated post-Pinatubo cooling at Ningaloo Reef is about 0.6°C (1992) to 0.9°C (1993).

record the SST variation of the Leeuwin Current (Gagan and Chivas, 1995). The predictability of the Ningaloo Reef coral-based SSTs may be unparalleled since it can be shown that SST changes in the WPWP are strongly correlated with, and lead by about 2.5 years, SST changes in the Leeuwin Current. This connection is illustrated in Figure 3a where lagged WPWP SST residuals, derived from satellite and ship-based SST data (Yan *et al*, 1992), are compared to the Ningaloo coral-derived SSTs. The closest correspondence of the WPWP and Ningaloo SSTs is obtained for the summer, after allowing a 32 month lag for «average» WPWP water to reach Ningaloo Reef. This correlation has been optimised (r=0.91, SD=0.33°C) by amplifying the WPWP residuals by a factor of 3.25. The fit is improved slightly (r= 0.94, SD=.28°C) by applying a 2-year running mean. Consequently, the ordinary SST variation in the Ningaloo coral record can be anticipated and removed to reveal unexpected cooling of 0.6°C (1992) and 0.9°C (1993) following the June 1991 eruption of Mt. Pinatubo (Fig. 3b). This cooling signal at Ningaloo Reef is likely to be produced by Pinatubo aerosol-induced cooling of the southwestern WPWP averaging 0.5°C by early 1992 which is sustained at least through early 1993.

This magnitude of volcanic cooling in the southwestern WPWP could have prolonged, in part, the extended 4-year (1991 -1994) negative phase of the Southern Oscillation. General circulation models suggest that when tropical regions cool, the strength of the Hadley cell circulation (and rainfall) are reduced. A weakened Hadley cell may serve to prolong an ENSO event since it is the tradewinds generated by this circulation that help confine warm water to the Western Pacific. Also notable is that the magnitude of volcanic cooling in the southwestern WPWP (0.5°C) is substantial compared to the ordinary interannual variation (SD=0.2°C, Fig. 3a), which includes the very strong El Niño (1982-83) and strong La Niña (1988). Furthermore, radiation flux anomalies recorded during the spaceborne Earth Radiation Budget Experiment showed that changes in the radiation balance throughout the tropics were not homogeneous; the largest decreases in net radiation occurred over the deep convective storm regions, including the WPWP. If the WPWP seasurface cooling is not matched elsewhere in the tropics, the relative increase in surface pressure over the WPWP may reduce the convergence of moist air (and convection) into the region thus weakening the Walker circulation to prolong an established ENSO.

Testing Climate Sensitivity With Ancient Corals

A key priority in global climate change research is to understand the sensitivity of the tropical climate to changes in mean global temperature (warming or cooling). Fossil corals recording relatively warm, Late Pleistocene interglacial climates may provide partial analogues of an earth warmed by greenhouse gases. Work is under way to apply the highresolution isotopic techniques described above to ancient corals to document the range of climate variation in the past. Pilot studies have been initiated at oceanic sites where there is potential to compare well calibrated records from modern corals with those from nearby fossil corals. Such sites include the Laundi Terraces of Indonesia and Orpheus Island in the Great Barrier Reef (Fig. 1).

Laundi Terraces. Published age-dates for the Laundi Terraces of Sumba Island suggest that this unique flight of coral terraces extends back to at least 800 ka BP (Pirazzoli *et al*, 1993). Reconnaissance examination of the terraces confirmed the potential of the area for documenting, in detail, the sensitivity of the Indo-Australian monsoon and the Indonesian Throughflow to changes in global temperature. In addi-

tion to being complimentary to the Ningaloo Reef research, the Laundi Terraces should provide access to Oxygen Isotope Stages 9 (*ca.* 300 ka) and 11 (*ca.400* ka) which are thought to mark the late Quaternary Earth's warmest periods.

Orpheus Island. Well-preserved massive *Porites* micro-atolls (6 m diameter) from Orpheus Island, Great Barrier Reef have been cored to reveal 100 years of continuous coral growth, and radiocarbon date to 5.8 ka BP. Examination of the coral UV fluorescence patterns, indicating the intensity of runoff from mainland rivers, suggests that monsoonal rainfall in northeast Australia was generally weaker and much less variable than at present. We documented the magnitude of possible ENSO events by examining seasonal SST and rainfall patterns using high-resolution, tandem measurements of coralline $\partial^{18}O$ and Sr/Ca (Gagan *et al,* 1995). Contemporary ENSO-induced droughts in northeast Australia coincide with cool SST anomalies (1-2°C) in the southwest Pacific. Near-weekly $\partial^{18}O$ and Sr/Ca data from a 12-year transect bracketing the largest drought on record, as indicated by UV fluorescence, show no evidence of even moderate El Niño-induced cooling. Depletions in skeletal $\partial^{18}O$ produced by individual rainfall events demonstrate that although monsoonal rainfall intensity was relatively weak, it commonly persisted for up to six months, extending well into the austral autumn. The results suggest that this period of the mid Holocene in the southwest Pacific was characterised by weaker ENSOs and more dependable but moderate rainfall, rather than the warmer conditions and higher rainfall that are generally associated with the mid-Holocene «climatic optimum».

Acknowledgements

We wish to thank J. Cali, G. Mortimer, and X. Wang for assistance with the mass spectrometry; D. Meyers and R. Karniewicz for logistical support at Ningaloo Reef; and C. Veron who identified coral species. Financial support was provided by the Australian National Greenhouse Advisory Committee.

References

Dunbar, R.B. and Cole, J.E.: (1992) Coral records of ocean-atmosphere variability. NOAA Climate and Global Change Program, Special Report No. 10, 38 pp.

Gagan, M.K., Chivas, A.R. and Isdale, P.J.: (1994) High-resolution isotopic records from corals using ocean temperature and mass-spawning chronometers, *Earth and Planetary Science Letters,* 121 :549-558.

Gagan, M.K. and Chivas, A.R.: (1995) Oxygen isotopes in Western Australian coral reveals Pinatubo aerosol-induced cooling in the Western Pacific Warm Pool, *Geophysical Research Letters,* 22: 1069-1072.

Gagan, M.K., Ayliffe, L.K., McCulloch, M.T., Anker, S., Hopley, D. and Isdale, P.J. :(1995) Sr/Ca and $\partial^{18}O$ in Great Barrier Reef corals and ENSO dynamics at 5 ka BP, EOS supplementary Issue 76:316.

Harrison, P.L. and Wallace, C.C.: (1990) Reproduction, dispersal and recruitment of scleractinian corals (cd. Z. Dubinsky), *Coral Reefs,* Amsterdam, 133-207.

Pirazzoli, P.A., Radtke, U., Hantoro, W.S., Jouannic, C., Hoang, C.T., Causse, C. and Borel Best, M.: (1993) A one million-year-long sequence of marine terraces on Sumba Island, Indonesia, *Mar. Geol,* 109:221-236.

Yan X.,-H., Ho C.,-R., Zheng, Q. and Klemas, V.: (1992) Temperature and size variabilities of the Western Pacific Warm Pool, *Science,* 258:1643-1645.

BEHAVIOUR OF THE GLACIAL INTERGLACIAL-GLACIAL TRANSITIONS RECORDED IN CHINA LOESS

Z.T. Guo

Institute of Geology, Chinese Academy of Sciences, P.B. Box 9825, Beijing 100029, China

Abstract

Two loess sections in the central Loess Plateau in China are studied to characterise the behaviour of the climatic transition from the penultimate glaciation to the last interglacial and that of the subsequent interglacial-glacial transition. Measurements on free iron and total iron contents and micromorphological observations converge to demonstrate that both transitions were marked by a severe climatic event at millennial scale, which cannot be directly attributed to the orbitally induced insolation changes and ice-volume variations. During these events, the Loess Plateau region was characterised by destruction of vegetation and strong aeolian dynamics, probably in relation with strong winter monsoon winds. Natural fire may have played an important role in the destruction of the pre-existed vegetation.

Introduction

In the recent years, paleoclimatic studies in a number of regions tend to show that the transitions between glacial and interglacial periods were associated with some catastrophic and abrupt events. In the North Atlantic region, the transition from the last glacial period to the Holocene (the last deglaciation) experienced an abrupt and striking cooling event (the Younger Dryas; Overpeck *et al;* 1989) which has been also identified in many other parts of the world (Kudras *et al.*, 1991; Van Camp and Gasse, 1993; Yan and Petit-Maire, 1994), while the termination of the last interglacial (marine $\partial^{18}O$ stage 5) is marked by massive discharge of icebergs into the ocean (Heinrich event 6) associated with the decrease in atmospheric temperature in the circum-Atlantic region (Bond *et al,* 1992). A similar event may have occurred right at the termination of the penultimate glaciation (transition $\partial^{18}O$ stage 6 to 5; Broecker, 1994). The transition of $\partial^{18}O$ stage 5 and 4 was also synchronous with a major volcanic eruption (Toba eruption)

73,500 years ago, which is thought to have greatly influenced the global climates (Rampino and Stephen, 1992). A question arisen is if synchronous changes have been documented in the loess-soil sequence in the Loess Plateau of China, commonly regarded as a near continuous climatic record of Quaternary paleoclimates (Liu, 1985; Kukla, 1987; Kukla *et al.*, 1988). Based on geochemical and micromorphological studies from two loess sections in the central Loess Plateau, this paper aims to study the behaviour of the climatic transition from the penultimate glaciation to the last interglacial and that of the subsequent interglacial-glacial transition.

Materials and Methods

Two loess sections are studied, located at Luochuan (35°45' N, 109°25' E) and Yichuan (36°03'N, 110°10' E) in Shaanxi Province. A stratigraphic summary is given in Figure 1, which is quite similar to that of the other loess sections (Liu, 1985; Kukla, 1987, Kukla *et al.*, 1988; Liu *et al.*, 1995). Since magnetic susceptibility is widely used in characterising the stratigraphic boundaries of the loess-soil sequence in China (Kukla et *al* 1988), it is also measured on dry samples taken at 10 cm intervals using a Bartington susceptibility meter and expressed in SI units (Fig. 1).

In earlier studies (Liu, 1985; Kukla, 1987; Liu *et al*, 1995), the top soil (Holocene soil S0) was correlated with marine $\partial^{18}O$ stage 1 (Fig. 1). The underlying loess unit L1 was correlated with $\partial^{18}O$ stages 2,3 and 4, the soil complex S1 with stage 5 and the loess unit L2 with stage 6. This correlation pattern has been confirmed by radiocarbon and thermoluminescense dating results from different localities (Lu et *al.*, 1988; Forman, 1991; Liu et *al.*, 1995) .

In this study, two methods are used to characterise the behaviour of the climatic transitions. Firstly, bulk samples were taken at 10 cm intervals from the lower part of L1, the whole of the S1 soil and the upper part of L2, to measure the ratio of free iron and total iron contents (Fed/Fet, Fed and Fet are expressed as Fe_2O_3 weight percent). Fed is extracted by dithionite-bicarbonate-citrate method (Meha and Jackson, 1960). The ratio Fed/Fet, widely used by European pedologists, is a measurement of iron liberated from iron-bearing silicate minerals by chemical weathering (Duchaufour, 1983), and thus an indication of chemical weathering intensity which is in close relationship with paleoclimatic conditions. It should be mentioned that the possibility of iron translocation in loess can be basically excluded as non evidence of clay illuviation and hydromorphic features were identified. Secondly, thirty-two non-disturbed and oriented samples were taken from the transitional parts (about 1 m in thickness) covering the L1 /S1 and S1 / L2 boundaries for micromorphological studies. This method proved particularly useful in characterising the abrupt climatic changes recorded in paleosols and eolian sediments (Fedoroff, 1996).

Results and Discussions

Weathering intensity

The variations of the Fet /Fed ratio in the studied sections are shown in Figure 2. The values are much higher in S1 soil than in the overlying and underlying loess. It may be inappropiate to interprete the fluctuations of the ratio within S1 soil, since the last one in the Loess Plateau is a soil complex having been affected by three pedogenic

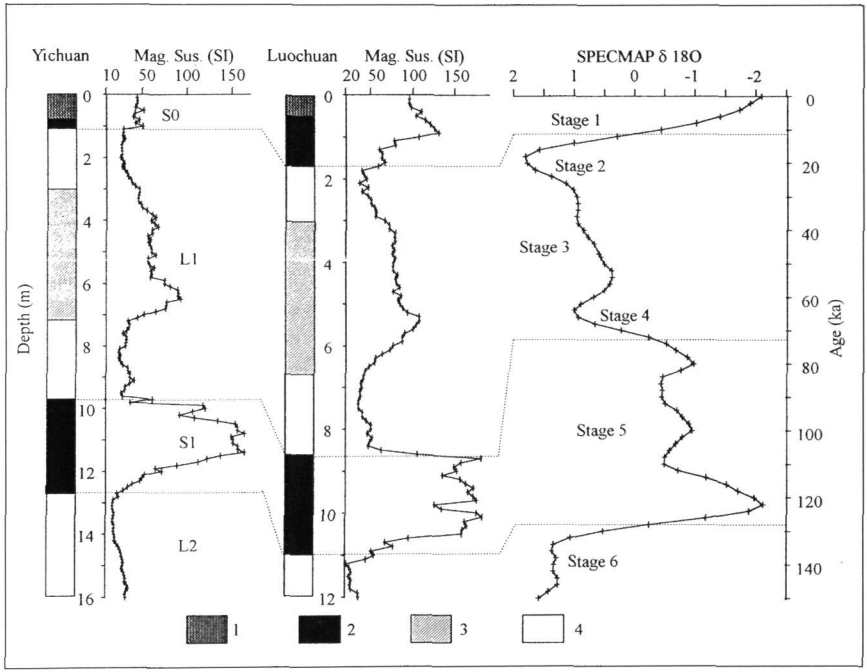

Figure 1. Stratigraphy and magnetic susceptibility of the Yichuan and Luochuan sections and correlation with SPECMAP marine $\partial^{18}O$ record ($\partial^{18}O$ data from Imbrie *et al.*, 1984). 1, Disturbed horizon; 2, palaeosol; 3, weakly developed palaeosol; 4, loess.

stages (Guo *et al.*, 1994; Liu *et al.*, 1995). The pedofeatures produced during the different pedogenic stages were overlapped, and, thus, influence the Fet / Fed ratio. In addition, the S1 soil experienced clay illuvial process, and translocation of iron along the profiles, can be expected.

The most significant features are the two peaks with lower values (Fig. 2). One locates just above the L1 /S1 boundary and another just below the S1 /L2 boundary. These peaks are clearly expressed in both sections, suggesting that they are climatically significant. The Loess Plateau is located within the east Asian monsoon zone and the modern climate is mainly controlled by two seasonally alternative monsoons, i.e. the warm-humid summer monsoon and the cold-dry winter monsoon (Liu *et al.*, 1995). Since the average soil temperatures in the region are below 0°C from late autum to early spring, under the modern interglacial conditions, chemical weathering of loess mainly depends upon the summer temperatures and precipitation, associated with the summer monsoon intensity, or / and dust accumulation rate associated with the winter monsoon intensity. Consequently, high Fet / Fed ratio can be interpreted as an indication of a strengthened summer monsoon or / and a weakened winter monsoon, and lower values indicate the inverse. The low Fet / Fed peaks therefore imply a significant weakening of summer monsoon or / and a strengthening of the winter monsoon.

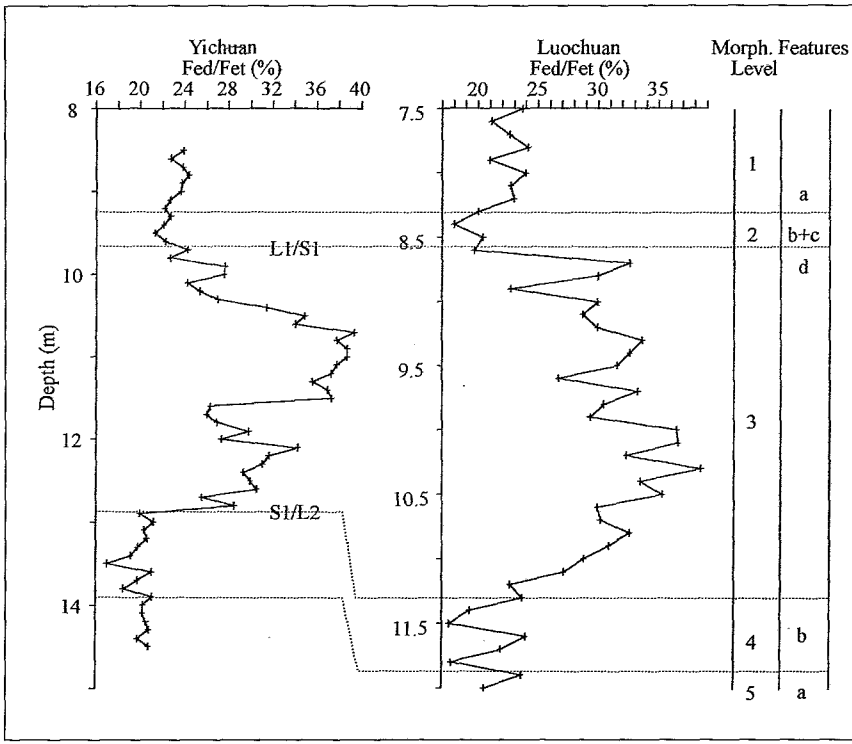

Figure 2. Variations of Fed/Fet ratio and ocurrence of selected micromorphological features in Yichuan and Luochuan sections. a. Loess with spongy microstructure; b, Loess with pseudo-sand microstructure; c, Charcoal particles; d, Fine silty textural feature.

Morphological features

The following morphological features have been identified. They are highly significant to the studied topics. Their stratigraphic occurence is shown in Figure 2.

(1) Abrupt L1 /S1 boundary: In both sections, the top of the S1 soil is truncated as indicated by an irregular and abrupt L1 / S1 boundary. Some soil fragments randomly distribute in the loess immediately overlying the boundary. However, non water-reworked features are observed. Truncation of the profiles was therefore related with aeolian erosion, suggesting strong aeolian dynamics and probably also a landscape with a very sparse vegetation cover, which is favourable to aeolian erosion.

(2) Loess with pseudo-sand microstructure: They are observed at the positions immediately overlying the L1 / S1 boundary and underlying the S1 / L2 boundary. In the field, they are massive with very few canalicular pores. Under the microscope, the groundmass contains a large amount of sand-sized (50-300 μm), rounded-subrounded aggregates (pseudo-sands) consisting of silty mineral grains and clay fraction. Some soil fragments are also observed. According to the experiments of Pye and Tsoar (1987), particles larger than 100 μm are unable to be transported by wind as suspended dust for long distance, and most of them would be deposited within 30 km from the source. The pseudo-sands were evidently derived from local materials, rather than typical aeolian

dust particles. Since non waterreworked feature is observed in these loess, the pseudo-sands must have been produced by aeolian erosion and transportation in saltation state, as is also supported by the rounded sharps. Consequently, the loess with this type of microstructure suggest a landscape with sparse vegetation cover and strong winds, thus dry-cold conditions.

(3) Charcoal particles: In the groundmass of the loess with pseudo-sand microstructure immediately overlying the L1 /S1 boundary, some (>1%) randomly distributed charcoal particles (generally >100 μm) are observed. The presence of charcoal particles has been reported from the aeolian sediments in tropical and temperate zones and is commonly regarded as evidence of natural fire (Fedoroff and Goldberg, 1982; Fedoroff, 1996). A question arisen is whether the fire is causally related with climatic change. The fact that charcoals particles are identified at L1 / S1 boundary in the loess with pseudo-sand microstructure may imply that natural fire preferably occurred during climatic deterioration and that natural fires may have played an important role in the degradation of the vegetation cover.

(4) Fine silty textural features: At the top part of the S1 soil in both sections, some silty textural features are observed, juxtaposing over all the other pedofeatures, suggesting that they were formed in the latest stage. They are similar to clay coatings in sharps, but with much lower transparency. They mainly consist of 2-5 μm sized silty particles, including some fine carbonate grains and charcoal particles. This type of textural feature in modern soils have been studied by many authors and are mainly found in soils with a surface crust, like soils denuded of vegetation (Courty and Fedoroff, 1985; Macphail *et al*, 1987). In paleosols, they are usually associated with climatic aridification and sometimes with natural fires (Courty and Fedoroff, 1985; Fedoroff, 1996). Consequently, the presence of these features at the top part of S1 soil can be interpreted as evidence of vegetation destruction during the climatic transition from Interglacial conditions to glacial conditions. Moreover, the fine charcoal particles in the textural features and those in the overlying loess may indicate a vegetation destruction, in relationship with natural fire.

(5) Loess with spongy microstructure: The groundmass of loess is characterised by a large amount of animal excrement and interconnected channels, mainly resulted from strong biological activity. This type of loess identified in both L1 and L2, but is more typical in L1 (Fig. 2). This microstructure evidently implies that the land surface was covered by a significant steppe since organic matter is indispensable for soil fauna living. These loess can be therefore regarded as weakly developed soils, thus evidencing more humid conditions. In fact, spongy microstructure is typical of steppe soils in semi-arid environments (Pawluk and Bal, 1985).

Behaviour of the climatic transitions

The significant morphological features of loess in the studied sections are summarised in Figure 2 and compared with the variations in Fet / Fed ratio (weathering intensity). It shows that the results provided by the two methods are highly consistent. Level 1, characterised by spongy microstructure and relatively higher Fed / Fet values, suggests relatively humid conditions during which the land surface was covered by a significant steppe cover. This level is stratigraphically correlated to the middle part of marine $\partial^{18}O$ glacial stage 4, (Fig. 1) . Level 2, a loess layer with pseudo-sands microstructure and very low Fed / Fet values, indicates severe climatic conditions with sparse

vegetation cover and strong winds. It immediately overlies the L1 /S1 boundary and correlates with the earliest part of marine $\partial^{18}O$ stage 4, thus marks the termination of the last interglacial ($\partial^{18}O$ stage 5) . The aeolian truncation of the S1 soil and the formation of the fine silty textural features in the top part of S1 were apparently occurred during this episode. The charcoal particles suggest that natural fire may have played an important role for the vegetation destruction. Level 3 corresponds to the entire S1 soil complex formed during the last interglacial (marine $\partial^{18}O$ stage 5). Paleopedological study in Xifeng (Guo, 1990), where modern climate conditions are somewhat similar to those for Luochuan and Yichuan, suggested a steppe-forest landscape for the early part, semi-arid warm steppe for the middle part and a dry steppe for the lastest part. Level 4, inmediately underlying the S1 /L2, marks the termination of the penultimate glaciation (marine $\partial^{18}O$ stage 6) . This episode is characterised by climatic conditions comparable to those for Level 2. The lowest Level 5 is comparable to Level 1, but suggests slightly less humid conditions according to the less developed spongy microstructure.

The transition from the penultimate glaciation to the last interglacial and the subsequent interglacial-glacial transition were therefore marked by a severe climatic episode in the Loess Plateau region, characterised by destruction of vegetation probably associated with both intensive aridification and natural fires. During these episodes, aeolian dynamic was particularly strong as indicated by the truncation of the S1 soil and the aeolian saltation process resulting in the pseudo-sand microstructure of loess. On the contrary, the preceeding episode (Level 5) and the following episode (Level 1) were characterised by more humid conditions resulting in a significant steppe cover although they still correspond to glacial stages. It should be mentioned that in the Xifeng section (Guo, 1990), two layers evidencing relatively weak cryogenic process were identified corresponding to the stratigraphic positions of Level 2 and 4 in this study, indicating strongly cold conditions.

According to the land-sea correlation pattern (Fig. 1), the ages of the S0 / L1, L1 / S1 and S1 / L2 boundaries should be $\approx$ 73 and $\approx$ 128 ka, respectively. Using these ages as control points and the magnetic susceptibility data, we have developed the time scales for the studied sections according to the method of Kukla et al. (1988). They dates the low Fed / Fet peak above S1 soil at $\approx$ 67-73 ka, lasting about 5,000 years. Assuming a similar accumulation rate for L2 loess, the low Fed / Fet peak below S1 should be $\approx$ 128-131 ka in age, lasting $\approx$ 3,000 years. Evidently, these events, occurred at the transitions between glacial and interglacial periods. They cannot be directly explained by either the orbitally induced insolation changes or the ice-volume variations. However, the age of the event at the termination of the penultimate glaciation may be correlated with that of an unnamed Heinrich layer in the North Atlantic, mentioned by Broecker (1994), while the one following the formation of the S1 soil is more or less synchronous with the Heinrich event 6 or the Toba super volcanic eruption. A very important question has therefore arisen for future studies: are these events dynamically linked and by what mechanisms?

Conclusions

(1) Geochemical and micromorphological studies converge to demonstrate that the transition from the penultimate glacial period to the last interglacial, and the one from the last interglacial to the last glacial period were marked by a severe climatic event at

millennial scale, which cannot be directly explained by either orbitally induced insolation changes or ice-volume variations, as reflected by marine $\partial^{18}O$ record.

(2) During these events, the Loess Plateau region was characterised by denudation of vegetation and strong aeolian dynamics, probably in relation with strong winter monsoon winds. Natural fire may have played an important role in the destruction of the vegetation.

Acknowledgements

This work was supported by the National Natural Science Foundation of China and is also a contribution to the IUGS-UNESCO Programme Climates of the Past (CLIP). The author is grateful to Drs. Wu Naiqin and Lu Houyuan for their collaboration for investigation and for the magnetic susceptibility data.

References

Bond, G., Heinrich, H., Broecker, W.S., Labeyrie, L., McManus, J., Andrews, J., Huon, S., Jantschik, R., Clasen, S., Simet, C., Tedesco, K., Klas, M., Bonani, G., and Ivy, S.: (1992) Evidence for massive discharges of icebergs into North Atlantic Ocean during the last glacial period, *Nature*, 360:245-249.

Broecker, W.S.: (1994) Massive iceberg discharges as triggers for global climate change, *Nature* 372:421-424.

Courty, M.A. and Fedoroff, N.: (1985) Micromorphology of recent and buried soils in a semiarid region of Northwest India, *Geoderma*, 35:287-332.

Duchaufour, Ph.: (1983) *Pédologie*, Tome 1: *Pédogenese et Classifcation*. Masson, Paris-New York- Barcelona- Milan, 477 pp.

Fedoroff, N. and Goldberg, P.: (1982) Comparative micromorphology of two Late Pleistocene paleosols (in the Paris Basin), *Catena*, 9:227-251.

Fedoroff, N.: (1996) Signatures dans les sols, les sédiments derivés de sols et les sites archéologiques d'événements abrupts (*in press*).

Forman, S.L.: (1991) Late Pleistocene chronology of loess deposition near Luochuan, China, *Quaternary Research*, 36:19-28.

Guo, Z.T.: (1990) *Succession des paléosols et des loess du centre-ouest de la China: approche micromorphologique*, These Université Paris VI, France, 266 pp.

Guo, Z.T., Liu, T.S. and An, Z.S.: (1994) Paleosols of the last 0.15 Ma in the Weinan loess section and their paleoclimatic significance, *Quaternary Science*, (3):256-269.

Imbrie, J., Hays, J.D., Martinson, D.G., McIntyre A., Mix, A.C., Morley, J.J., Pisias, N.G., Prell, W.L. and Shackleton, N.J.: (1984) The orbital theory of Pleistocene climate: support from a revised chronology of the marine $\partial^{18}O$ record. *In* Berger, A., Imbrie, J., Hays, J., Kukla, G., Saltzman, B. (eds) *Milankovitch and Climate*, Part 1, 269-305.

Kudrass, H. R., Erlenkeuser, H., Vollbrecht, R. and Weiss, W.: (1991) Global nature of Younger Dryas cooling event inferred from oxygen isotope data from Sulu sea cores, *Nature*, 349:406-409.

Kukla, G.: (1987) Loess stratigraphy in central China, *Quaternary Science* Review, 6:191219.

Kukla, G., Heller, F., Liu, X.M., Xu, T.C., Liu, T.S., and An, Z.S.: (1988) Pleistocene climates in China dated by magnetic susceptibility, *Geology*, 16:811 -814.

Liu, J.Q., Chen, T.M., Nie, G.Z., Song, C.Y., Guo, Z.T., Li, K., Gao, S.J., Qiao, Y.L. and Ma, Z.B.,: (1994) Dating and reconstruction of the high resolution time series in the Weinan loess section of the last 150,000 years, *Quaternary Science*, (3):193-202.

Liu, T.S.: (1985) *Loess and Environment*, China Ocean Press, Beijing, 251 pp.
Liu, T.S., Guo, Z.T., Liu, J.Q., Han, J.M., Ding, Z,L., Gu, Z.Y, and Wu, N.Q.: (1995) Variations of eastern Asian monsoon over the last 140,000 years, *Bull Soc. Geol France*, 166:221-229.
Lu, Y.C., Zhang, J.Z., and Xie, J.: (1988) Thermoluminescence dating of Loess and paleosols from the Lantian section, Shaanxi Province, China, *Quaternary Science Review*, 7:245-250.
Macphail, R., Romans, J.C.C., and Robertson, L.: (1987) The application of micromorphology to the understanding of Holocene soil development in the British Isles; with special reference to early Cultivation. *In* Fedoroff N. Courty M.A. and Bresson L.M. (eds) *Soil Micromorphology* A.F.E.S., 647-656.
Mehra, O. and Jackson, M.L.: (1960) Iron oxide removal from soil and clay by a dithionite-citrate system buffered with sodium bicarbonate, Clay *and Clay Minerals*, 7:317-327.
Overpeck, J.T., Peterson, L.C., Kipp, N., Imbrie, J., and Rind, D.: (1989) Climate change in the circum-North Atlantic region during the last deglaciation, *Nature*, 338:553-557.
Pawluk, S. and Bal, S.: (1985) Micromorphology of selected mollic epipedons. *In* Douglas L.A and Thompson M.L. (eds) *Soil Micromorphology and Soil Classifcation*, Madison, 63-84.
Pye, K. and Tsoar, H.: (1987) The mechanics and geological implications of dust transport and deposition in deserts with particular reference to loess formation and dune sand diagenesis in the northern Negev, Israel, *Geological Society* Special Publication, 35:139156.
Rampino, M.R. and Stephen, S.: (1992) Volcanic winter and accelerated glaciation following the Toba super-eruption, *Nature*, 359:50-52.
Van Campo, E. and Gasse, F.: (1993) Pollen - and diatom - inferred climatic and hydrological changes in Sumxi Co Basin (western Tibet) since 13,000 yr BP, *Quaternary Research*, 39:300-313.
Yan, Z.W. and Petit-Maire, N.: (1994) The last 140 ka in the Afro-Asian arid/semi-arid transitional zone, *Palaeogeography Palaeoclimatology, Palaeoecology*, 110:217-233.

LAST GLACIAL CLIMATIC VARIATIONS ON EASTERN INDONESIAN WARMPOOL AREA. CENDERAWASIH BAY OCEAN-MOUNTAIN PALEOCLIMATE PROJECT: STATE OF THE ART

W. S. Hantoro[1], M. Prentice[2], L. Handayani[1] and I. Narulita[1]

1 Research and Development Center for Geotechnology, Indonesian Institute of Sciences. J 1 Cisitu Sangkurian 21/154 D, Bandung 40135, Indonesia
2 Glacier Research Group, Institute for the Study of Earth, Oceans, and Space (EOS), Indonesia

Abstract

Irian Jaya (West New-Guinea) is the southwestern limit of the Pacific Warmpool Area, with a relatively steep and deep basin to the north. To the south, it is flanked by a shallow epicontinental platform, connecting it with the Australian continent Forming a so called «bird head» physiography, the island is divided by east-west trending high mountains (Jaya wijaya). One snowy peak is 4800 m high; it is one of the equator ice cap that offers good information on the last glaciation, which produced a huge ice mass, down to 3500 m altitude, forming a good preserved glacier sequence. Post glaciation left mountain lakes whose sediments yield climatic evolution, pollen and isotopic data.

Trees and speleotherms may preserve other natural witnesses of the climatic variations, as well as short and long records.

The neck of the bird is a large bay (Cenderawasih) facing north, receiving the small amount of drainage that comes from the northern flank of Jayawijaya Mountain. A large portion of drainage is received in the basin and transported by Memberamo river, to be settled in the deep trough.

Records of deterioration in the sea surface can be traced back to centuries by using massive Porites micro atolls, forming the rich reef that fringes the islands in the bay.

Cenderawasih Ocean-Mountain Paleoclimate Project will be implemented during five years, as a multi-lateral cooperation, under the coordination of the Indonesian government The aims of the project are to obtain a climatic model since the last glacial period, based on the most complete and continuous record covering the different environment in the Equator.

Introduction

There are few places in the tropical area where the witnesses of the post-glacial process are still to be found as well preserved geological formations. The high mountain belt of Irian Jaya (Jayawijaya) offers a complete sequence of glacial deposits from the last glacial period, and possibly of previous glacial periods. It is believed that Irian Jaya, the western rim of the Pacific basin, has played an important role, together with the West Pacific Warmpool Area in the north, to contribute in the low hemispheric climate mechanism in the Pacific area. Samples from glacial deposits in high mountains and other geological formations, as well as samples obtained from marine, coastal, lowlands, lake deposits, etc. in Irian Jaya. The samples keep a readable, complete record of the Quaternary natural changes. A comprehensive study, using various data coming from different environments is current. Field work for glaciers and pollen studies will be conducted in the high mountain where a tectonic study is under way in order to understand the Quaternary tectonism that had uplifted marine sediments, forming an East-West trending high mountain range. This Pliocene tectonism had been accompanied by intrusion which brought rich copper and gold mineralisation. High and low altitude lake sediments contain pollen that yield the paleovegetation of the surrounding area. Records of marine environment changes can be obtained both from massive corals and from continuous deep sea cores in Cenderawasih Bay.

Background information

Role of the Pacific Warm-Pool in regional, tropical and extra-tropical climatic change.

The proposed records are important, because the West Tropical Pacific warm-pool is one of the most influential components of the global climate (Lucas and Lindstrom, 1991; Glantz *et al*, 1991; Cane, 1992). It is poorly known, which is a serious obstacle to the understanding of global change. Even the first-order question of the sensitivity of WTP warm-pool, albeit concerned with past coolings, represents a significant contribution to the current debate concerning the future. Response to such large regional and global changes, as experienced during the last glacial cycle, implies a wide sensitivity to future forcing. Observe a possible significant variability, at time scales less than 500 yrs, reflects an important contribution to the knowledge of future changes.

Comparison of magnitude and phasing of WTP changes with paleoclimate records from other areas will help to sort out the causal mechanism for all changes considered. A specific climate-change mechanism that should be understood is the global importance of the tropical water vapor flux to the extratropics, through greenhouse, albedo, and surfacewater boyancy effects.

Role of Ice-Sheets in Global Climate Change:

Northern Hemisphere ice-sheet changes are implicated in large-scale temperature fluctuations in the North Atlantic basin, during the last glacial cycle (Bond et al, 1993). Just how large a role ice sheets play is a critical issue. If their role is small, then some key mechanisms, such as poleward water vapor transport, are at large to cause similar changes in the future (Lehman *et al*, 1993). A strong role for ice sheets has been argued principally from ice modeling excercises (MacAyeal, 1993). Important, high-resolution unambiguous evidence of ice-volume change is scarce. The isotopic record of continuous global icevolume change, that will result from the proposed study, should strongly test the ice-sheet control hypothesis and contribute important data to the debate.

Objective of the programme

The goal of the proposed study is to use various records coming from different environments, in order to reconstruct the climatic and tectonic (vertical movement) history of Irian Jaya, during Isotope stage 2 (for climate and environmental changes) and during the Quaternary (for tectonic history).

For the high mountain program, the main goal is to use glacial and pollen records to reconstruct the climate history of Peak Jaya, Irian Jaya, during Isotope stage 2, in order to quantify West Pacific Warm pool change and relate it to far-field paleoclimate change. A working hypothesis is proposed for the phenomenal change in glaciation of the Peak Jaya region since the Last Glacial maximum. Glacier configurations are specified in terms of the six major erosional levels of glaciation etched into the highlands. These levels are regarded as marking the Extreme Level Advances (ELA) for the glaciers that eroded them. Each glacier front position is classified according to the elevation of the lowest cirque that contributed ice to that front. One interpretation of the pattern is in terms of monotonic retreat from stage 2 maximum glaciation, with an ELA at 3400 above mean sea level (amsl) to present-day glaciation, with an ELA above 4660 amsl.

Physiography of Jaya Wijaya

Jaya Wijaya is the part of the extreme east-west trending central mountains. It divides Irian Jaya in two, south and north, regions, before the mountain axis turns to the north-west, forming the neck of the bird.

The crest of the cordillera in the Jayawijaya region consists of a huge block of Miocene limestone that extends about 30 km to the east-west, only 7 km to the north and south. The upper altimetric profile of the mountain (>3000 m amsl) shows that the southern flank plunges precipitously to the coastal plain, relatively steeper than the northern flank that steps down gently with two principal flats (Dugundugu and Discovery Valley) forming Zengillorong, Kemabu and Ekabu Plateaus (Fig. 1). The valleys are floored by sedimentary and metamorphic rocks. NW Kemabu rim has a 3400 m high peak. The deepest valley of Kemabu plateau is Soth Kemabu river, it runs on about 3250 amsl. A main drainage valley goes to the east before it joins the Memberamo to drain the plateau. The West Kemabu valley incises the plateau to the west and drains the Kemabu valley to Cenderawasih Bay.

The remaining ice cap still found in Peak Jaya is reported to continue to melt. Some glacier lakes are found at different altitudes. Glacier deposits widely cover the northern flank of Jaya Wijaya Mtn, downing to Kemabu valley, still observed at about 3400 m amsl. On the southern flank, glacier deposits are observed but they are less important than to the north. Rapid unroofing seems to have happened on the southern flank of the Jayawijaya Mt.

Regional Geology

The Jayawijaya mountain range develops as the consequence of the plate convergence and northwards move of the Australian continental crust, subducted by the Pacific oceanic plate. Characterized by Australian rock types, Jayawijana seems to be built by the uplifting and upthrusting of marine deposits series against the Pacific series of

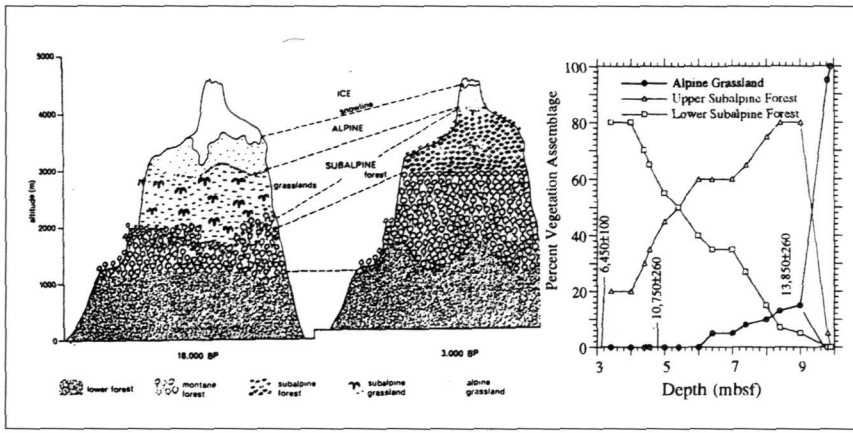

Figure 1. North-south topographic profiles accros the Mt. Jaya massif today. Major hypothetical unroofing levels are labelled.

Cyclop mountain range, to the north. Kemabu, Zengillorong and Ekabu Plateaus seem to be a present intra mountain basin that ends to the west of the Cenderawasih Bay. The main structural pattern in Jayawijaya Mt. develops east-southeast to west-northwest. It tectonically cuts and borders marine Neogene sediments.

Understanding the vertical tectonic movement is one of the important keys to the study of the glacial history in Jayawijaya Mt. Range. Pliocene magmatism was accompanied by granit intrusion through Miocene limestone, that produced mineralisation and rich ore of gold and copper. Thermal history and dating can provide temporal and mechanism data on the Quaternary tectonism that uplifled marine sediments, producing high mountains. Estimation of the first glaciation in this range can be obtained from both an hypothesis of steady uplifl and relict of old glacier sediments, but it seems difficult to realise.

Method

We propose to map the glacier sediments by using satellite images and aerial photographs, to sample the lake sediments, to radiocarbon-date them and to make geochemical analyses. Modeling is proposed, as it can support the assesment of paleoenvironmental studies.

Previous Investigations

Hope et al (1976) inferred that all glacial evidence below the meadow reflects mass wastage. Peterson and Cope (1972) interpreted a diamicton at about 1700 amsl in the lower Afhawagon Valleys, as a till reflecting an extensive LGM glaciation. Considering the 1000 m cliff from the meadows (over which the Meren-Carstensz ice lobe must have completely fraetured), any glacier ice below the cliff was reconstituted.

The extent of stage 2 ice and the associated ELA depression which have been reported previously probably extend to 3650 amsl (Hope et al, 1976). Dates of basal or-

ganics at the Ijomba (Discovery) and Ertsberg (Carstensz) locations indicate ice front recession (Discovery and Carstenzs ice lobes) back to an elevation of about 3600 amsl at about 13.4 ka (Hope and Peterson, 1976).

Tentative results

Extensive sequences of moraines, some of them 150 m high, indicate that large glaciers descended from the cordillera crest and covered the southern Kemabu and Zengillorong Plateaus, south of Sungai South Kemabu. Moraines, till sheets, and drumlinized bedrock forms were also located north of Sungai South Kemabu, on the northern rim of the Kemabu Plateau, as well as east of Sungai Zengillorong, on Zengillorong Plateau. Assuming that glaciers descended to the moraines on the northern side of the plateau rim, supposed by at <3000 amsl, the northern Kemabu Plateau ice-field must also have descended south to Sungai South Kemabu and nearly merged with the higher and more extensive southern ice-field, near Sungai South Kemabu. The glacier features on the low and narrow Wina Kangai Range, located just east of the northern Kemabu rim icefield, across Sungai Zengillorong, between the villages of Illaga and Beoga (Fig. 2), are also recognised. Assuming that the peak elevation of the Wina Kangai plateau is about 3500 m amsl, the ELA of the former Wina Kangai ice cover should have been about 3400 m amsl. If we are correct about the northern Kemabu and Wina Kangai icefields, then the stage 2 ELA was significantly lower than the previously reported 3650 m amsl and was likely about 3400 m amsl. There is significant evidence for a glacier outlet in Lembah (valley), Cemara draining ice from the eastern Kemabu plateau, as well as from the southern Zengillorong Plateau. This suggests that the saddle area between the Kemabu and Zengillorong Plateau was glaciated, which was not previously proposed. Another area of glacier cover, not noted previously, is in the western Kemabu region, north of S. Dega in the vicinity of Puncak Putigibuli.

Radiocarbon dates from basal peats from Lembah Hogayaku, on the Kemabu Plateau (northeast of Peak Jaya), indicate that the outermost moraines are stage 2. Peat collected from a 2.75 m depth, near the outlet of lower Danau Hohayaku, are dated 14.8 ± 0.2 ka. This old date is the oldest deglaciation date non available for Irian Jaya. It agrees exactly with dates from the North Atlantic and South America. The peat separated glacial mud from overlying algal ooze, it probably reflects glacial-lake infilling following ice retreat. Peat samples have been obtained downstream from the lake, in a lower area between the end of moraines, dating 11.6 ± 0.4 Ka. This date probably indicates erosion and delayed colonization at an inter-moraine site.

Discussion and Conclusions

This work has confirmed a very expanded glacier cover and a much lowered ELA during the LGM, in the Mt Jayawijaya area. Deglaciation was underway by 14.8 ka and LGM cooling in the Jayawijaya highlands was about 8°C. The small LGM glacial system that covered the lowest summits is used in this region to interpret lowered ELAs for the large stage 2 glacial systems that descended from the cordillera crest through the finger valley. A good example is the small LGM icefield on the Wina Kangai Range (Fig. 2). If the icefield has existed at the LGM, the mean annual 0°C isotherm should have been at or below the top of the outwards range 3500 m amsl. Given the negligible seasonality in

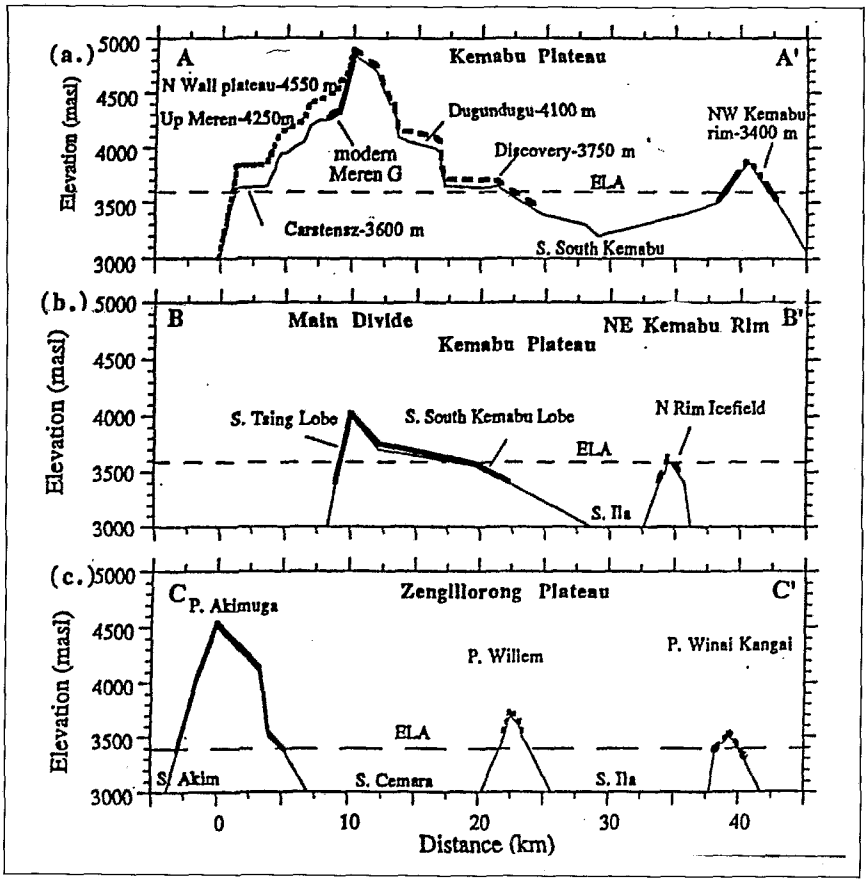

Figure 2. North-south topographic profiles for the LGM (b-c). Thick lines depict glacier surface. ELAs are at 3.600 amsl in (a,b) and 3.400 amsl.

this region, the mean annual temperature for a glacier to have existed there must have been 0°C (Fig. 3). The key difference between this situation and the one for the large stage 2 glacier, is that the latter glaciers could theoretically have been supplied by significantly greater-than-present snow accumulations, significantly lowering their ELAs. For the large stage 2 glacier, the mean annual 0° C isotherm, which is currently at about 4600 m amsl (Allison and Bennet, 1976), needs not have been depressed anywhere near to the ELA of the LGM. The working hypothesis that results from the reliance of a small glacial system, featuring a very restricted vertical elevation range is that, during the LGM, the mean annual 0°C isotherm was depressed at least 1 km below its present position. A LGM lapse-rate derived from GCMmodeling (Rind and Peteet, 1985), the extent of the highland cooling estimation down to the warm-pool itself, suggests that SST at the LGM sea level, 120 m lower than present sealevel, was cooler by about 5°C than at present, more than twice the cooling inferred from the paleooceanographic

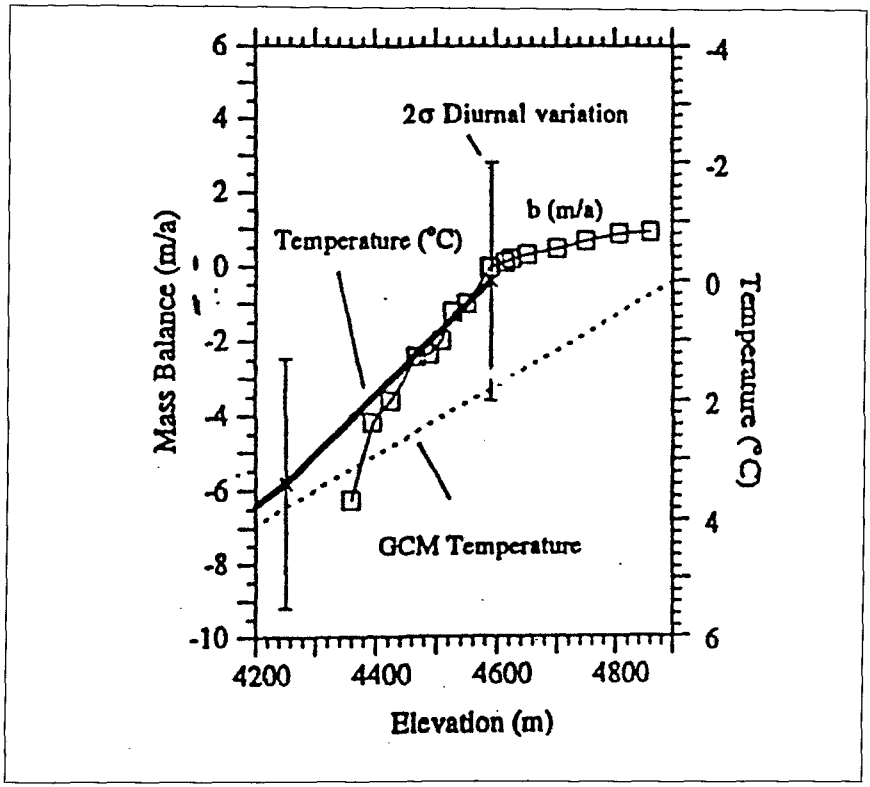

Figure 3. Climate mass balance relations for P. Jaya in 1971-1972. The net balance is average for the Cartensz and Meren Glaciers (Allison, 1976). Mean annual temperature is projected from the elevation of the highest measurements (4251 amsl) using the LGM lapse rate from the GISS GCM. Assuming no vertical gradient in accumulation, the ablation gradient is linearly related to the temperature gradient. Hence, a ratio of mass balance change to temperature change is established which integrates the complexities of ablation in this region. However, temperature on the glaciers is inferred as acumulation. Further, no data exist to calibrate temperature change at the ELA to precipitation change. Monitoring of glacier balance and weather in 1995-1997 would provide key data to derive these relations when contrasted with similar data from 1971-1972.

record (Fig. 4).

Another key difference that have to be calculated and added to the lowering of LGM's ELAs is the fact that a huge ice cap, extending down to 3400 m amsl must induce an extra exogen influence to the down loading of the basement. A release the ice cap must then be followed by an isostatic rebound.

Pollen data from stage 2 sites, well to the east in the Baliem Valley (Hope et al., 1993 unpublished) support this interpretation since they indicate the persistence of wet conditions. This fits several pollen spectra from Papua New Guinea (Hope and Peterson,1976) which record a more extensive cloud forest. The considerable lowering

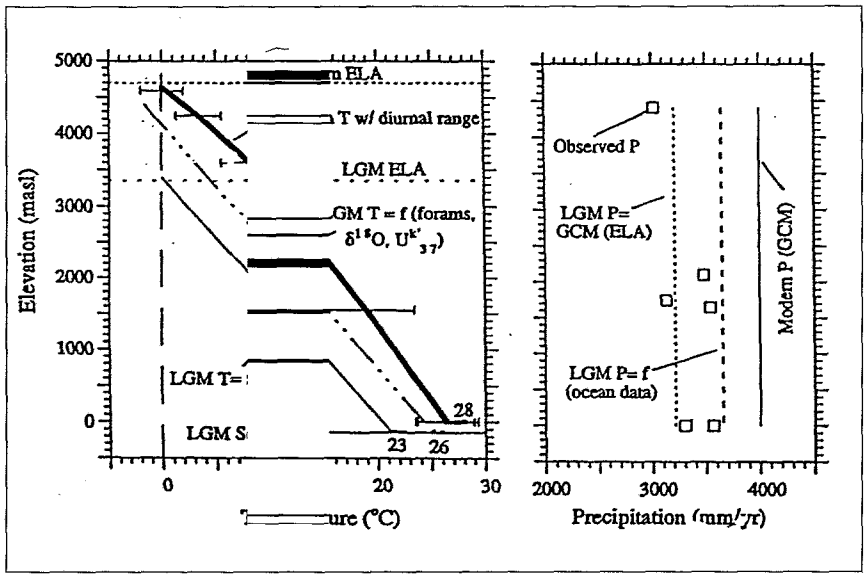

Figure 4. Present and postulated LGM atmospheric temperature (a) and precipitation (b) distributions for the western Pacific "warm-pool" region. Thick solid line gives the average observed lapse rat e for Irian Jaya (Allison and Bennet, 1976).
(a) The LGM lapse rate based on the marine record (dash-dot line) is anchored at the prevalent interpretation of 1.5°C of SST cooling (e.g. Thunnel et al., 1994) for a sea-surface at-120 bmsl. This SST is extended using the GISS GCM lapse rate derived by Rind and Pettet (1985) for the LGM, 0.59°C/100m. based on CLIMAP (1981) SST estimates. The ELA-based lapse rate, thin solid line, extends from the 0°C isotherm at 3,400 amsl using the GISS GCM lapse rate of 0.6°C/100m.
(b) Boxes show observed annual precipitation for P. Jaya region (Allison and Bennet, 1976). The vertical gradient is negligible but data above 2,000 amsl are sparse. Solid line gives GCM simulation of present annual precipitation in the grid-box containing the field area (Rind and Peteet, 1985). Dashed lines depict LGM precipitation modeled by the GISS for CLIMAP-based SST and for 2°C cooler than inferred by CLIMAP (Rind and Peteet, 1985).

of the treeline, from 4000 m, to day to about 2200 m for the LGM, may have been a response to low CO2 concentrations and not to aridity, since wet communities dominate the vegetation.

Acknowledgments

I would like to express my appreciation to PT. Freeport Indonesia for the field support during the reconnaissance work at Kemabu Plateau, Jayawijaya Mt. and to Dave Mayes who was fully helpful in preparing field work.

References

Bond, G., Broecker W., Johnsen, S., McManus, J., Labeyrie, L., Jouzel, J. and Bonani, G.: (1993) Correlations between climaxte records from North Atlantic sediments and Greenland ice, *Nature*, 365:143-147.

Cane, M.A.: (1992) Tropical Pacific ENSO models: Enso as a mode of the coupled system. *Climate System Modeling*. Cambridge University Press, Cambridge: 583-616.

Glantz, M.H.R., Katz, R.W. et al.: (1991) *Teleconnections Linking Worldwide Climate Anomalies*, Cambridge University Press, Cambridge.

Hope, G.S., Peterson, J.A., Allison, L. and Radok, U.: (1976) *The equatorial glaciers of New Guinea* (1th ed), A.A. Balkema, Rotterdam.

Hope, G.S. and Peterson, J.A.:(1976) Paleoenvironments. In G.S. Hope, J.A. Peterson, U. Radok & L. Allison (eds), *The Equatorial glaciers of New Guinea*, A.A Balkema, Rotterdam: 173-206

Lehman, S.J.: (1993) Ice sheets, wayward wind and sea change, *Nature*, 365:108-110.

Lucas, R. and Lindstrom, E.: (1991) The mixed layer of the Western Equatorial Pacific Ocean, 96:334.358.

MacAyeal D.R.: (1993) Binge/purge oscillations of the Laurentide Ice Sheets as a cause of the North Atlantic's Heinrich Events, *Palaeoceanography*, 8,6:775.

Peterson, J.A. and Hope, G.S.: (1972) Lower limit and maximum age for the last major advance of the Carstensz glaciers, West Irian, *Nature*, 240:36-37.

ENVIRONMENTS OF MAINLAND SOUTHEASTERN AUSTRALIA AT THE CLIMATIC EXTREMES OF THE LAST GLACIAL CYCLE-EVIDENCE FROM POLLEM

A.P. Kershaw

Centre for Palynology and Palaeoecology, Department of Geography and Environmental Science, Monash University, Clayton, Vic.3168, Australia

Abstract

The height of the last glacial period, centred on 17,000 years BP, and the Mid Holocene period, around 6000 BP, represent, in many parts of the globe, the extremes of climatic conditions experienced over the last glacial cycle. They provide a useful envelope of natural climatic variability against which any future human-induced climate change can be assessed.

In Australia, evidence for late Quaternary climates is patchy with most available data from the more humid margins of the continent where conditions have been most condusive to the accumulation of continuous sediment sequences (Harrison and Dodson, 1993, Kershaw, 1995). Within these regions, the most substantial paleoclimatic evidence is derived from a range of sites analysed for pollen within mainland southeastern Australia. From these records, a data base has been constructed to allow some assessment of regional patterns of vegetation and inferred climates for critical periods including those at the identified climatic extremes. This pollen data base is probably the most substantial outside of the well studied regions of northeastern North America and Europe.

The study area

All pollen records are located within the state of Victoria and adjacent portions of southeastern South Australia and southeastern New South Wales (Fig. 1). The region extends between 34° and 39° S and experiences a temperate climate. The general weather is controlled primarily by the subtropical high pressure systems that track from west to

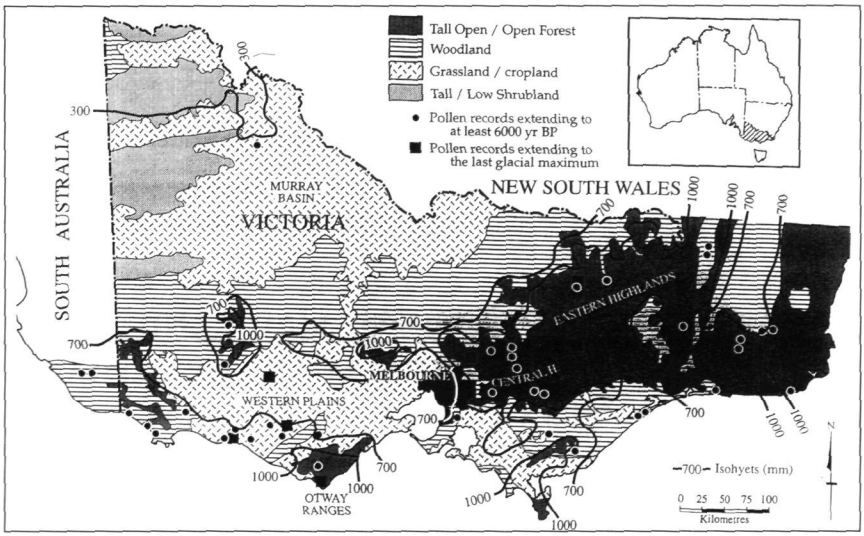

Figure 1. Location of pollen records in mainland southeastern Australia in relation to modern vegetation and mean annual precipitation.

east and are centred south of the region in summer and between 30° and 35° S in winter. These systems are separated by rain-bearing low pressure systems which bring rain mainly in winter. The influence of these westerlies decreases from west to east and in the very east of the region the heaviest rain is produced by strong depressions which develop over the seas to the east. In this eastern area rainfall is fairly evenly distributed through the year. Occasionally the whole region is influenced by incursions of moist tropical air that is responsible for some of the heaviest rainfall.

The distribution of rainfall is greatly influenced by topography and proximity to the coast with highest totals in the Southeastern and Central Highlands and their outliers to the west, and lowest values in the lowlying Murray Basin in the northwest. This distribution pattern has a major influence on the distribution of vegetation (Fig. 1). Vegetation description follows Specht (1970). Those areas receiving above about 1000 mm are dominated, at least in topographically suitable locations, by tall open eucalypt forests with an understorey of ferns and mesomorphic shrubs. Within these areas, rainforest occurs as small, isolated patches in topographically-protected situations where rainfall exceeds about 1200 mm per annum. As rainfall decreases, the eucalypt canopy becomes more open to form open forests which grade into woodlands around about the 700 mm isohyet. Both open forests and woodlands have an understorey of sclerophyll shrubs or grasses. Within the drier western part of the region and in coastal areas, Casuarinaceae can become co-dominant with eucalypts in the canopy. The canopy layer becomes very sparse in parts of the Western Plains and Murray Basin but here determination of the natural vegetation is made difficult by extensive clearing for agriculture. In the dry northwest tall open shrublands with a eucalypt or Casuarinaceae canopy dominate old Pleistocene dunes while Chenopodiaceous shrublands occur in low, frequently saline areas.

Temperature variation has a much less obvious influence on vegetation distributions except on the high mountains where cooler conditions have resulted in the development of subalpine eucalypt woodland above about 1400 m, and very restricted alpine grassland, herbfeld and heath above 1600 to 1700 m.

Recent pollen-environment relationships

The establishment of relationships between modern environments and pollen spectra derived from them provides the essential basis for interpretation of past pollen assemblages in vegetation and climatic terms. The most useful recent pollen spectra are derived from sites revealing fossil pollen records and the location of those sites whose records extend back through at least a substantial part of the Holocene are shown, in relation to major present vegetation types and rainfall isohyets, on figure 1. Pollen percentages of major, or indicator, taxa for each of these sites is shown on figures 2a and b. Percentages are based on a dry land pollen sum which includes all selected taxa except for Chenopodiaceae which can grow locally on some saline sites. The samples are from just prior to the first impact of European settlement, as determined from the lack of introduced pollen, as these samples have been demonstrated to reflect native vegetation variation much better than present day spectra from the sites (Kershaw *et al.*, 1994; Kershaw and Bulman, 1996).

As expected from its dominance within the region, *Eucalyptus* is the best represented taxon with highest values, frequently above 60%, in those areas supporting dense canopied tall open forest. By contrast, Casuarinaceae, although represented at all sites, achieves its best representation in the more open-canopied woodlands in the west and along the coast. Values greater than 5% are mainly restricted to environments receiving less than 1000 mm per year and which have a mean annual temperature above 13°C. *Nothofagus* values reflect well the distribution of this dominant of cool temperate rainforest which is mainly found in the Central Highlands and in the Otway Ranges. Values over 2% are restricted to sites receiving in excess of 1200 mm of rain. The pattern of representation of the indicator of tall open forest, *Pomaderris*, is less restricted to the distribution of parent plants with some occurrence in a large proportion of sites in the region. However, values greater than 5% are only found at sites within tall open forest and, from the more extensive data set of Kershaw et al (1994), values greater than 2% are restricted to sites experiencing more than an average of 870 mm of rainfall per year.

The major understorey taxa, Poaceae and Asteraceae, have broad geographical representation but patterns that are less clear than those of the major woody taxa *Eucalyptus* and Casuarinaceae. High percentages occur in woodland and open herbaceous areas within the Western Plains and, particularly for Poaceae, in subalpine to alpine regions. From the more extensive data set of Kershaw *et al* (1994), highest Asteraceae values, above 30%, are restricted to the dry northwest which experiences a rainfall less than 650 mm and a mean annual temperature in excess of 15°C. The pollen here is probably derived mainly from opportunistic annuals. Asteraceae values are also relatively high within some tall open forests which have an abundance of small tree composites in their understorey. The morphological type of Asteraceae pollen with blunt spines is very rare and there is debate about the origin of the source plants with very few potential contenders present in the vegetation of the region. The geographical spread of Chenopodiaceae pollen indicates broad regional dispersal although high percentages are largely restricted

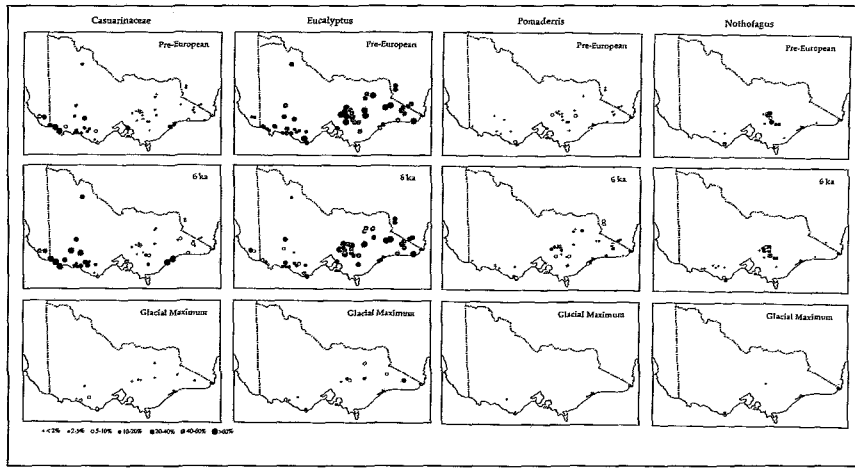

Figure 2 a. Pollen percentages, relative to a pollen sum of dry land taxa, of predominantly tree taxa for time slots from site records in mainland southeastern Australia.

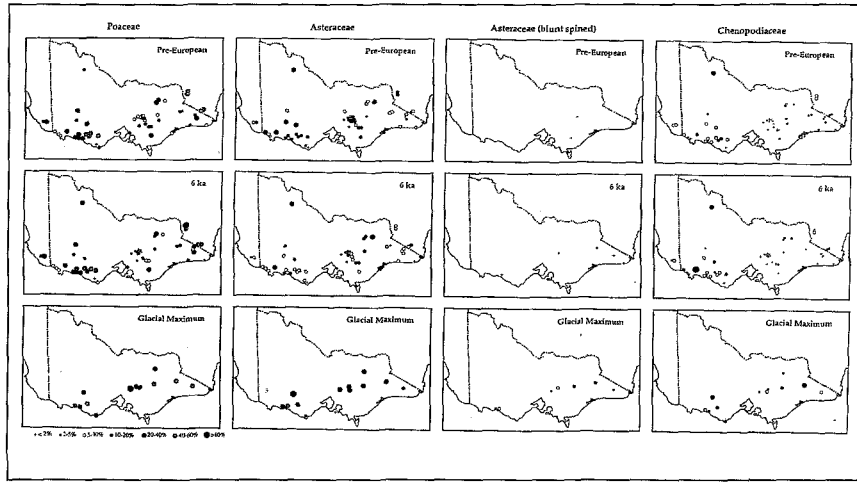

Figure 2 b. Pollen percentages, relative to a pollen sum of dry land taxa, of predominantly herbaceous and shrub taxa for time slots from site records in mainland southeastern Australia.

to more saline coastal and inland sites. The two values exceeding 5% in southern New South Wales probably represent efficient wind transport from drier areas and a low dilution effect from pollen of alpine species surrounding these sites.

Conditions during the last glacial

Of the fifty-one records which cover at least the last 6,000 years, only 12 extend back to the last glacial period. The fact that these records are predominatly restricted to highland areas which presently receive high precipitation, and to deep volcanic craters in the Western Plains which have favourable moisture balances due to bisection of the regional water table, suggests strongly that precipitation levels were much lower than today. The very low values of woody taxa, the very limited distribution of taxa of wetter forests, *Pomaderris* and *Nothofagus*, and the relatively high values for the salt tolerant Chenopodiaceae in the higland sites, provide support for this proposal. However, the sclerophyllous taxa *Eucalyptus* and Casuarinaceae can tolerate very dry conditions: in the study area they still form a significant proportion of the vegetation under mean annual precipitation levels below 300 mm. It is unlikely that rainfall was this low throughout the region as the presence of some pollen from wetter forest taxa indicates their survival within the region through this period.

It is expected that temperatures were also cooler during this period. Estimates of temperature ranging from greater than 4°C to 6°C lower than today have been calculated from individual highland studies based on the assumption that the treeline was below the sites, but the low values for woody taxa in most lowland pollen spectra indicate the absence of any defined treeline. Consequently these are not reliable estimates. However, similar estimates have been derived from other studies. The presence of limited glaciation in the Snowy Mountains, within the very eastern part of the region, indicates a reduction of at least 6°C in higland areas (Colhoum and Peterson, 1986) while predicted temperatures for the southern part of Australia from the COHMAP model were up to 4°C below present (Kutzbach *et al*, 1993).

Comparisons of the fossil with modern spectra provide very limited information on glacial climates. Domination of the vegetation of the whole region by Poaceae and Asteraceae would suggest a regional cover of steppe grassland which is not represented in the area today. The lack of present vegetation and presumably climatic analogues is reinforced by the widespread occurence of Asteraceae (spineless) pollen which is characteristic of glacial assemblages through the Quaternary of southeastern Australia but is scarse during the Holocene and previous interglacials (Kershaw *et al.*, 1991).

Factors other than average temperatures and precipitation that may have been important determinants of vegetation cover include generally higher wind speeds and incursions of cold polar air as postulated for the existence of similar treeless vegetation in the mid latitudes of New Zealand (McGlone, 1988). Evidence for wind speeds some 20% higher than present is indicated by widespread sand dune activity in southeastern Australia (Wasson, 1989) while incursions of cold air would have been facilitated by a more northerly position of the westerly wind belt as predicted from the COHMAP model (Kutzbach et a/, 1993), at least during winter. Under these conditions, forest and woodland vegetation would probably have been able to survive in protected moist pockets. The pattern of representation of woody plant pollen is consistent with this hypothesis. The low but consistent values for *Eucalyptus* and Casuarinaceae suggest localised sur-

vival throughout the region while the relatively high individual values for *Eucalyptus* in the far east of the area and for *Nothofagus* in the Otway Ranges site indicate the actual presence of refugia in protected stream valleys.

Conditions at the Holocene 'optimum'

High values for all the tree taxa indicate the period of maximum expansion of forest vegetation and structurally more dense vegetation than today throughout most of the region. From the glacial distribution of *Eucalyptus* and Casuarinaceae pollen, it is possible that many contained species simply expanded their distributions locally without any major migration. Casuarinaceae achieved substantially higher percentages than those of today although its predominant distribution in the drier western part of the region and along the coast was similar to that of present. *Eucalyptus*, on the other hand, appears to have slightly lower values, especially in the western region. This could mean either that it took longer to achieve dominance, perhaps due to less efficient dispersal than Casuarinaceae, or that conditions have become increasingly more favourable for it. Evidence for increased burning which is likely to have been tied to greater climatic variability in the latter part of the Holocene (McGlobe *et al.*, 1992) would certainly have favoured fire-promoting eucalypts.

In contrast to *Eucalyptus* and Casuarinaceae, a greater degree of dispersal may have been required by *Pomaderris* to achieve its mid Holocene distribution as its glacial record is very sparse. This taxon demonstrates a much greater representation, if not a substantially greater geographical range, of tall open forest than today with a number of records exceeding the percentages of any modern spectrum. The response of the rainforest tree Nothofagus was much more modest. It substantially increased its representation to levels higher than today but only within the Central Higland and Otways areas where it appears to have been contained throughout the recorded period. Considering the response of *Pomaderris*, it is unlikely that *Nothofagus* achieved its potential climatic range, an observation that is supported by its present day absence from areas which, from bioclimatic analyses (Busby, 1984), are within its present climatic envelope. One reason for this restricted expansion is the vulnerability of the taxon to fire which may have prevented the colonisation of areas beyond sheltered valley situations. This is in contrast to *Pomaderris* which is considered to require periodic fire for its regeneration beneath the dense eucalypt canopy of tall open forests (Ashton and Attiwell, 1994). Another factor is the limited dispersal of capacity of *Nothofagus* whose wind transported seeds travel only a few metres from parent trees (Howard, 1973).

In line with the general increase in representation of tree taxa, there are marked reductions in the relative proportions of herbaceous taxa to values which, on average, are slightly lower than those in the recent spectra. The decreases in Asteraceae are greater than those of Poaceae in the Western Plains area where, despite effectively increased precipitation, a dominant grass layer appears to have been maintained. This may be due to the heavy textured soils which are not condusive to the development of a dense tree canopy. Conversely, the decline of grasses is relatively greater in the eastern highlands where Asteraceae percentages have probably been supported to some extent by the tree composites of tall open forest. Chenopodiaceae values are also reduced but only to levels recorded at present.

Overall, the major patterns of taxon representation are sufficiently similar to those of today to suggest that major climatic gradients have been fairly constant through at least the last 6000 years. There is little doubt that effective precipitation was higher in the mid Holocene than today but, as with the glacial period, temperatures are difficult to determine. Higher values than today for *Pomaderris* at high elevation sites where precipitation is unlikely to have been limiting could suggest that temperatures were higher although a generally better representation of parent plants may have artificially inflated pollen percentages beyond the actual distribution of *Pomaderris*.

The only quantitative estimate of climate centred on 6000 years BP is derived from an examination of *Nothofagus* representation in the records from the Central Highlands (McKenzie and Busby, 1992). All sites show evidence, from pollen and macrofossils, of the presence of *Nothofagus* 6000 years ago but the taxon is absent now from both lower and higher altitude sites. From bioclimatic estimates of the sites and the modern distribution of the taxon, it was determined that precipitation needed to have been only slightly higher than present but that summer temperatures must have been at least 2°C cooler in summer and perhaps marginally warmer in winter to have supported the 6000 year distribution of the taxon. This estimate is not inconsistent with lower summer temperatures predicted by COHMAP largely on the basis of lower insolation levels than today in the Southern Hemisphere (Webb *et al.*, 1993).

Conclusions

The mapping of pollen records for major taxa at the height of the last glacial and Mid Holocene has provided a general and consistent picture of vegetation and climatic conditions for times considered to represent the climatic extremes of the last glacial cycle. The climate was substantially cooler, drier and windier than today at the height of the last glacial but the lack of modern vegetation and presumably climatic analogues has prohibited detailed climatic reconstruction. The Mid Holocene was probably effectively wetter than present but may have also been somewhat cooler in summer. The major climatic features of this period are that it was likely to have been milder and climatically less variable than today.

Acknowledgements

I thank Dave Bulman for great assistance in the production of the data base, the Australian Research Council for financial support and Gary Swinton and Phil Scamp for drafting the text figures.

References

Ashton, D.H. and Attiwill, P.M.: (1994) Tall open-forests. *In* R.H. Groves (ed.) *Australian Vegetation* 2nd edn., Cambridge University Press. Cambridge, 157-196.

Busby, J.R.: (1986) A bioclimatic analysis of *Nothofagus cunninghamii* (Hook.) Oerst. in southeastern Australia, *Australian Journal of Ecology,* 11:1-7.

Colhoun, E.A. and Peterson, J.A.: (1986) Quaternary landscape evolution and the cryosphere: research progress from Sahul to Australian Antarctica. *Australian Geographical Studies* 24:1 45-1 67.

Harrison, S.P. and Dodson, J.: (1993) Climates of Australia and New Guinea since 18,000 yr B.P. *In* H.E. Wright Jr, J.E. Kutzbach, T. Webb III, W.F. Ruddiman, F.A. Street-Perrot & P. J. Bartlein (eds.) *Global Climates since the Last Glacial Maximum* University of Minnesota Press. Minneapolis, 265-293.

Howard, T.M.: (1973) Studies in the ecology of *Nothofagus cunninghamii* Oerst. 1. Natural regeneration on the Mt. Donna Buang Massif, Victoria, *Australian Journal of Botany,* 21:6778.

Kershaw, A.P.: (1995) Environmental change in Greater Australia through the Pleistocene/ Holocene transition, *Antiquity,* 69:656-675.

Kershaw, A.P. and Bulman, D.: (1996) A preliminary application of the analogue approach to the interpretation of late Quaternary pollen spectra from southeastern Australia, *Quaternary International* 33:61-71.

Kershaw, A.P., Bulman, D. and Busby, J.R.: (1994) An examination of modern and pre-European settlement pollen samples from southeastern Australia: assessment of their application to quantitative reconstruction of past vegetation and climate, *Review of Paleobotany and Palynology,* 82:83-96.

Kershaw, A.P., D'Costa, D.M., McEwen Mason, J.R.C. and Wagstaff, B.E.: (1991) Palynological evidence for Quaternary vegetation and environments of mainland southeastern Australia, *Quaternary Science Reviews* 10:391-404.

Kutzbach, J.E., Guetter, P.J., Behling, P.J. and Selin, R.: (1993) Simulate climatic changes: results from the COHMAP climate-model experiments. *In* H.E. Wright Jr., J.E. Kutzbach, T. Webb III, W.F. Ruddiman, F.A. Street-Perrot and P. J. Bartlein (eds) *Global Climates since the Last Glacial Maximum,* University of Minnesota Press. Minneapolis, 24-93.

McGlone, M.S.: (1988) New Zealand. *In* B. Huntley and T. Webb III (eds.) Vegetation History, Kluwer. Dordrecht, 567-599.

McGlone, M.S., Kershaw, A.P. and Markgraf, V.: (1992) El Niño/Southern Oscillation climatic variability in Australasian and South American paleoenvironmental records. In H.F. Díaz and V. Markgraf (eds.) *El Niño Historical and Paleoclimatic Aspect of the Southern Oscillation,* Cambridge University Press. Cambridge, 435-462.

McKenzie, G.M. and Busby, J.R.: (1992) A quantitative estimate of Holocene climate using a bioclimatic profile of *Nothofagus cunninghamii* (Hook.) Oerst., *Journal of Biogeography,* 19:531 -540.

Specht, R.L.: (1970) Vegetation. *In* G.W. Leeper (ed) *The Australian Environment* 4th edn., CSIRO and Melbourne University Press. Melbourne, 46-67.

Wasson, R.J.: (1989) Desert dune building, dust raising and palaeoclimate in the Southern Hemisphere during the last 280,000 years. *In* T. Donnelly and R. Wasson (eds.) CLIMANZ 3, CSIRO. Canberra, 123-137.

Webb T.III, Ruddiman W.F., Street-Perrot F.A., Markgraf V., Kutzbach J.E., Bartlein P.J., Wright Jr., H.E. and Prell, W.L.: (1993) Climatic changes during the past 18,000 years: regional syntheses, mechanisms and causes. *In* H.E. Wright Jr., J.E. Kutzbach, T. Webb III, W.F. Ruddiman, F.A. Street-Perrot & P.J. Bartlein (eds.) *Global Climates since the Last Glacial Maximum,* University of Minnesota Press. Minneapolis, 514-535.

THE QUATERNARY DEPOSITS IN LANZAROTE AND FUERTEVENTURA (EASTERN CANARY ISLANDS, SPAIN): AN OVERVIEW

J. Meco[1], N. Petit-Maire[2], M. Fontugne[3], G. Shimmield[4] and A. J. Ramos[1]

1 Departamento de Biología, Universidad de Las Palmas de Gran Canaria, Campus de Tafira, 35017 Las Palmas, España.
2 URA 164, CNRS, case 907, 13288 Marseille Cedex 09, France.
3 Centre des Faibles Radioactivités. Laboratoire Mixte CNRS-CEA, Avenue de la Terrasse, F91198 Gif-sur-Yvette Cedex, France.
4 Dunstaffnage Marine Laboratory, P.O. Box 3, Oban, PA34 4AD, Scotland, U.K.

Abstract

The main Quaternary formations observed in Fuerteventura and Lanzarote (Canary Islands) are aeolian deposits marine terraces and lava flows.

The sand from of all dunes derive from marine deposits containing final Miocene and early Pliocene fauna. The successive regression left the marine bioclastic sand esposed to aeolian erosion. The dunes contain interbedded levels of land snail shells and insect brood cells. Part of the dunes were covered by Pliocene lava flows. A thick calcareous crust developed at their tops. In some areas the sand eroded from those ancient formations built new dunes, anew buried by Upper Pleistocene lava flows. Several layers of little-evolved palaeosols are intercalated into the aeolian sediments. The Mollusca fauna was radiocarbon (c.42 ka; 28-27 ka; 23 Ka; c.15 and 13.8 ka; 9.8-9 ka) and U/Th dated (c.95 ka; c. 138 ka; c.183 ka; c. 235 ka and >350 ka).

Pleistocene fossiliferous marine terraces correspond to isotopic stage 5e and 1. The stage 5e terraces are located at + 5m above msl. Their faunal assemblage (Strombus bubonius) indicates water temperatures much higher than at present and was U/Th and ESR dated at c. 125 ka. Holocene terraces are located at elevations slightly higher than modern beaches and approximately 1 m lower than the Pleistocene terraces. The fauna has been radiocarbon dated c. 4 and 2 ka.

Aeolian formations

The sand from of all dunes in Fuerteventura and Lanzarote islands derive from Messinian marine deposits containing final Miocene and early Pliocene warm water faunas: *Hinnites ercolaniana*, *Chlamys pesfelis*, *Gigantopecten latissimus*, *Ancilla glandiformis*, *Lucina leonina*, *Rothpletzia rudista* and abundant *Strombus coronatus*, *Nerita emiliana* and *Gryphaea virleti* (Meco, 1977, 1981, 1982, 1983), together with large quantities of calcareous algae. Such deposits exist in southern Lanzarote, western and southern Fuerteventura as well as in Gran Canaria. They are younger than the basal flow unit at Ajui in Fuerteventura, (5.8 + 0.5 my; Meco and Stearns, 1981) and older than the lava flow at Janubio in Lanzarote (6.6 + 0.3 my; Coello *et al*, 1993).

The post Messinian regression left the marine bioclastic sand exposed to aeolian erosion. It spread over the islands, except for the highest peaks. Part of them were covered at 2.9 my, 2.7 my, 2.4 my and 1.8 my by lava flows, e.g at Barranco de la Cruz, Barranco de Los Molinos, Puerto de Los Molinos and Aljibe de la Cueva (Meco and Stearns, 1981; Coello *et al*, 1992). Those dunes (e g. at Agua Tres Piedras, Meco, 1993 contain interbedded levels of land snail shells, insect brood cells and alluvial deposits. A thick calcareous crust developed on their tops, as well as on the sand scattered over volcanic and plutonic rocks, probably during the early Pleistocene. The sand eroded from those ancient formations (either from the cliffs' faces, or when the calcareous crust was eroded by torrential flows, or from the aeolian erosion of the beach during marine regressive phases), built new dunes which were, in some areas, buried anew by lava flows. Such is the case for those from Montaña Arena and Bayuyo volcanoes wich overlie the Lajares and Cañada Melian dunes in Fuerteventura Pl. I. Several layers of little-evolved palaeosols are intercalated into the aeolian sediments. They are extremely rich in fossil land snails shells (Theba geminata, Hemicycla sarcostoma, Rumina decollata; Fig. 3) and in incredibly numerous insect brood cells (Petit-Maire *et al*, 1986, 1987). Those cells have been determined as Antophoridae and taxonomically associated with Eucera sp; the perforations in the wall of the cells and the existence of unopened cells indicate a preimaginal mortality of c. 47 % due to predation and fungal attacks (Ellis and Ellis-Adams, 1993). Those observations testify to active past biogenic activity and biodiversity within the palaeosols, but also testify to occasional dust flows from the Sahara, since dust is necessary for the brood cells to be constructed by the insects. At several places (Table 1), the Mollusca fauna was radiocarbon and U/Th dated (Petit-Maire *et al*.1986,1987; for detailed stratigraphy and sedimentology cf Damnati et al.,1996, Damnati this volume, Bouab and Lamothe, this volume). Table 1 gives the results of all analyses the validity of which is to be discussed, given the wide uncertainty of radiocarbon ages older than 25 ka and the problems related with Uranium dating of terrestrial Mollusca shells.

Serious problems arise about the validity of some of these ages. The radiocarbon ones around 30 ka are suspicious. However their large number at different sites must probably indicate a real period of humid conditions (also validated by similar observations in the Sahara; Yan and Petit-Maire, 1994, Petit-Maire et al, 1995). Moreover, some of the results are validated by U/Th TIMS and by OSL ages.

Therefore, despite the uncertainty of dating, one recognizes several wetter periods during which pedogenesis and development of biodiversity could take place at this western margin of the Sahara. The three most recent ones, corresponding to the top layers of

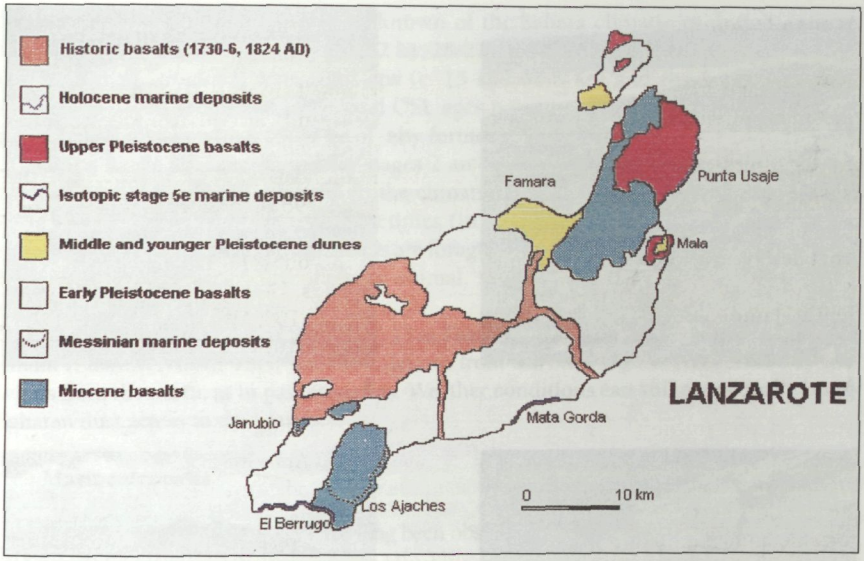

Figura 1. Geological outline of Lanzarote island.

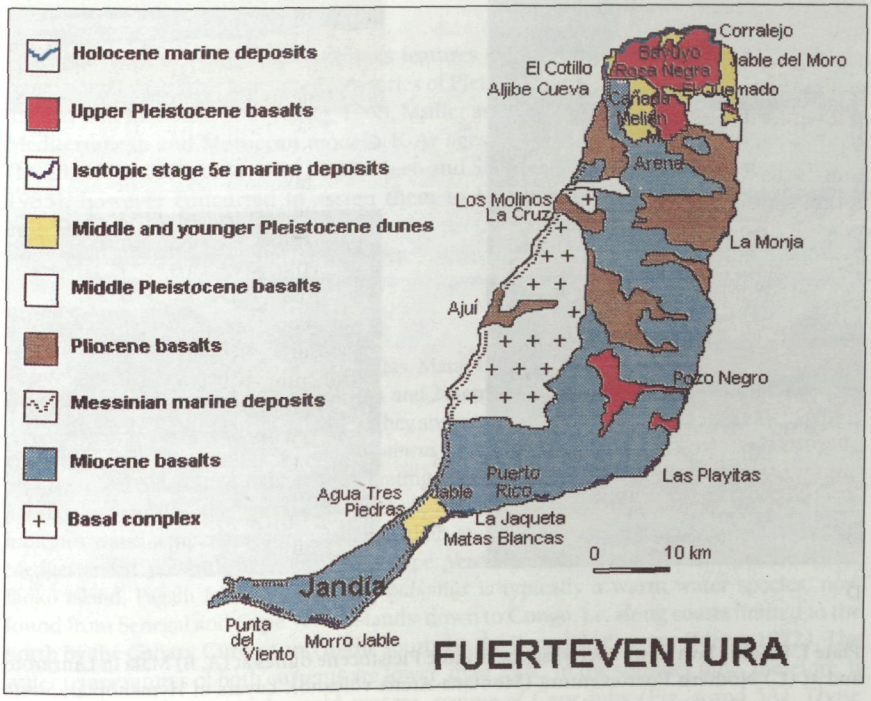

Figure 2. Geological outline of Fuerteventura island.

A

B

D

C

E

Plate I. Basaltic lava flows overlying the Middle Pleistocene dunes at (A, B) Mala in Lanzarote and at (C) Nothern Fuerteventura (Montaña Arena volcano). Layers of Hymenoptera nests and land snails (D), and fossil roots (E) in paleodunes at Cañada Melián section.

Fuerteventura formations, fit what is known of the Sahara climatic evolution: one to three wet episodes during stage 3 (c. 42 ka; 28-27 ka; 23 ka), two short wetter episodes corresponding to global warming steps (c. 15 and 13.8 ka) and the Early Holocene (beginning at 9.8 ka). Some U/Th and OSL ages point to stage 5. Older ones indicate possible wet phases which could be of any former interglacial.

Not a single age corresponds to stages 2 an 4, which pleads for the validity of the results. Besides, the above episodes fit the climatic evolution in the Sahara (Petit-Maire *et al.*, 1995) . However, the ages sometimes (in particular in Mala section) do not fit stratigraphy: considering that land snails are foraging species, they possibly may be found fossilized in layers older than the very animal. Still, these ages indicate wet periods during which they could live.

At present, mobile dunes exist (Fig. 1) at Famara (Lanzarote), (Fig. 2) Corralejo and Jandia (Fuerteventura). Their sand also derives from the older dunes, remobilised by the winds from the north, as in past scenarios. Weather conditions can still occasionally bring Saharan dust across to the islands.

Marine deposits

Fossiliferous marine terraces have long been observed along the coasts of the eastern Canary Islands. They correspond to the Mio-Pliocene and to isotopic stages 5e and 1.

Mio-Pliocene terraces

Sequences of emergent strandlines features («raised beaches») in the eastern Canary Islands have been attributed to a series of Pleistocene levels (Crofts, 1967; Lecointre, Tinkler and Richards, 1967; Klug, 1968; Muller and Tietz, 1975; Klaus, 1983) following Mediterranean and Moroccan models. K-Ar ages, more complete paleontological data (Meco, 1975, 1977,1981,1982,1983; Meco and Stearns, 1981) and ESR dating (Radtke, 1985), however concurred to assign them to Mio-Pliocene (Messinian) deposits on emergent coastal platforms.

We shall not discuss them in this paper.

Stage 5e terraces

At Mata Gorda, El Berrugo, Las Playitas, Matas Blancas (Photo 6 A, B), Puerto Rico, Punta del Viento and Morro Jable beaches (Fig. 1 and 2) terraces located at +5 m above msl have been observed since 1975 (Meco, 1975,1977). They are very fossiliferous. The fauna includes *Strombus bubonius, Conus testudinarius* (= *Conus ermineus*), Harpa rosea (= *Harpa doris*), *Murex saxatilis* and the coral *Siderastrea radians* Proliferating large *Patella* (group *Patella ferruginea*), *Thais haemastoma* and 15 other species (Meco *et al.*, 1987) are also present. This faunal assemblage indicates water temperatures much higher than at present. *Harpa rosea* never found in the Mediterranean, presently lives only in the Cape Verde Islands and the Gulf of Guinea (Gabon, Bioko Island, Pagalu Island). *Strombus bubonius* is typically a warm water species, now found from Senegal and Cape Verde Islands down to Congo, *i.e.* along coasts limited to the north by the Canary Current and to the south by the Benguela Current (Meco, 1972). The water temperatures of both currents are lower than 23 °C in the summer time, therefore, it cannot live in the present day cold current regime of Cape Juby (Fig. 4 and 5A). Those

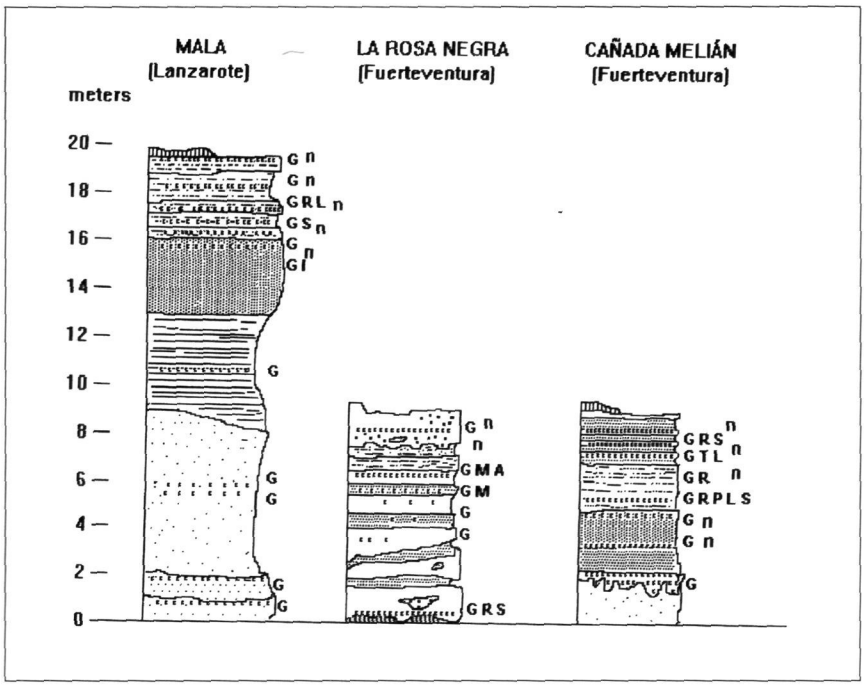

Figure 3. Mollusca fauna from the sections in Quaternary aeolian formations, Eastern Canary Islands. Layers of land snails are interbedded into the sand dunes. (Geochronology and lithostratigraphy studied by Bouab and Lamothe, this volume, and Damnati, this volume). The number of species (biodiversity) increases with humidity. A: *Theba pisana cf arietina* (Rossmässler 1846) G:*Theba geminata* (Mousson 1857); I: *Theba impugnata* (Mousson 1857); L: *Pomatias laevigatum* (Webb & Berthelot 1833); M: *Monilearia lancerottensis* (Webb & Berthelot 1833); n: Hymenoptera nests; P: *Parmacella auriculata* Mousson 1872; R: *Rumina decollata* (linné 1758); S: *Hemicycla sarcostoma* (Webb & Berthelot 1833); T: *Trochoidea despreauxii* (d'Orbigny 1839).

References of the original descriptions

Linne, C. von: (1758) *Systema Naturae Regnum Animale, edit. decima.* Lipsiae, p.773, n°608.

Mousson, A.: (1857) in G. Hartung. Die geologischen Verhältnisse der Inseln Lanzarote und Fuerte Ventura. *Naturwissens chaften*,15: 132-133.

Mousson, A.: (1872) Révision de la faune Malacologique des Canaries. Naturwissens chaften 25:9, Pl.1 figures 1-2

Orbigny, A. d': (1839) *in* P.B. Webb & S. Berthelot, *Histoire Naturelle des Iles Canaries*, 2,2:1-72, Pl.1, Figures 13-14,24-25, Pl.2, figure 30.

Rossmässler, E.A.: (1846) Diagnosen einiger neuen Binnen-Mollusken, *Zeitschr. Malakozool.*, 3:172.

Webb, P.B. & Berthelot, S.: (1833) Synopsis molluscarum terrestium et fluviatilium quas in itineribus per insulas Canarias observarunt, *Ann. Sci. nat.* 28:307-326.

deposits were attributed (Meco, 1975,1977; Meco et al, 1987) to the last interglacial under the name of Jandian, from the Jandía Peninsula in Fuerteventura. They were U/Th and ESR dated from 103 ka to 178 ka (Table 2).

Such terraces *with Strombus bubonius* are also known during stage 5 along the Mediterranean coast (Meco, 1977). In the southern coast of Spain they are dated 180 ka, 150 ka, 128 ka, 110 ka, 95 ka, 85 ka, 80 ka and 30 ka (Zazo et al.,1981; Hillaire-Marcel *et al.*, 1986). This wide range of ages is likely to be rather attributable to the method's uncertainties or to the reworking of older shells into the last interglacial deposits, as observed today when *Strombus bubonius* removed from the Pleistocene beach is found at Matas Blancas in the current beach sediments.

The colonisation of the eastern Canary Islands during stage 5 implies SSTs much higher than nowadays and a disappearance of the upwelling along the Senegalian and Saharan coasts, allowing larvae migration during the summer. The analysis of isotopic SSTs from Matas Blancas *Strombus bubonius* is in progress by Bard *et al.* (Cornu et al.,1993). However, a problem arises, considering the absence of *Strombus bubonius* in the 5e (Ouljian) terraces of the Atlantic coast of northern Africa (Ortlieb 1975; Meco, 1977), which could be explained by the fact that the main path of inflowing Atlantic tropical warm water into the Mediterranean (Alboran Sea) is around two large anticyclonic gyres, easily observable on satellite imagery (Fig. 4 and 5B).

Holocene terraces

Beach rocks are preserved at scattered localities in Fuerteventura and Lanzarote (Fig. 1 and 2), at elevations slightly higher than modern beaches and approximately 1 m lower than the Pleistocene terraces. After the ancient name of Fuerteventura (Erbania), they have been named Erbanian (Meco *et al.*, 1987).

Those deposits contain boulders from the Jandian sandstone and conglomerates. The Erbanian sea carved a notch in the cliffs-walls of «Los Jameos del Agua» cave, in Lanzarote, at approximately 2 m above present msl. It also carved a coastal erosion platform in the Jandian conglomerates, as seen at Las Playitas in Fuerteventura. The last marine pulsation (Erbanian II) left a berm and beach-rocks, for example at La Jaqueta, Puerto Rico and La Monja. The fauna in this berm is analogous to the one living along the modern littoral zone. It is characterized by the abundance of *Cerithium vulgatum*, reaching up to 70% in the collected samples, and by the decrease of Patella (11%) and *Thais hameastoma* (2%) in relationship to the Jandian fauna, which typically contains more *Patella* (almost 56%) and *Thais haemastoma* (17%) than the Erbanian .

The fauna has been radiocarbon dated at four different sites in Fuerteventura (Table 3). Those radiocarbon ages indicate two periods of ocean stillstands, one around 4 ka and another after 2 ka. At La Monja and La Jaqueta, an alluvial deposit is interbedded between those two pulsations (Erbanian I and II). It is possibly related with a similar deposit recorded inland, dated 3.3±0.1 ka (Rognon and Coudé-Gaussen, 1987).

Material	Site	14C age BP	U/Th corrected age	OSL age	Author(s)
Land snails	Famara	0.3±0.05 ka			Hillaire-Marcel et al,1995
Land snails	Jandía	7.93±0.7ka			Gif- 9070
Land snails	Corralejo	8.84 ±0.7ka			Gif- 9063
Land snails	Jandía	9.8±0.14 ka			Petit-Maire et al., 1986
Land snails	Jandía	13.85±0.2 ka			Rognon et al., 1989
Land snails	Corralejo	15±0.2ka			Petit-Maire et al.,1986
Land snails	Corralejo	23.22±0.35 ka			Gif - 9057
Land snails	P. Negro	23.6± 0.55 ka			Petit-Maire et al.,1986
Land snails	Famara	26.76±0.23 ka			Hillaire-Marcel et al.,1995
Land snails	Famara		27.4 ± 2.1 ka		Hillaire-Marcel et al.,1995
Land snails	Rosa N .	28.46 ± 0.63ka			LGQ - 142
Egg-shell	Jandía	28.95 ± 0.53 ka			Gif-9054
Land snails	Jandía	29.66± 0.7ka			Gif-8847
Land snails	Famara		30.2±0.9 ka		Hillaire-Marcet et al 1995
Land snails	Famara		30.6±0.9 ka		Hillaire-Marcet et al 1995
Land snails	Famara		31.2±0.6 ka		Hillaire-Marcet et al 1995
Land snails	Famara		31.6±0.9 ka		Hillaire-Marcet et al 1995
Marine shell*	Jandía	31.7±1.1 ka			Gif-9059
Land snails	Jandía	31.8±0.15 ka			Gif-9059
Egg-shell	Jandía	32.1±1.1 ka			Walker et al. 1990
Land snails	Famara		32.3±2.2 ka		Hillaire-Marcel et al.,1995
Land snails	Rosa N.	32.5±1.2 ka			LGQ-143
Land snails	Rosa N.	>33.8 ka			LGQ-141
Land snails	Rosa N.	>33.8 ka			LGQ-140
Land snails	Famara	33.91± 0.38 ka			Hillaire-Marcel et al., 1995
Land snails	Famara	34.2±0.37 ka			Hillaire-Marcel et al., 1995
Land snails	Famara	37.42±0.4g ka			Hillaire-Marcel et al., 1995
Land snails	Famara	38.73±0.5 ka			Hilaire-Marcel et al., 1995
Land snails	Famara	38.27±0.72 ka			Hilaire-Marcel et al., 1995
Marine shell*	Jandía	≥40 ka			Gif - A-93246
Land snails	Famara	40.76±0.6 ka			Hillaire Marcel et al., 1995
Land snails	Famara		from 41 to 27 ka		Hilaire-Marcel et al., 1995
Land snails	Famara		42.2±1 ka		Hilaire-Marcel et al., 1995
Land snails	Famara		43.15±07 ka		Hilaire-Marcel et al., 1995
Land snails	Famara		53.8±2.8 ka		Hilaire-Marcel et al., 1995
Land snails	Mala		94.9±07 ka		Shimmield
Land snails	Mala		138.3±5.02 ka		Shimmield
Land snail	Mala		138.3±7.4 ka		Shimmield
	Rosa N.			181±27 ka	Bouab & Lamothe, this vol.
Land snail	C. Melián		182.4±6.6 ka		Shimmield
	Rosa N.			183±27 ka	Bouab & Lamothe, this vol.
Land snails	C.Melián		224.4±4.9 ka		Shimmield
Land snails	C.Melián		229.0±7.5 ka		Shimmield
Land snails	Mala		235±4.65 ka		Shimmield
Land snails	C.Melián		241±4.9 ka		Shimmield
	Rosa N.			318±45 ka	Bouab & Lamothe, this vol.
Land snails	Mala		>350 ka		Shimmield
Land snails	Mala		>350 ka		Shimmield
Land snails	C.Melián		>350 ka		Shimmield

*Brought by fossil shearwater or by prehistoric man

Table 1. Radicarbon, U/Th TIMS and OSL ages of the Pleistocene/Holocene dunes.

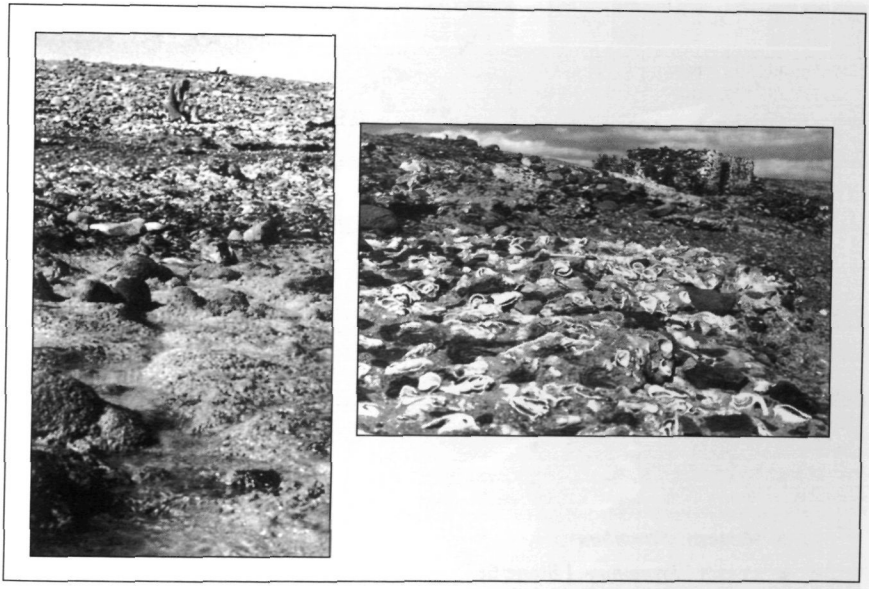

Photo 6. *Strombus bubonius* in a stage 5e beach-rock at Matas Blancas, leewards of Jandía Peninsula, Fuerteventura.

Material	Site	U/Th age	ESR age	Author(s)
S. bubonius	Morro Jable	103 (116-91) ka		Radtke, 1985
S. bubonius	Matas Blancas	103.8±2 ka		Zazo et al. 1993
S. bubonius	Puntas del Viento		104.8 ka	Radtke, 1985
S. bubonius	Matas Blancas	106±7 ka		Meco et. al.,
S. bubonius	Puerto Rico		108 ka	Radtke, 1985
S. bubonius	Matas Blancas	112±7 ka		Meco et.al.,1992
S. bubonius	Matas Blancas		128.7 ka	Radtke, 1985
S. bubonius	Puerto Rico		135 ka	Radtke, 1985
S. bubonius	Matas Blancas	136 (154-122) ka		Radtke, 1985
S. bubonius	Matas Blancas		137.6 ka	Radtke, 1985
S. bubonius	Puerto Rico		147.2 ka	Radtke, 1985
S. bubonius	Matas Blancas	178±43.8 ka		Zazo et.al., 1993

Table 2. U/Th and ESR ages of stage 5e marine terraces.

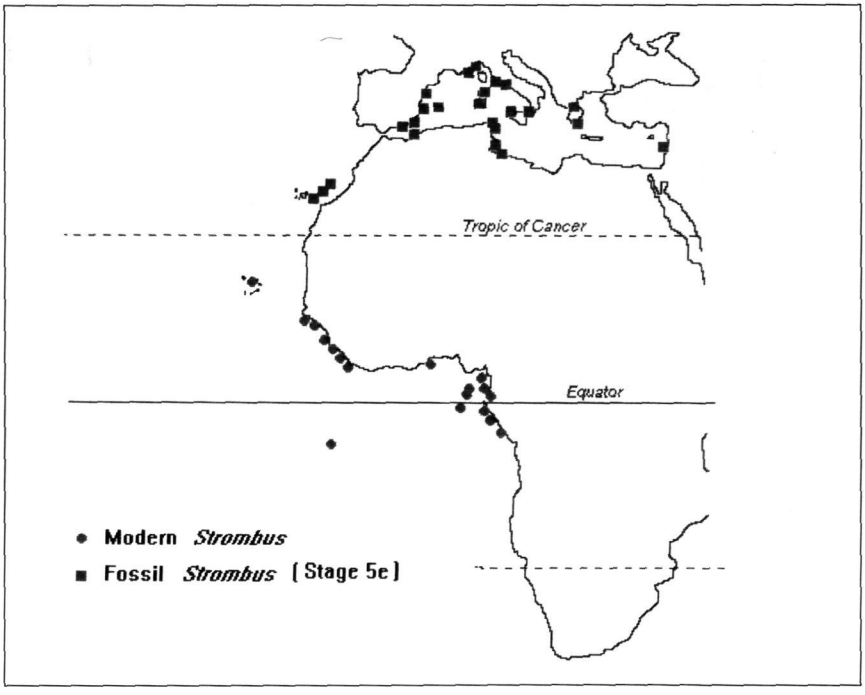

Figure 4. Geographical distribution of *Strombus bubonius* at present and during the last interglacial period.

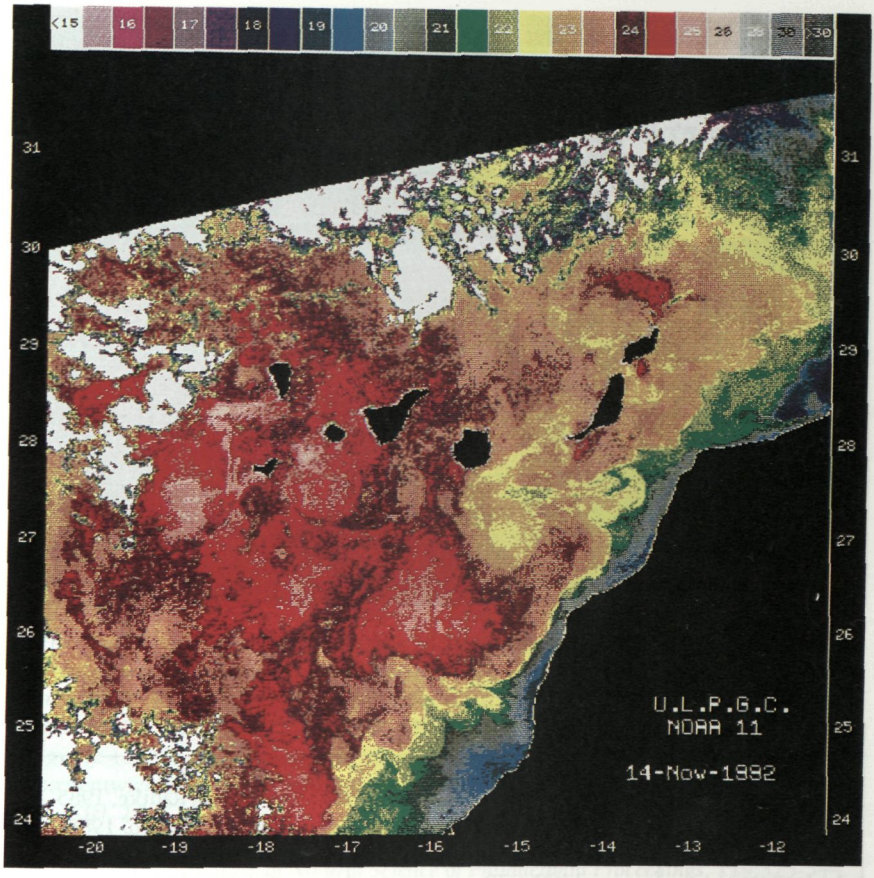

Figure 5A. Sea surface temperatures derived from NOAA/AVHRR satellite imagery show the North -African coast upwelling (A) and the main path of inflowing Atlantic warm water into the Mediterranean Sea (B). It could explain the differences observed between the Ouljian fauna, when compared with the Jandian and Tyrrhenian faunas.

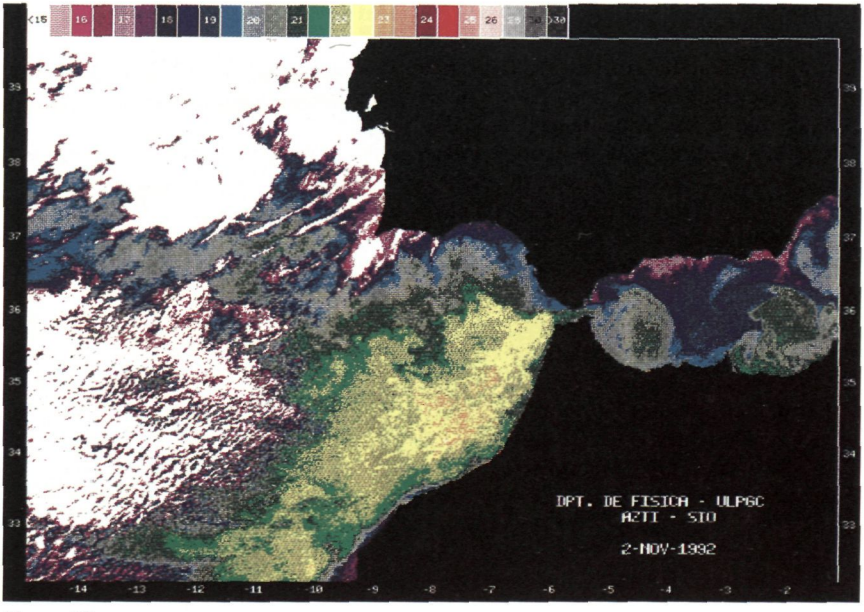

Figure 5B.

Site	^{14}C BP age	Authors
La Monja	1020 + 40	(Gif-9061)
Puerto Rico	1140 + 70	(Ki-2336) Radtke, 1985
La Jaqueta	1249 + 149	(LGQ-83) Meco, 1988
La Jaqueta	1363 + 151	(LGQ-82) Meco, 1988
La Jaqueta	1400 + 70	(Gif-7039) Meco et al.,1987
Puerto Rico	1940 + 70	(Ki-2336) Radtke, 1985
Corralejo	3640 + 100	(Gif-5346) Meco et al.,1987
La Monja	3960 + 70	(Gif-9060)
La Monja	4350 + 50	(Gif-9058)

Table 3. Radiocarbon dating of Holocene marine terraces

References

Chamley, H.,Coudé-Gaussen, G., Debrabant, P., and Rognon, P.: (1987) Contribution autochtone et allochtone à la sédimentation quaternaire de l'Ile de Fuerteventura (Canaries): altération ou apports éoliens ?, *Bull Soc géol. France*, (8) 3,5:939-952.

Coello, J., Cantagrel, J.-M., Hernan, F., Fúster, J.-M., Ibarrola, E., Ancochea, E., Casquet, C., Jamond, C., Díaz de Téran, J.-R., and Cendrero, A.: (1992) Evolution of the eastern volcanic ridge of the Canary Islands based on new K-Ar data, *Journal of Volcanology and Geothermal Research*, 53:251-274.

Cornu, S., Patzold, J., Bard E., Meco, J., and Cuerda-Barceló, J.: (1993) Paleotemperature of the last interglacial period based on $\partial^{18}O$ of *Strombus bubonius* from the western Mediterranean Sea, *Palaeogeography, Palaeoclimatology, Palaeoecology*, 103:1-20.

Crofts, R.: (1967) Raised beaches and chronology in north west Fuerteventura, Canary Islands, *Quaternaria*, 9:247-260.

Driscoll, E.M., Hendry, G.L. and Tinkler, K.J.: (1965) The geology and geomorphology of Los Ajaches, Lanzarote, *Geological Journal* (Liverpool), 4:321-334.

Ellis, W.N. and Ellis-Adam, A.C.: (1993) Fossil brood cells of solitary bees on Fuerteventura and Lanzarote, Canary Islands (Hymenoptera: Apoidea), *Ent. Ber. Amst.*, 53,12:161-173.

Hillaire-Marcel, C., Carro, O., Causse, C., Goy, J.L. and Zazo, C.: (1986) Th/U dating of Strombus bubonius-bearing marine terraces in southeastern Spain, *Geology*, 14:613-616.

Hillaire-Marcel, C., Ghaleb, B., Gariépy, C., Zazo, C., Hoyos, M., and Goy, J.-L.: (1995), USeries Dating by the TIMS Technique of Land Snails from Paleosols in the Canary Islands, *Quaternary Research*, 44:276-282.

Klaus, D.: (1983) Verzahnung von Kalkrusten mit Fluss- und Strandterrassen auf Fuerteventura, Kanarische Inseln, *Ess. Geogr. Arb.*, 6:93-127.

Klug, H.: (1968) Morphologische Studien auf den Kanarischen Inseln. Beitrage zur Kustenentwicklung und Talbildung auf einem vulkanischen Archipel, *Schr. Geogr. Inst. Univ. Kiel*, 24, 3.

Lecointre, G., Tinkler, K.J., and Richards, G.: (1967) The marine Quaternary of the Canary Islands, *Academy of Natural Science of Philadelphia Proceedings*, 119:325-344.

Macau Vilar, F.: (1958) Tubos volcánicos en Lanzarote «La Cueva de los Verdes» *Anuario de Estudios Atlánticos*, 11 :437-468.

Meco, J.: (1972) Données actuelles pour l'étude paléontologique du Strombus bubonius Lamarck in H.J. Hugot (Ed) *VI Congr. Panafr. Préhist Etud. Quat Dakar 1967*, Chambéry Imprimeries Réunies. 391-394.

Meco, J.: (1975) Los niveles con «Strombus» de Jandía (Fuerteventura, Islas Canarias), *Anuario de Estudios Atlánticos*, 21 :643-660.

Meco, J.: (1977) *Los Strombus neógenos y cuaternarios del Atlántico euroafricano. Taxonomía, biostratigrafía y paleoecología* Ed. Cabildo Gran Canaria. Madrid. 207 p. (Thesis Universidad Complutense de Madrid, 1976).

Meco, J.: (1981) Neogastrópodos fósiles de las Canarias orientales, *Anuario de Estudios Atlánticos*, 27:601 -615.

Meco, J.: (1982,1983) Los Bivalvos fósiles de las Canarias orientales, *Anuario de Estudios Atlánticos* 28:65-125 and 29:579-595.

Meco, J.: (1993) Testimonios paleoclimáticos en Fuerteventura *Tierra y Tecnología*, 6:41-48

Meco, J., Petit-Maire, N., and Reyss, J.L.: (1992) Le Courant des Canaries pendant le

stade isotopique 5 d'apres la composition faunistique d'un haut niveau marin a Fuerteventura (28°N) *C.R. Acad. Sci. Paris,* 314 Série II: 203-208.

Meco, J., Pomel, R.S., Aguirre, E., and Stearns, C.-E.: (1987) The Recent Marine Quatemary of the Canary Islands, *Trabajos sobre Neógeno-Cuafernario del CSIC Madrid,* 10:283-305 .

Meco J. and Stearns C.-E. (1981) Emergent littoral deposits in the Eastern Canary Islands, *Quaternary Research, 15:* 199-208.

Muller, G. and Tietz, G.: (1975) Transformation of carbonate sands into limestone and dolostone, Fuerteventura, Canary Islands, Spain, *Proceedings IX^th International Congress of Sedimentology Nice,* 143-148.

Ortlieb, L.: (1975) Recherches sur les formations plio-quaternaires du littoral ouest-saharien (28°30' - 20°40' lat.N), *Travaux* et *Documents* de l' *O.R.S. T.O.M.,* 48:1-267.

Petit-Maire, N., Delibrias, G., Meco, J., Pomel, S. and Rosso, J.C.: (1986) Paléoclimatologie des Canaries orientales (Fuerteventura), C.R. *Acad. Sci. Paris,* 303:1241-1246.

Petit-Maire, N., Rosso, J.-C., Delibrias, G., Meco, J., and Pomel, S.: (1987) Paleoclimats de l'Ile de Fuerteventura (Archipel Canarien) *Palaeoecology of Africa and the surrounding islands,* 18:351-356.

Petit-Maire, N., Sanlaville, P. and Yan, Z . W.: (1995) Oscillations de la limite nord du domaine des moussons africaine, indienne et asiatique, au cours du demier cycle climatique, *Bull. Soc. géol. Fr,* 166,2:213-220.

Radtke, U.: (1985) Untersuchungen zur zeitlichen Stellung mariner Terrassen und Kalkrusten auf Fuerteventura (Kanarische Inseln, Spanien), *Kieler geographische Schriften,* 62:73-95.

Rognon, P. and Coudé-Gaussen, G.: (1987) Reconstitution paléoclimatique à partir des sèdiments du Plèistocène supérieur et de l'Holocène du nord de Fuerteventura (Canaries), Z. *Geomorph. N.E,* 31,1:1-19.

Rognon, P., Coudé-Gaussen, G., Le Coustumer, M.-N., Balouet, J.C. and Occhietti, S.: (1989), Le massif dunaire de Jandia (Fuerteventura, Canaries): évolution des paléoenvironnements de 20 000 BP à l'actuel, *Bulletin ASEQUA,* 1:31-37.

Tinkler, K. J.: (1966) Volcanic chronology of Lanzarote (Canary Islands), *Nature,* 209:11221123.

Walker, C.A., Wragg, G.M. and Harrison, C.J.O.: (1990), A new shearwater from the Pleistocene of the Canary Islands and its bearing on the evolution of certain *Puffinus* shearwaters, *Historical Biology,* 3:203-224.

Yan, Z.W. and Petit-Maire, N.: (1994) The last 140 ka in the Afro-Asian arid/semi-arid transitional zone, *Palaeogeography, Palaeoclimatology, Palaeoecology,* 110:217-233.

Zazo, C., Goy, J.L., Hoyos, B., Dumas, J., Porta, J., Martinell, J., Baena, J., and Aguirre, E.: (1981) Ensayo de sintesis sobre el Tirreniense peninsular español, *Estudios geol.,* 37:257262.

Zazo, C., Hillaire-Marcel, C., Hoyos, M., Ghaleb, B., Goy, J.-L., and Dabrio, C.J.: (1993) The Canary Islands, a stop in the migratory way of Strombus bubonius towards the Mediterranean around 200 ka. Subcomm. Mediterranean and Black Sea Shorelines INQUA, *Newsletter,* 15:7-11.

IN-PHASE HOLOCENE CLIMATE VARIATIONS IN THE PRESENT-DAY DESERT AREAS OF CHLNA AND NORTHERN AFRICA

N. Petit-Maire and Z. Guo

URA 164, CNRS, Case 907, 13288 Marseille Cedex 9, France
Institute of Geology, Academy of Sciences, Beijing, China

Abstract

The comparison of holocene radiocarbon ages for lacustrine or paludal deposits in the presently hyperarid core of the Sahara desert (mean annual rainfall less than 100 mm) and for evolved palaeosols in the presently arid regions of China show an evolution roughly in phase, marked by two optima at 9.5 to 7 ka and 5.5 to 5 ka. A very severe arid episode peaked between 4 and 3.6 ka.

560 radiocarbon dates from lake deposits in the present-day Sahara desert, and 158 radiocarbon dates on organic matter from palaeosols in the arid parts of China are sufficient in number, homogeneous and well reparted enough to allow the comparison of their frequencies in terms of arid / humid variations during the Holocene. The % of dates in each region has been plotted within intervals of 400 years, widely covering the errors on the recorded ages, between the beginning of the Holocene (10 ka) and the onset of the current aridity generally determined for those areas at 3 ka (Yan and Petit-Maire 1994, Petit-Maire *et al* 1995).

Both curves (fig. I) show an evolution roughly in-phase, despite short lags for China, due to the fact that pedogenesis is slower than the direct aquifer rise induced by increase of rainfall. The Holocene is marked in both the Sahara and arid China by two humid episodes: the first one, between 9.5 and 7 ka, interrupted by a short, somewhat drier event at *c.* 8 ka, peaks between B and 7.5 ka. After 7 ka and until 5.5 ka, palaeosols in the chinese deserts and many lakes and swamps in the Sahara have disappeared.

After 5.5 ka, aquifers rise quickly in northern Africa and an active pedogenesis results into palaeosols dated *c.* 5 ka in China. At *c.* 4,5 ka, a very abrupt new onset of severe aridity occurs, it culminates at 3.8 ka and ends at c. 3.5 ka. At the lowest latitudes

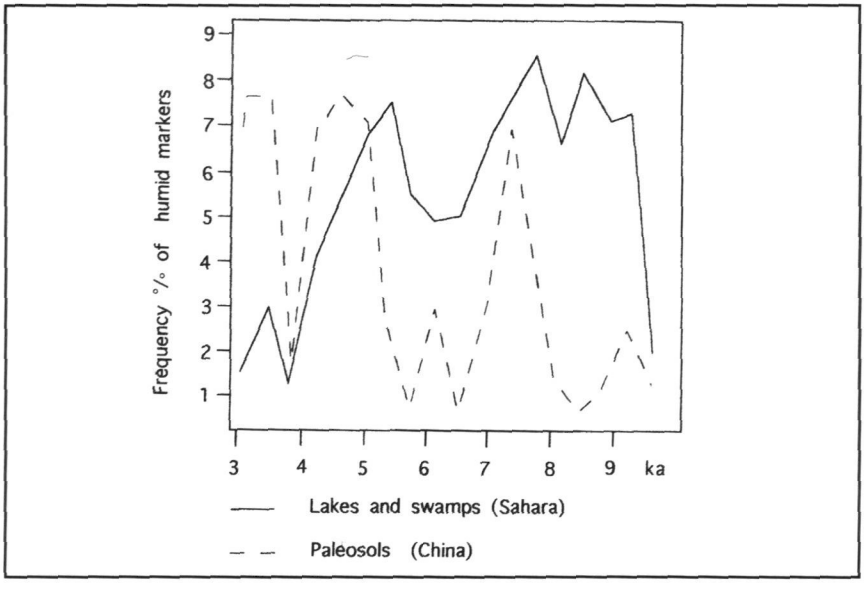

Figure 1. Compared (Holocene) age frequencies of surface fresh water (Sahara) and palaeosols (arid areas in northern China). The frequencies are calculated at a 400 yrs interval and expressed as percent of the total number of data (560+158).

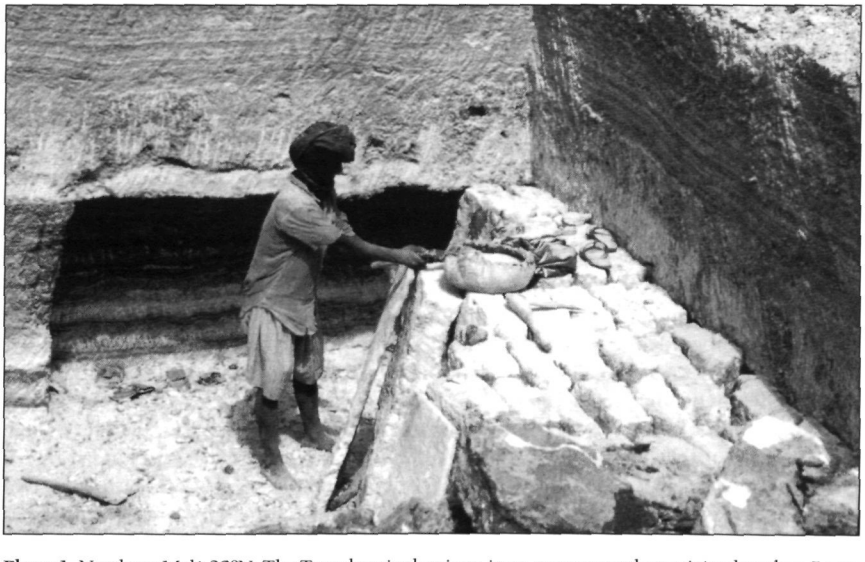

Photo 1. Northern Malí, 23°N. The Taoudenni salt mines, in an area presently receiving less than 5 mm mean annual rainfall, result from the evaporation, some 4,000 years ago, of a large saline lake. The exposed sections, completed by cores, have provided a continuous record of the Holocene climatic variations, close to the Tropic of Cancer (Fabre and Petit-Maire, 1988; Petit-Maire *et al.*, 1991).

in China, a short climatic regeneration preceeds the general aridification observed throughout the transitional zone after 3 ka (Yan and Petit Maire, 1994). In the Sahara also, only the lowest latitudes, at the margins of the Sahel retreating southwards, nearby the large rivers or along the Atlantic coast, still benefit from some surface fresh water.

Those results are confirmed by the dating of continuous lacustrine sections in the Taoudenni Basin, along the Tropic of Cancer in the Sahara (Fabre and Petit-Maire, 1988; Petit-Maire (ed.), 1991. Ph. 1)

The onset of the Holocene long-term humid phase and its degradation is certainly related with the orbital forcing, maximal at 11 ka, while the shorter-term (a few centuries to one millenium) oscillations are not. One may consider other forcings such as variability of solar radiation (cf the Little Ice Age during the Maunder minirnum) or volcanic activity (fitting events at 8.2 ka, at c. 6 ka and at 3.8 ka (Bryson 1995).

The dry episodes had an important impact upon human cultures, in particular the last severe arid event which, throughout the Old World, totally upset the socio-economic systems and civilisations: it corresponds to collapse of the Indus culture at 3.7 ka (Mughal, 1990), in Mesopotamia to unusual dust events at 3.8-3.7 ka (Weiss, 1997), in northeastern Syria to disappearance of all archaeological sites and abrupt sedimentary changes between 4 and 3.5 ka (Hole, 1997, Courty and Weiss, 1997, in the southern Levant to collapse of early Bronze Age society (Rosen, 1997) in Palestine to wide environmental changes at 3.8-3.6 ka (Butzer,1997), in southeastern Ukraine to severe aridification at 4.1 -3.5 ka (Gerasimenko, 1997), in the Dead Sea record to a 100 m level drop at 3.7 ka (Frumkin *et* al., 1991), in Anatolia to low levels of Lake Van as soon as 4.2 ka {Weiss, 1997), in the Aegean to droughts ts at 3.7 ka (Manning, 1997) in Egypt to collapse of the centralised govemement, reduced Nile discharge and degradation of the flood plain at *c.* 3.7 ka (Hassan, 1997), and to disappearance of settlements in Iberia between 4.0 and 3.5 ka (Lillios, 1997). At lower latitudes, in east Africa, Lake Turkana records lower levels at 3.9 ka (Johnson, 1995). The consistence of these data highly conforts the validity of our curve.

It is remarkable that the Holocene climatic optimum in the considered continental records is not at 6 ka, a date generally adopted for modelisations, which better fits delayed responses to external forcings, such as the final ocean level rise.

References

Bryson R.: (1988) Late Quaternary volcanic modulation of Milankovitch climate forcing. *Theor. Appl.* Climatlogy, 39: 115-125.

Butzer K.W.: (1997) "Sociopolitical Discontinuity in the Near East c. 2200 BCE: Scenarios from Palestine and Egypt". *In:* Dalfes H.N., Kukla G., Weiss R. (eds). *Third Millenium BC Climate Change and old World Collapse.* Springer Verlag, Berlin, NATO ASI Series I 49: 245-296.

Courty M.A., Weiss H.: (1997) "The Scenario of Environmental Degradation in the Tell Leilan Region, NE Syria, during the Late Third Millenium Abrupt Climate Change". *In:* **Dalfes H.N., Kukla G., Weiss R.** (eds). *Third Millenium BC Climate Change and Old World Collapse,* Springer Verlag, Berlin, NATO ASI Series I 49: 107-148.

Fabre J., Petit-Maire N.: (1988) Holocene climatic evolution at 22°-23°N from two paleolakes in the Taoudenni area (northem Mali). *Palaeogeography, Palaeoclimatology, Palaeoecology,* 65 133-148.

Frumkin A., Magaritz M., Carmi I., Zak I.: (1991) The Holocene climatic record of the salt caves of Mount Sedom, Israel. *The Holocene,* 1.3: 191-200.
Gerasimenko N. P.: (1997) "Environmental and Climatic Changes Between 3 and 5 ka BP in southeastern Ukraine". *In:* **Dalfes H.N., Kukla G., Weiss R.** (eds). *Third Millenium BC Climate Change and Old World Collapse* Springer Verlag, Berlin, NATO ASI Series I 49: 371-400.
Hassan F.A.: (1997) "Nile Floods and Political Disorder in Early Egypt". *In* : **Dalfes H.N., Kukla G., Weiss R.** (eds). *Third Millenium BC Climate Change and Old World Collapse* Springer Verlag, Berlin, NATO ASI Series I 49: 1-24.
Hole F.: (1997) "Evidence for Mid-Holocene Environmental Change in the Westem Khabur Drainage, Northeastern Syria". *In* : **Dalfes H.N., Kukla G., Weiss R.** (eds). *Third Millenium BC Climate Change and Old World Collapse,* Springer Verlag, Berlin, NATO ASI Series I 49: 39-66.
Johnson T.C.: (1995) "Abrupt Climate change in Holocene Records from African Lakes", *EOS* supplement november 7, 1995: 011B-8.
Lillios K.T.: (1997) "The Third Milleniurn BC in Iberia: Chronometric Evidence for Settlement Histories and Socio-cultural Change". *In* : **Dalfes H.N., Kukla G., Weiss R.** (eds). *Third Millenium BC Climate Ckange and Old World Collapse,* Springer Verlag, Berlin, NATO ASI Series I 49: 173-192.
Manning S.T.: (1997) "Cultural Change in the Aegean c.2200 BC". *In:* **Dalfes H.N., Kukla G., Weiss R.** (eds). *Third Millenium BC Climate Change and Old World Collapse,* Springer Verlag, Berlin, NATO ASI Series I 49: 149-172.
Mughal R.: (1990) The Decline of the Indus Civilization and the Late Harappan Period ill the Indus Valley. *Lahore Museum Bulletin, 3.2: 1-17.*
Petit-Maire N.: (ed.) (1991) Paléoenvironnements du Sahara. Lacs holocènes à Taoudenni (Mali). Editions du CNRS, Marseille-Paris: 239 pp.
Petit-Maire N., Sanlaville P., Yan Z.W.: (1995) Oscillations de la limite nord du domaine des moussons africaine, indienne et asiatique au cours du demier cycle climatique. *Bull Soc géoL Fr, 166,* 2: 213-220.
Rosen A. M.: (1997) "Environmental Change and Human Adaptational Failure at the End of the Early Bronze Age in the Southern Levant". *In:* **Dalfes H.N., Kukla G., Weiss R.** (eds). *Third Millenium BC Climate Change and Old World Collapse,* Springer Verlag, Berlin, NATO ASI Series I 49: 25-38.
Weiss H.: (1997) "Late Third Milleniurn Abrupt Climate Change and Social Collapse in West Asia and Egypt". *In* **Dalfes H.N., Kukla G., Weiss R.** (eds). *Third Millenium BC Climate Change and Old World Collapse,* Springer Verlag, Berlin, NATO ASI Series I 49: 711-723.
Yan Z. W., Petit-Maire N.: (1994) The last 140 ka in the Afro-Asian climatic transitional zone. *Paleogeography, Palaeoclimatology, Palaeoecology,* 110: 217-233.

MUTUAL INFLUENCING BETWEEN THE ATLANTIC OCEAN AND THE MEDITERRANEAN SEA DURING THE QUATERNARY

E.J. Rohling

Dept. of Oceanography, University of Southampton, Highfield, Southampton, Hampshire SO17 1BJ, United Kingdom.

Abstract

Results are presented for runs of a recent hydraulic control model for the exchange transport through the Strait of Gibraltar with independent variations in sea level and Mediterranean net evaporation. Sea level lowering causes a decrease in in/outflow and a strong increase in the inflow-outflow salinity contrast, while the total salt flux from the basin remains constant Reduction of net evaporation causes a decrease in both in-/outflo and the inflow-outflow salinity contrast, so that the total salt flux is reduced. Reduced salt flux into the Atlantic Ocean would potentially influence the salinity and formation of North Atlantic Deep Water. The maintained total salt flux related to sea level lowering is deceptive as regards its potential influence on NADW. Not only would the volume of Medioterranean outflow be reduced, but -more importantly - it would also be of a much higher density than today. The density difference between Mediterranean outflow and deep water in the North Atlantic during the las glacial maximum appears to be more than twice the present value. It seems likely that glacial Mediterranean outflow would have settled at much greater depth in the Atlantic, which would have hindered its salinity-contribution to any deep water formed in the North Atlantic. The modeled sea-level and net evaporation dependent variations in inflow volume into the Mediterranean are considered to have had important consequences 1) near the Strait of Gibraltar (e.g., influence on frontal development in the Alboran Sea, and 2) throughout the Mediterranean (e.g., shoaling of the interface between intermediate and surface waters into the euphotic layer).

Introduction

The only place for water exchange between the Atlantic Ocean and the Mediterranean Sea is the Strait of Gibraltar, which consists of 1) a shallowest passage ('sill') of only 284m depth, and 2) a narrowest passage ('narrows') of up to 880 m depth (Bryden

and Kinder, 1991). An excess of evaporation over total freshwater input ('net evaporation') drives surface water inflow from the Atlantic into the Mediterranean and subsurface water outflow from the Mediterranean into the Atlantic. The subsurface outflow consists of intermediate and deep waters (e.g., Stommel *et al,* 1973; Kinder and Parilla, 1987; Kinder and Bryden, 1990) that are formed through evaporation and cooling within the Mediterranean (e.g., Wust, 1961; MEDOC group, 1970; POEM group, 1992).

The exchange through the Strait of Gibraltar has been the focus of a large number of modeling and observational studies (overviews in Bryden and Kinder, 1991; 1991b; Bryden et *al.* 1994). In this paper, I discuss the effects of variations of sea level and Mediterranean net evaporation in the recent Bryden and Kinder (1991) hydraulic control model for exchange through the Strait of Gibraltar (hence called BK model). This model uses a condition for maximum exchange for flow through the Strait, which implies that there should be a control region inside the Strait - i.e., sill and narrows - bounded at both sides by supercritical flow (Farmer and Armi, 1986; Bryden and Kinder, 1991; Macdonald et *al,* 1994; Bryden et *al,* 1994). There is about 20% offset between observed exchange transport values that are lower than the predictions from the steady maximal exchange model. Part of this offset could be ascribed to time-dependent processes such as atmospheric and tidal forcing and interfacial mixing (*cf* Candela et *al,* 1989; Candela, 1991), and part presumably results from the omission of friction and rotation in the model (Bryden *et al,* 1994). Even though the steady BK model predictions appear to be slightly higher than the observed exchange, it still provides a sound basis for determining the long-term averaged variations of the recent geological past, especially when the results are expressed in terms of changes relative to the modern-scenario predictions.

In the present paper, results from BK model runs with independent variations in net evaporation and sea level will be presented. Thus the model evaluates the effects of changes in the Mediterranean net evaporation and sea level on 1) the properties and volume of subsurface Mediterranean Outflow Water (MOW), and 2) the volume of Atlantic surface water inflow into the Mediterranean. The former determines the total salt flux from the Mediterranean and the depth at which it influences the Atlantic Ocean, while the latter influences hydrography both near the strait in the Alboran Sea, and on larger scales throughout the Mediterranean.

Relevance

It is important to understand the history of MOW, since it provides a source of high salinity waters for the intermediate and deep circulation of the North Atlantic (Reid, 1979;1994; Price *et al.,* 1993; Price and O'Neil-Baringer, 1994). Reid (1979) argued that the influence of the high salinity Mediterranean outflow extends to the Norwegian Sea, and would thus be important for the formation of the relatively salty North Atlantic Deep Water (NADW). Ultimately the (partly) Mediterranean derived salinity of NADW would influence the formation of Antarctic bottom water in the Weddell Sea. In the present paper, variations in the properties and volume of MOW dictated by changes in sea level and Mediterranean net evaporation will be discussed in the context of Reid's (1979) hypothesis that the Mediterranean outflow would dominate the world ocean thermohaline circulation, beacuse of its salt input into the Atlantic.

It is furthermore important to understand the history of Gibraltar exchange, since inflow variations appear to have influenced Mediterranean hydrography (see discus-

sion). Ongoing observational palaeoceanographic research in the Mediterranean concentrates on well-dated high resolution records, eventually enabling detailed comparison with the palaeoceanographic history of the Atlantic Ocean. To interpret timing of, and leads and lags between, events in the Atlantic and the Mediterranean, however, a basic understanding of the bahaviour of the exchange transport through the Strait of Gibraltar as a function of sea level and net evaporation will be vitally important.

Model

i. Bryden and Kinder (BK) model

To build their hydraulic control model for exchange through the Strait of Gibraltar, Bryden and Kinder (1991) digitised the cross-strait profiles at the sill and the narrows from a recent map (IGN-SECEG, 1988), then plotted width versus depth symetrically about the center line for each cross section and described best-fit triangles for each cross-section. This resulted in a triangle representing the sill section with a surface width of 22.3 km and a sill depth of 284 m, and one representing the narrows with a surface width of 13.8 km and a depth of 880 m. In the configuration of the Strait of Gibraltar, with the narrows on the inward (=Mediterranean) side of the sill, the maximum exchange solution needs to take both passages into account, and assumes that the exchange flow is hydraulically critical at both the sill and the narrows (Farmer and Armi, 1986; Dalziel, 1990; Bryden and Kinder, 1991). Subsequently, Bryden and Kinder (1991) combined the hydraulic theory with salt and mass conservation arguments. The resulting model showed that 1) the inflow-outflow transports (volumes) are relatively insensitive to the amount of net evaporation from the Mediterranean, varying only by about 25% for a doubling in net evaporation, but also that 2) the salinity difference between the Mediterranean and Atlantic waters is more sensitive, increasing by 60% for a doubling in net evaporation.

ii. The BK model with variable sea level

Rohling and Bryden (1994) used the BK model, imposing variations in sea level in the Strait of Gibraltar between +10 and -120 m, which modified the sill and narrows crosssections.This range of sea level positions would cover most of the known glacial-interglacial variability (Chappell and Shackleton, 1986; Fairbanks, 1989). Net evaporation from the Mediterranean was kept at a constant value of 56 cm yr^{-1}, the value that produces the most realistic results for present-day exchange transport and inflow-outflow salinity contrast in the BK model.

Results

In the following, either inflow or outflow volume is mentioned where appropriate for the argument to be made. It should be emphasized, that these volumes are only fractionally different, according to conservation of mass arguments (inflow=outflow + net evaporation; where the in-/outflow volumes are many times larger than the net evaporation). Any change in these volumes will, therefore, be virtually identical for both.

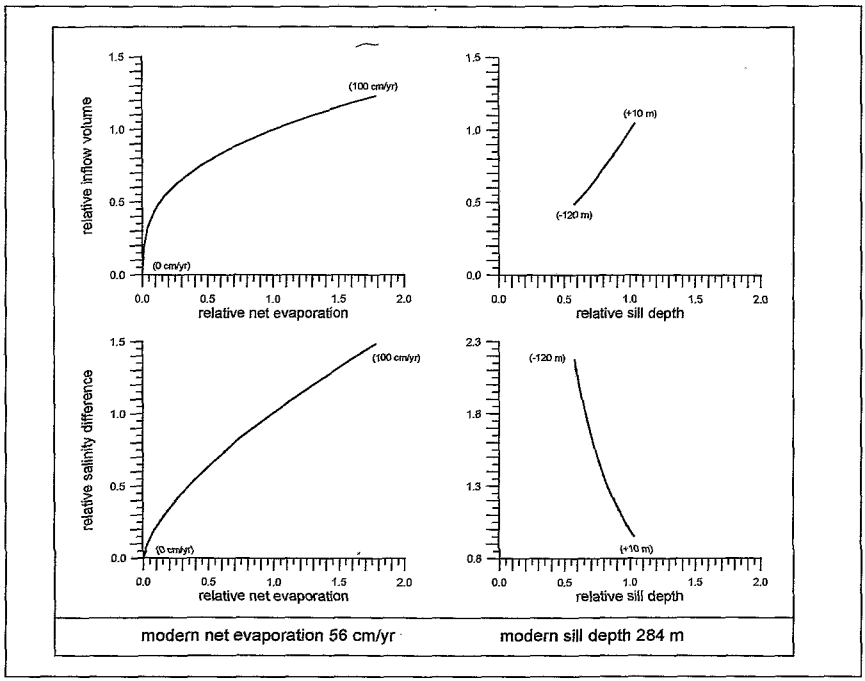

Figure 1. Results from the Bryden and Kinder (1991) model with variations in sea level (cf. Rohling and Bryden, 1994) and in Mediterranean net evaporation. "Relative net evaporation"=net evaporation/present - day net evaporation; "Relative sill depth"= sill depth /present day sill depth; "Relative salinity difference"=inflow-outflow salinity difference/present day inflow-outflow salinity difference; "Relative inflow volume"=volume of surface water inflow into Mediterranean/present-day volume of surface water inflow into the Mediterranean. Ratios relative to the present are used to eliminate (quasi) systematic deviation of steady hydraulic control model from true (observed) values. All ratios equal 1.00 for the present-day. A value of, for instance, 1.20 would indicate a 20% increase, and a value of 0.60 a 40% decrease, relative to the present.

Figure 1 shows how inflow volume into the Mediterranean through the Strait of Gibraltar and the salinity difference between inflow and outflow, would vary with variations in net evaporation and sill depth (i.e., sea level). All values are represented as ratios relative to the modern values. Several conclusions can be drawn immediately: 1) with respect to the inflow volume, the influence of changes in net evaporation is much less dramatic than that of sea level, except when net evaporation is reduced by more than 70%; 2) with respect to the inflow-outflow salinity difference, the influence of changes in net evaporation is again much less dramatic than that of sea level. Furthermore, it appears that: 3) sea level lowering causes reduced outflow of strongly increased salinity, and 4) decreasing net evaporation causes reduced outflow of reduced salinity. Of course, neither 3) nor 4) is surprising, both being visualisations of the conservation of mass and salt arguments within the BK model.

Discussion and conclusions

i. Influence of the Mediterranean on the Atlantic

According to Reid's (1979) hypothesis, changes in the salt flux from the Mediterranean and in the density of MOW are potentially important for the world ocean thermohaline circulation. As illustrated in Fig. 1, sea level lowering by itself does not appreciably affect the total salt flux from the Mediterranean into the Atlantic. However, the salinity (i.e., density) is considerably increased, affecting the depth at which MOW would settle in the Atlantic.

Today, temperature of MOW is roughly 13°C (Kinder and Parilla, 1987; Macdonald *et al.,* 1994). With a rough world-wide surface water salinity increase of 1.25 psu during the last glacial maximum (LGM) due to freshwater storage in the ice-caps, inflow salinity would be near 37.5 psu. Assuming LGM net evaporation over the Mediterranean to have been equal to the present, the inflow outflow salinity difference would be about 2.2 time its modeM value (Fig. 1; modern value ≈1.9 psu; Bryden and Kinder, 1991), giving 2.2* 1.9=4.2 psu. The LGM salinity of MOW would then be 37.5+4.2=41.7 psu. If MOW temperature was equal to its present value, its density would have been 1031.6 kg m^{-3}, and if MOW temperature was about 10°C, its density would have been 1032.2 kg m^{-3}. These values far exceed the likely density values of deep waters in the North Atlantic at that time, which were recently estimated to have been max. 1028.5 kg m^{-3} (Maslin et *al.,* 1995). Today, the density difference between MOW and ambient waters is about 1.5 kg m^{-3} (Price *et al,* 1993), and the above calculation suggests that it was in the order of 3.1 to 3.7 kg m^{-3} during the LGM. Entrainment of ambient waters today rapidly reduces the MOW density, while quickly doubling and eventually almost quadrupling its volume (Price *et al.*, 1993). During the LGM, similar entrainment processes would have prevailed, and the initial volume of outflow would be roughly half of the present (Fig. 1). With the strongly increased initial density contrast, however, it is not unlikely that the Mediterranean outflow settled at much greater depth in the Atlantic, reducing its potential to play any role of significane in increasing surface salinities at high northern latitudes.

Contrary to sea level change, a change in Mediterranean net evaporation does strongly affect the total salt flux from the basin. A decrease in net evaporation would have caused both a decrease in outflow volume, and a decrease in its salinity (Fig. 1). Less water, of reduced salinity/density, would have entered the Atlantic Ocean. Decreased net evaporation is believed to have (in part) triggered deposition of organic rich sediments (sapropels) in the eastern Mediterranean, and sometimes also in the western Mediterranean (see review in Rohling, 1994). Some of these periods occurred during glacial intervals, with substantially lowered sea level, but most occurred during relatively warm intervals, with sea levels higher (sapropel S5, isotopic stage 5e) or perhaps only several 10s of meters lower than today. For instance, considering S1 - one of the more poorly developed sapropels - net evaporation may have been reduced to about 70% of its modern value (Fig. 1: relative in/outflow volume then is 0.86, and relative salinity difference 0.80) while the sea level imposed component of relative in-/outflow reduction was about 0.9 (Rohling, 1994). The total resultant outflow volume, therefore, can be calculated as 100*(0.86*0.90)≈77%, while the inflow-outflow salinity contrast was only about 80% of its present value. Combined, these reductions determine a substantial decrease in the total salt flux from the Mediterranean into the Atlantic, which may have influenced the formation of NADW in the early Holocene following Reid's (1979) hypothesis.

ii. Influence of Atlantic inflow variations on the Mediterranean

In a recent study Rohling et *al* (1995) discussed the planktonic foraminiferal record of the Alboran Sea. In their newly analysed core KS310, as well as in previously published records (Pujol and Vergnaud-Grazzini, 1989), a rapid faunal change was observed around 8000 BP, from a dominance of *Neogloboquadrina pachyderma* (right-coiled) to *Globorotalia inflata*. Comparison with plankton tow results from the western Mediterranean basin showed that this change likely reflects the onset around 8000 BP of more or less modern conditions in the Alboran Sea, with distinct geostrophic fronts separating the jet of Atlantic inflow from ambient Mediterranean waters. Using the BK model with variable sea level, Rohling *et al.* (1995) calculated that the inflow volume around that time would have amounted to a maximum of about 86% of the modern value. This is a maximum estimate since Mediterranean net evaporation around 8000 BP was probably reduced relative to present (*cf.* evidence reviewed in Rohling, 1994), which would have caused further reduction of the inflow volume. The study concluded that the modern front-dominated conditions in the Alboran Sea prevail only when inflow volume is at least 86% of the present. Background against which to view this frontal development is provided by previous studies, which concentrated on a more general description of the late Quaternary environmental history of the Alboran Sea (e.g., Turon and Londeix, 1988; Abrantes, 1988; Vergnaud-Grazzini and Pierre, 1991).

Other studies examined a more Mediterranean-wide response to inflow reductions due to sea level lowering and/or decreases in net evaporation (Rohling, 1991a;1991b; Rohling and Bryden, 1994; Rohling, 1994). These investigations focussed on the link between inflow reductions and shallowing of the interface between surface water and intermediate water in the Mediterranean, which would have improved the availability of the nutrients contained in Mediterranean intermediate water (MIW) (cf. McGill, 1961; Minas, 1971) to the base of the euphotic layer, resulting in development of a deep chlorophyll maximum (DCM). This 'pycno-/nutricline shoaling' concept originated from an explanation for consistent periods of high abundance of *Neogloboquadrina pachyderma* (righ-coiled) in especially eastern Mediterranean planktonic foraminiferal records, which were found in full glacial intervals (low sea level) and in most sapropels (reduced net evaporation) (Rohling and Gieskes, 1989). Additional evidence for DCM development was derived from calcareous nannofossil assemblages (Castradori, 1993), while evidence for pycnocline shoaling during deposition of sapropels S6 and especially S7 was obtained from a stable isotope study on planktonic foraminifera with different depth-habitats (Ganssen and Troelstra, 1987).

iii. Scope for further research

During the Quaternary glacial-interglacial cycles, deep water hydrography in the world ocean has differed from the modern configuration on longer (glacial-interglacial), and shorter (millenial or shorter) time scales (e.g., Maslin *et al*, 1995; Bertram *et al.*,1995; Beveridge *et al.*,1995). By focussing on the timing, leads and lags between changes in NADW formation and both 1) changes in global sea level, and 2) variations of the Mediterranean climate, future studies may validate the implication of Reid's (1979) hypothesis that the Mediterranean Outflow history contributed to changes in world ocean deep circulation. Such palaeoceanographic work requires high-quality core material and high resolution, multidisciplinary investigations. This work could be based on, and benefit from, a number of previous studies (e.g., Zahn *et al.*,1987; Caralp, 1988; Vergnaud-Grazzini *et al*,1 989).

In addition, realistic models of the circulation through the Strait of Gibraltar, in the Alboran Sea and in the Mediterranean as a whole should be applied to evaluate the sensitivity of the system. Comparison of model results with fossil data will portray what portion of the total variability can be explained with each main perturbation identified from the geological record (e.g., sea level lowering, net evaporation reduction). This comparison would highlight whether additional mechanisms have also been responsible for a significant portion of the variability. A possible example would be the dynamics of the subsurface (outflow) layers, which may play as important a role in the dynamics of gyres and fronts in the Alboran Sea as surface water inflow (Heburn and La Violette, 1990). Obviously, such processes will be far more difficult to constrain from the geological record.

References

Abrantes, F.: (1988) Diatom productivity peak and increased circulation during the latest Quaternary: Alboran Basin (western Mediterranean), *Mar. Micropaleontol.,13:79-96*

Bertram, C.J., Eldersfield, H., Shackleton, N.J. and MacDonald, J.A.: (1995) Cadmium/calcium and carbon isotope reconstructions of the glacial northeast Atlantic Ocean, *Paleoceanography,* 10:563-578.

Beveridge, N.A.S., Elderfield, H. and Shackleton, N.J.: (1995) Deep thermohaline circulation in the low-latitude Atlantic during the last glacial, *Paleoceanography,* 10:643-660.

Bryden, H.L. and Kinder, T.H.: (1991) Steady two-layer exchange through the Strait of Gibraltar, *Deep-Sea Res,* 38:S445-S463.

Bryden, H.L. and Kinder, T.H.: (1991b) Recent progress in Strait dynamics, *Reviews of Geophysics* **supplement,** 617-631.

Bryden, H.L., Candela, J. and Kinder, T.H.: (1994) Exchange through the Strait of Gibraltar, *Prog. Oceanogr.*, 33:201-248.

Candela, J.: (1991) The Gibraltar Strait and its role in the dynamics of the Mediterranean Sea, *Dyn. Atm. Oceans, 15*:267-299.

Candela, J., Winant, C.D. and Bryden, H.L.: (1989) Meteorologically forced subinertial flows through the Strait of Gibraltar, *J. Geophys. Res,* 94:12, 667-12, 679.

Caralp, M.-H.: (1988) Late glacial to Recent deep-sea benthic foraminifera from the northeast Atlantic (Cadiz Gulf) and western Mediterranean (Alboran Sea): palaeoceanographic results, *Mar. Micropaleontol,* 13:265-289.

Castradori, D.: (1993) Calcareous nannofossils and the origin of eastern Mediterranean sapropels, *Paleoceanography,* 8:459-471.

Chappell, J. and Shackleton, N.J.: (1986) Oxygen isotopes and sea level, *Nature,* 324:137140.

Dalziel, S.B.: (1991) Two-layer hydraulics: a functional approach, *J. Fluid Mechanics,* 223: 135-163.

Fairbanks, R.G.: (1989) A 17,000 year glacio-eustatic sea level record: influence of glacial melting on the Younger Dryas event and deep-ocean circulation, *Nature,* 342:637-642.

Farmer, D.M. and Armi, L.: (1986) Maximal two-layer exchange over a sill and through the combination of a sill and contraction with barotropic flow, *J. Fluid Mechanics,* 164:53-76.

Ganssen, G. and Troelstra, S.: (1987) paleoenvironmental changes from stable isotopes in planktonic foraminifera from easter Mediterranean sapropels, *Mar. Geol,* 75:221-230.

Heburn, G.W. and La Violette, P.E.: (1990) Variations in the structure of the anticyclonic gyres found in the Alboran Sea, *J. Geophys. Res.*, 95:1599-1613.

Kinder, T.H. and Bryden, H.L.: (1990) Aspiration of deep waters through straits. *In: L J* Pratt (ed.) *The physical oceanography of sea straits,* Kluwer, The Netherlands, 295-319.
Kinder, T.H. and Parilla, G.: (1987) Yes, some of the Mediterranean outflow does come from great depth, *J. Geophys Res,* 92:2901 -2906.
Macdonald, A.M., Candela, J. and Bryden, H.L.: (1994) An estimate of the net heat transport through the Strait of Gibraltar. *In:* P.E. La Violette (ed.) Seasonal and Interannual variability of the western Mediterranean Sea, *Coastal and Estuarine Studies,* American Geophysical Union, Washington DC, USA, 46:13-32.
Maslin, M.A., Shackleton, N.J. and Pflaumann, U.: (1995) Surface water temperature, salinity and density changes in the northeast Atlantic during the last 45,000 years: Heinrich events, deep water formation, and climatic rebounds, *Paleoceanography,* 10:527-544.
McGill, D.A.: (1961) A preliminary study of the oxygen and phosphate distribution in the Mediterranean Sea, *Deep-Sea Res.,* 8:259-269.
MEDOC group: (1970) Observation of formation of deep water in the Mediterranean Sea, *Nature,* 277:1037-1040.
Minas, H.J.: (1971) Résultats préliminaires de la campagne «Mediprod 1» du Jean Charcot (115 Mars et 4-17 Avril 1969), *Investigacion Pesquera* (Barcelona), 35:137-146.
POEM group: (1992) General circulation of the eastern Mediterranean, *Earth Sci. Rev.,* 32:285-309.
Price, J.F. and O'Neil-Baringer: (1994) Outflows and deep water production by marginal seas, *Prog Oceanogr.,* 33: 157-196.
Price, J.F., O'Neil-Baringer, M., Lueck, R.G., Johnson, G.C., Ambar, I., Parilla, G., Cantos, A., Kennelly, M.A. and Sanford, T.B. :(1993) Mediterranean outflow mixing and dynamics, *Science,* 259:1277-1282.
Pujol, C. and Vergnaud-Grazzini, C.: (1989) Palaeoceanography of the last deglaciation in the Alboran Sea (western Mediterranean). Stable isotopes and planktonic foraminiferal records, *Mar Micropaleontol.* 15: 153-179.
Reid, J.L.: (1979) On the contribution of the Mediterranean Sea outflow to the Norwegian-Greenland Sea, *Deep-Sea Res.,* 26: 1199-1223.
Reid, J.L.: (1994) On the total geostrophic circulation of the North Atlantic Ocean:Flow patterns, tracers and transports, *Prog. Oceanogr., 33, 1*
Rohling, E.J.: (1991a) A simple two-layered model for shoaling of the eastern Mediterranean pycnocline due to glacio-eustatic sea level lowering, *Paleoceanography,* 6:537-541.
Rohling, E.J.: (1991b) Shoaling of the eastern Mediterranean pycnocline due to reduction of excess evaporation: implications for sapropel formation, *Paleoceanography,* 6:747-753.
Rohling, E.J.: (1994) Review and new aspects concerning the formation of eastern Mediterranean sapropels, *Mar Geol,* 122: 1 -28.
Rohling, E.J. and Bryden, H.L.: (1994) A method for estimating past changes in the eastern Mediterranean freshwater budget, using reconstructions of sea level and hydrography, *Proc. K. Ned Akad. We, Ser B., Phys. Sci.,* 97:201-217.
Rohling, E.J. and Gieskes, W.W.C.: (1989) Late Quaternary changes in Mediterranean Intermediate Water density and formation rate, *Paleoceanography,* 4:531-545.
Rohling, E.J., Dulk, M. den, Pujol, C. and Vergnaud-Grazzini, C.: (1995) Abrupt hydrographic change in the Alboran Sea (western Mediterranean) around 8,000 yrs BP, *Deep-Sea Res. I,* 42:1609-1619
Stommel, H., Bryden, H. and Mangelsdorf, P.: (1973) Does some of the Mediterranean outflow come from great depth?, *Pure and Applied Geophys,* 105:879-889.

Turon, J.-L. and Londeix, L.: (1988) Dinoflagellate assemblages in the western Mediterranean (Alboran Sea): evidence of the evolution of palaeoenvironments since the last glacial maximum, *Bull Cent. Rech. Explor. Prod. Elf-Aquitaine,* 12:313-344.

Vergnaud-Grazzini, C. and Pierre, C.: (1991) High fertility in the Alboran Sea since the last glacial maximum, *Paleoceanography,* 6:519-536.

Vergnaud-Grazzini, C., Caralp, M., Faugeres, J.-C., Gonthier, E., Grousset, F., Pujol, C. and Saliege, J.-F.: (1989) Mediterranean outflow during through the Strait of Gibraltar since 18,000 years BP, *Oceanol Acta,* 12:305-324.

Wust, G.: (1961) On the vertical circulation of the Mediterranean Sea, *J. Geophys Res,* 66:3261 -3271.

Zahn, R., Sarnthein, M. and Erlenkeuser ,H.: (1987) Benthic isotope evidence for changes of the Mediterranean outflow during the late Quaternary, *Paleoceanography,* 2:543-559

GROUND THERMAL CONTRACTION IN NORTHWESTERN EUROPE RELATED WITH LAST INTERGLACIAL ICE SHEET DYNAMICS

B. van Vliet-Lanoë

Géosciences, UPR 4661 du CNRS, Université de Rennes 1, 35042 Rennes cédex, France.

Abstract

The study of ice wedge polygons in Europe and of their diagenesis allows to emphasize of their recurrence throughout the last Glacial, alternating with loessic sedimentation. They are associated with continuous and ice poor permafrost. Their development is not related with orbital forcing, but more probably to catabatic winds related with the cyclic thickening of ice sheets. Their degradation seems correlated with their thinning, synchronous with the Heinrich events in the northern Atlantic.

Introduction

Permafrost is a subsurface horizon remaining at negative temperature all over the year. Most studies concerning the last glacial permafrost are related to evidence of thermal cracking such as ice wedge casts, sand wedges, soil wedges and cryoturbations. An ice wedge is essentially a thermal crack, open each year, during the winter, in the frozen soil and filled in summer by the deep freezing of melt water into the permafrost upper layer. Thermal cracking in soil is related to abrupt coolings (as those associated with catabatic winds) and ice content in the frozen soil (Lachenbruch, 1966) . Moreover, thermal cracking and permafrost are independent (Svenson, 1977). Successive, joint, vertical ice layers build the ice wedge (Black, 1976). Present-day high Arctic forms use to reach deeper than 3 m. A sand wedge is a thermal crack in the frozen ground filled seasonally by sand translocation (or ice+sand); it characterises the southern region of permafrost (Romanovskii, 1985). Ice wedges are usually considered as the only indication for continuous permafrost. A soil wedge is a crack, not necessarily thermal, filled by fine soil translocation. Many authors have studied the deformation of the frozen

layers adjacent to the wedge, but little attention has been paid to the deformations occurring within the active layer, thawing seasonally, during the growth and the decay of the ice wedge.

Methods

The work of Romanovskii (1985) has shown that many wedge-like forms are related, for rheological reasons, to the southern permafrost region, such as peat or sands wedges. Recent data from Siberia (Soloviev, 1973) and Mackensie delta (Murton and French, 1994) have shown the importance of the degradation forms for the ice wedges understanding of abrupt climate change, e.g. at the onset of the Holocene. Other data collected by the author in Svalbard, Northern Quebec and Ungava (Van Vliet-lanoe *et al.*, 1995) have shown the relationship between short warming events, retrogressive slow degradation of ice wedges and eolian sedimentation during the general cooling trend prevailing in these regions since the Subboreal, and especially during the Little Ice Age. These situations are very similar to those occurring during the last Pleniglacial isotopic stage 2. It is the reason why we shall first discuss the behaviour of permafrost and ice wedges in the Arctic Holocene. During the glacial, vegetation is discrete or thin and the development of ice wedges is essentially restricted to poorly drained sectors such as lowlands, downslopes or depressions.

Holocene data

The permafrost history in the Holartic and the Neartic shows a drastic retreat of its extension in both regions, related with the deglaciation, and the taiga extension mainly during the high summer insolation (c. 15 ky BP up to c. 6 ky BP). Thermokarstic features induced by the abrupt warming during the Late Glacial and after the Youngest Dryas, allowed the development of alas (thermo-erosion lakes) such as in Siberia (Soloviev, 1976) or in the Mackensie delta (Murton and French, 1994). Permafrost disappeared from northern Europe (mountains excepted). In northern America, it was restricted roughly to the northwestern Territories and the NE part of northern Quebec.

In the end of the Hypsithermal or the Atlanticum, summer insolation depleted (Berger, 1989) and permafrost aggradated in 3 major steps. The first aggradation occurred around 4500 BP, associated with ice wedge growth. It restored periglacial activity both in N. America and in Siberia (Fig. 1); palsa (frozen decametric peat/ mineral mounds) developed in peat bogs in Scandinavia and N. Quebec; perennial hydrolaccolite of ice (pingo) developed in former alas in Siberia and Mackensie, or in the valley bottoms, as in Svalbard. This led to the formation of a double layered permafrost in Siberia, a thick unfrozen material zone (talik) being squeezed between the relict fossil permafrost and the new aggradation (Soloviev, 1976). A second major cooling phase is recorded since 2 ky BP (Roman period) on both sites of the Atlantic Ocean, associated with a second main phase of ice wedge growth, extension of palsa bogs and a young generation of pingo. It is important to note that the loess activity in Svalbard started at that time and did not stop since then.

A last major phase of permafrost aggradation occurred during the Little Ice Age (1450-1910), seemingly associated with the 3 minima of solar activity (Jones, 1990): the present-day extension of permafrost is related with this cooling and, despite the warm-

CHRONOLOGY		(Svalbard) Adventalen 78° N	(Svalbard) Gasebu 79° N	Scandinavia 68 - 69°N	N. Quebec 57 à 63° N	Summer Insolation (Berger, 1979)
SUBATALNTIQUE	1910	aeolian and niveo-aeolian	niveo-aeolian	aeolian crytubartions solifluction	aeolian, sand wedges,palsas, sofluction	
	1750		aeolian	stabilisation	stabilisation	
				aeolian crytubartions	aeolian ice wedge growth cryoturbations	
	1000-1450 A.C.	stabilisation		warming fires	warming fires	
		aeolian	aeolian	crytubartions		
	450-850 A.C.	stabilisation	?	stabilisation		
		reactivation of erosion and deflation, groeth os the second generation of pingo, ice wedge activity	?	?	ice wedge activity	
SUBBOREAL	3000-2200 B.P.	muck and peat	mull	peat	peat	
	4500 B.P.	growth of large pingo and ice wedge activity	ice wedge activity	cryoturbations palsas growth	ice wedge growth palsas growth	
	ATLANTIQUE (Hypsithermal)	emmersion	sandur stabilisation	pedogenesis	pedogenesis	

Figure 1. Chronology of ocurrence of ice wedges and other associated permafrost features in the North Atlantic area during the late Holocene cooling.

ing of the early 20th century, is about 1/3 of the Last Glacial Maximum extent. Pedogenesis stopped since the 1000 AD in most of the Subarctic to high Arctic locations, replaced locally by peat growth. In northern Quebec, this cooling is associated with complex sand/soil wedges in the discontinuous permafrost zone, ice wedge growth in Svalbard and N. Ungava. Since 1947, on both sites of the Atlantic only and in southern Beringia (Jones, 1990; Van Vliet-La2noe *et al.*, 1994), cooling strongly accentuates, associated with recurrent thermal cracking and with increasing storminess.

Last Glacial data

Most studies on Last Glacial permafrost are related to thermal cracking, recorded as ice wedge casts and sand wedges. Mapping of permafrost extension during the Last Glacial Maximum in Europe, using ice wedges and other data, such as fragipan horizon (compact subsurface soil horizon with a platy fabric derived from ice lenses growth in the permafrost table), flat bottom cryoturbation or generalised gelifluction, allow to determine a discontinuous and a continuous zone (Fig. 2) with some abnormal boundaries around the Alps Mountains. Moreover, a chronostratigraphical study of permafrost extension, especially in Belgium and NW France has allowed to determine two main phases of permafrost aggradation at 60 ky BP and at 28 ky BP (Van Vliet-Lanoe, 1989). Permafrost installation in western Europe (Van Vliet-Lanoe, 1989) is related to low insolation rates in spring and summer, as plotted by Berger (1979), and to low precipitation.

A new analysis of ice and sand wedges from western Europe (Fig. 3) demonstrates clearly that, in loess or in sand covers, the ice wedges casts were small and represent

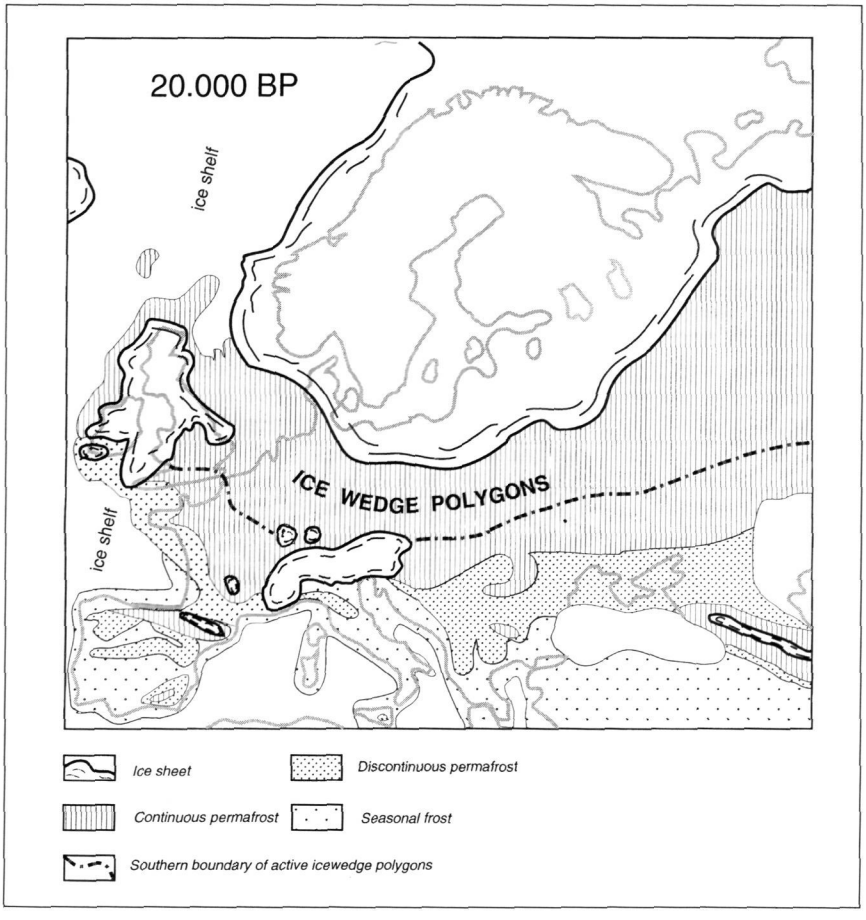

Figure 2. Location of ice wedge polygons and permafrost extension during the Last Glacial Maximum.

juvenile forms, especially south of the Seine river (Van Vliet-Lanoe, 1995). During the last glacial phase, the development of ice wedges was essentially restricted to poorly drained sites, growing during short events. Cryotubation was syngenetic with the ice wedge growth, as in the Arctic today, and continued locally in the wedge filling in wet topographical conditios during the degradation phase (deformation by differential frost heave; Van Vliet-Lanoe, 1987). These features can be confused with loading, sometimes of co-seismic origin.

Sand wedges occurring in the vicinity of the ice sheets, such as those described by Kolstrup (1993) in Denmark show, a complexity similar to those occurring in continuous permafrost during the Holocene in the Subarctic. The other sand wedges occurred on permafrost in sand covers or along the glacial margins, usually during short (but not necessarily dry) cooling events. They were usually not more developed than these of the

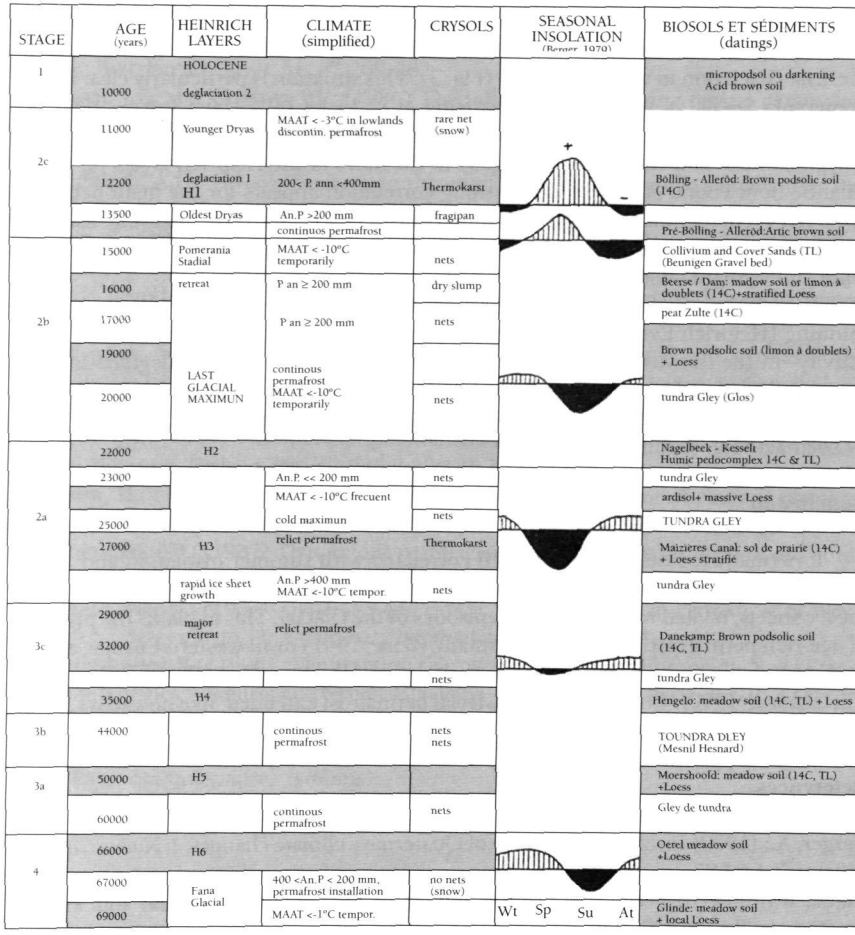

Figure 3. Chronology of Heinrich events, permafrost, ice wedge polygones, palaeosols and climate during the Last Glacial Maximun.
MAAT: mean annual air temperature; AnP.: annual precipitation.

Little Ice Age in N. Quebec. In western Europe, the Last Glacial permafrost, adjacent to the ice wedges, is relatively ice poor: most of the decay forms are simple, attesting that the degradation was slow, plastic (loam) to fragile (sand), without, in most cases, running water during summer. It only leads to the creation of shallow polygonal V trenches, further filled by loess or by aeolian sand, which confirms previous signals extracted from the other periglacial features (Van Vliet-Lanoë, 1989).

Thermokarsts are rare in loess, except around 27 ky BP, surprisingly during the second phase of permafrost aggradation, and at the onset of the Late Glacial warming in western Europe, (13-11 ky BP), leading locally to V shaped valley development; they are

more frequent in eastern Europe where the climate inertia is the lowest. A cyclic answer of ice wedge growth -wedge decay- loess/ sand deposition occurred several time during the Last Glaciation in western Europe (Fig. 3). This situation is particularly clear for the Pomerania Stadial, a glacial surge occurring at c. 15 ky BP. Orbital forcing does not explain this cyclicity of thermal cracking. When plotting the periods of activity of the polygonal nets and comparing it (Fig. 3) to the dates of the Heinrich layers on the N. Atlantic floor (Bond *et al.*, 1993), a strong correlation appears for the main nets. The observed cyclicity of ice wedges development can be explained by the cyclic ice sheet instability (Boulton and Payne, 1994). A thick ice cap induces high pressure, catabatic wind and drought, associated with ice wedge growth.

Abrupt short warmings, about 70 years long, related with the ice cap surge and thinning (Heinrich Events) allow a restored cyclonic circulation in summer, and flood activity in the outwash plains, associated with retrogressive wedges degradation and loess/sand deposition in late summer. Minor events (about 1-2 ky period) within the cycles correspond to the Dansgeard-Oeshger events (Bond *et al.*,1993), possibly ruled by solar activity (Lehman, 1993).

Conclusion

If permafrost extension seems well correlated with summer insolation and astronomical forcing, ice wedge activity is an accidental, climate controlled, event induced by the ice sheets, related with the coolest episodes of the Glacial. This explains the presence of ice-rich permafrost in southern Germany (Bose, 1991) or in western Europe, associated with rare ice wedge casts and their absence in the Po valley (Cremaschi and Van Vliet-Lanoe, 1990). Continuous Last Glacial permafrost extended, like nowadays, south of the ice wedge casts region (Fig. 2).

References

Berger, A.: (1979) Insolation signature of Quaternary climate changes. *Il Nuovo Cimento*, Milano, 2,1:63 87.

Black, R.F.: (1976) Periglacial features indicative of permafrost: ice and soil wedges. Quaternary *Research,* 6:3-26.

Bond, G., Heinrich, H., Broecker, H., Labeyrie, L., McManus J., Andrews, J., Huon, S., Jantschik, R., Clasen, S., Simet, C., Tedesco, K., Klas, M., Bonami, G. and Ivy, S.: (1993) Evidence for massive discharges of icebergs into the North Atlantic ocean during the last glacial period, *Nature*, 365:143-147.

Bose, M.: (1991) A palaeoclimatic interpretation of frost-wedge casts and eolian sand deposits in the lowlands between Rhine and Vistula in the Upper Pleniglacial and late Glacial, Z. *Geomorph.N.F,* **suppl. 90:15-28.**

Boulton, S.G. and Payne, T.: (1994) Mid Latitude ice sheets through the Last Glacial Cycle: glaciological and geological reconstruction. Nato ASI Series, Edit. J.C. Duplessy and M.T. Spyridakis, SpringerVerlag 122:177-212.

Cremaschi, M. and van Vliet-Lanoe, B.: (1990) Traces of frost activity and ice vegetation in Pleistocene loess deposits of Northern Italy. Deep seasonal freezing or permafrost ? *Quaternary Intemational,* 5:39-48.

Hyatt, J.A.: (1990) Reconstruction of Holocene periglacial environments in the Panngnirtung area based on ice wedge characteristics, *Nordicana,* 54:17-21, NR Canada.

Jones, P.D.: (1990) Le climat des mille dernieres années, La *Recherche*, 21,219:304-312.
Kolstrup, E.: (1993) Complex frost wedge casts as indicators of ice age environmental change *Würzburger Geogr. Ar.*, 87:269-282.
Kutzbach, J.E. and Guetter, P.J.: (1986) The influence of changing orbital parameters and surface boundary conditions on climate simulations for the 18000 years, *Jour. Atmos Sc*, 43: 1726-1759.
Lachenbruch, A.H.: (1966) Contraction theory of ice wedge polygons: a qualitative discussion. *Permafrost Inter. Conf. Proc Nat Acad. Sc & Nat. Res Council USA publ.*, 1287:63-71.
Lehman, S.: (1993) Ice sheets, wayward winds and sea change, *Nature*, 365:108-110.
Murton, J.B. and French, H.M.: (1993) Thaw modification of frost-fissure wedges, Richards Island, Pleistocene Mackensie Delta, Western Arctic Canada, *Joumal of Quaternary Sc.*, 8,3: 185-196.
Romanovskii, N.N.: (1985) Distribution of recently active ice and soil wedges in the USSR. *In* M. Church and O. Slaymaker (eds), *Field and theory-lectures in Geocryology:* 154-165.
Solovyev, P.A.: (1973) Thermokarst phenomena and landforms due to frost heaving in Central Yakoutia, *Biuletyn Peryglacjalny*, 23:135-155.
Svensson, H.: (1978) Ice wedges as a geomorphological indicator of climatic changes, *Danske Meteor Inst, Klimat Meddel* 4:9-17.
Van Vliet-Lanoë B.: (1987) Dynamique périglaciaire actuelle et passée. Apport de l'étude micromorphologique et de l'expérimentation, *Bull. A.F.E.Q.*, 2:113-132.
Van Vliet-Lanoë B.: (1989) Dynamics and extent of the Weichselian Permafrost in Western Europe (stages 5e to 1), *Quaternary International*, 3/4:109-114.
Van Vliet-Lanoë B.: (1996) Contraction thermique des sols en Europe du Nord Ouest et dynamique des inlandsis au Dernier Glaciaire, *C.R. Acad. Sci. Paris*, sér. II, 322 .
Van Vliet-Lanoë B., Allard M. and Payette S.: (1995) Formes de croissance et de dégradation des coins de glace et de sols actuels. Application au pergélisol quaternaire. *Géogr. Phys. & Quaternaire*, (soumis).

UNIVERSIDAD DE LAS PALMAS DE GRAN CANARIA
SERVICIO DE PUBLICACIONES